

國立交通大學

光電工程研究所

碩士論文

絕熱式光方向耦合器的干擾與寬頻議題

Adiabatic Optical Directional Coupler:

Crosstalk and Broadband Issues



研究生：彭煒仁

指導教授：祁 甦 教授

陳奇峯 教授

中華民國九十二年六月

絕熱式光方向耦合器的干擾與頻寬議題

Adiabatic Optical Directional Coupler:

Crosstalk and Broadband Issues

研究生：彭煒仁

Student : Wei-Ren Peng

指導教授：祁 姓 教授

Advisor : Prof. Sien Chi

陳奇峯 教授

Prof. Chi-Feng Chen

國立交通大學

光電工程研究所

碩士論文

A thesis

Submitted to Institute of Electro-Optical Engineering

College of Electrical Engineering and Computer Science

National Chiao Tung University

In partial Fulfillment of the Requirements

For the Degree of

Master

In

Institute of Electro-Optical Engineering

June 2003

Hsinchu, Taiwan, Republic of China

中華民國九十二年六月

絕熱式光方向耦合器的干擾與寬頻議題

學生: 彭煒仁

指導教授: 祁 甦

教授

陳奇峯

教授

國立交通大學光電工程研究所碩士班

摘要

在波長多工光通訊系統下，我們通常需要寬頻元件來處理所有的信號。其中一個適當元件便是具有對光極化，光波長以及元件長度不敏感特性的絕熱式光方向耦合器。此論文中我們對具有寬頻特性的絕熱式光方向耦合器做干擾以及頻寬的計算與模擬，並比較數種特別結構下的特性分析。最後我們得到全能量耦合器在長度 1.2 公分下可使 1.29 到 1.7 μm 波長的交錯能量達 98% 以上，同時我們得到絕熱式濾波器可在 2 公分長度下使干擾降低-20dB 以下並且得到 106nm 的寬頻特性。

Adiabatic Optical Directional Coupler:

Crosstalk and Broadband Issues

Student: Wei-Ren Peng

Advisor: Prof. Sien Chi

Prof. Chi-Feng Chen

Institute of Electro-Optical Engineering

National Chiao Tung University

Abstract

Under WDM system, we often need a broadband device addressing all the signals. One of the candidates is the adiabatic coupler which exhibits advantages of insensitive to polarizations, wavelengths and length of the device. In this thesis we proposed and analyzed several special adiabatic coupler profiles through computing and simulating their crosstalk and bandwidths, and their results are compared. We proposed the full coupler of length 1.2cm which can make the crossing power over 98% of the input under the wavelength from 1.29 to 1.7um. Filters that exhibit bandwidth of 106nm near 1.55um and low crosstalk less than -20dB whether in 1.31 or 1.55 bands are also provided in this thesis.

致謝

首先感謝交通大學提供的所有資源，感謝光電所祁姓老師和中正大學助理教授陳奇峯學長對我論文的指導與建議，同時也感謝實驗室眾多師兄弟對此論文的任何建議與幫忙，感謝我的母親及兄弟對我的關懷與愛護。因為要感謝的人太多，只好謝天了。

最後僅將我的論文獻給我最敬愛的父親。

彭煒仁

國立交通大學

中華民國九十二年六月

Contents

Abstract (Chinese)/

Abstract/

Acknowledgement/

Contents/

Figure Caption/

Chapter 1

Introduction and Overview

1.1 Preface / 1

1.2 Motivation / 2

1.3 Outline of the thesis / 3

Chapter 2

The coupling principle and model

2.1 Normal modes of uniform coupled waveguides / 5

2.2 Mode Interference Directional Couplers / 8

2.3 Quasi-Normal modes in Tapered Coupled Waveguides / 11

2.4 Adiabatic Directional Couplers / 14

2.5 Broadband Aspect of ADC's / 16

Chapter 3

Analysis and simulation of adiabatic full couplers

3.1 Constant local beat length couplers

3.1.1 the crosstalk issue / 18

BPM simulation / 23

3.1.2 the broadband issue / 27

3.2 Uniform tapered mode couplers

3.2.1 the crosstalk issue / 31

	BPM simulation / 34
	3.2.2 the broadband issue / 36
3.3	Linearization of device layout
	3.3.1 the crosstalk issue / 38
	BPM simulation / 39
	Further Discussion / 40
	3.3.2 the broadband issue / 41
Chapter 4	
	Application aspect
	4.1 Broadband optical switch / 67
	4.2 Broadband optical filter / 69
Chapter 5	
	Conclusion / 80
Reference / 81	

Figure Caption

Fig. 1-1	Real guide approximated as the series local guides.....	3
Fig. 1-2	General layout of an adiabatic coupler.....	4
Fig. 1-3	Function of the front end of a transceiver.....	4
Fig. 2-1	(a)Even mode (b)Odd mode of a coupler.....	8
Fig. 2-2	Beat and coupling length.....	9
Fig. 2-3(a)	Variation of the phase constant b and coupling coefficient C.....	12
Fig. 2-3(b)	The corresponding waveguide layout of Fig. 2-3(a).....	12
Fig. 3-1	A typical loss pass filter.....	42
Fig. 3-2	Dynamic crosstalk of case 1.....	42
Fig. 3-3	Variations of $q(k)$ of case 1.....	43
Fig. 3-4	Variations of $d(k)$ and $C(k)$ of case 1.....	43
Fig. 3-5	Variation of effective index versus waveguide width.....	44
Fig. 3-6	Antisymmetric waveguide pairs.....	44
Fig. 3-7	Waveguide layouts of case 1.....	45
Fig. 3-8(a)	Dynamic power flow of case 1, $D = 2$	46
Fig. 3-8(b)	Dynamic power flow of case 1, $D = 3.5$	46
Fig. 3-8(c)	Dynamic power flow of case 1, $D = 6$	47

Fig. 3-9(a)	Power in guide 1, case 1, $D = 2$, scanned from 1.29 to 1.7 μm	47
Fig. 3-9(b)	Power in guide 2, case 1, $D = 2$, scanned from 1.29 to 1.7 μm	48
Fig. 3-9(c)	Loss in case 1, $D = 2$, scanned from 1.29 to 1.7 μm	48
Fig. 3-10(a)	Power in guide 1, case 1, $D = 3.5$, scanned from 1.29 to 1.7 μm	49
Fig. 3-10(b)	Power in guide 2, case 1, $D = 3.5$, scanned from 1.29 to 1.7 μm	49
Fig. 3-10(c)	Loss in case 1, $D = 3.5$, scanned from 1.29 to 1.7 μm	50
Fig. 3-11(a)	Power in guide 1, case 1, $D = 6$, scanned from 1.29 to 1.7 μm	50
Fig. 3-11(b)	Power in guide 2, case 1, $D = 6$, scanned from 1.29 to 1.7 μm	51
Fig. 3-11(c)	Loss in case 1, $D = 6$, scanned from 1.29 to 1.7 μm	51
Fig. 3-12	Variations of coupling coefficients of case 2.....	52
Fig. 3-13	Dynamic crosstalk of case 2.....	52
Fig. 3-14	Variations of the asynchronicity parameter of case 2.....	53
Fig. 3-15	Variations of half the difference of phase constants, $d(k)$	53
Fig. 3-16	Waveguide layouts of case 2.....	54
Fig. 3-17(a)	Dynamic power flow of case 2, $D = 2$	55
Fig. 3-17(b)	Dynamic power flow of case 2, $D = 3.5$	55
Fig. 3-17(c)	Dynamic power flow of case 2, $D = 6$	56
Fig. 3-18(a)	Power in guide 1, case 2, $D = 2$, scanned from 1.29 to 1.7 μm	56
Fig. 3-18(b)	Power in guide 2, case 2, $D = 2$, scanned from 1.29 to	

1.7um.....	57
Fig. 3-18(c) Loss in case 2, $D = 2$, scanned from 1.29 to 1.7um.....	57
Fig. 3-19(a) Power in guide 1, case 2, $D = 3.5$, scanned from 1.29 to 1.7um.....	58
Fig. 3-19(b) Power in guide 2, case 2, $D = 3.5$, scanned from 1.29 to 1.7um.....	58
Fig. 3-19(c) Loss comparisons of case 2, $D = 3.5$	59
Fig. 3-20(a) Power in guide 1, case 2, $D = 6$, scanned from 1.29 to 1.7um.....	59
Fig. 3-20(b) Power in guide 2, case 2, $D = 6$, scanned from 1.29 to 1.7um.....	60
Fig. 3-20(c) Loss comparisons of case 2, $D = 6$	60
Fig. 3-21 Linearization of adiabatic coupler.....	61
Fig. 3-22 Variations of $C_{AB}(z)$ and $r(z)$ of case 3.....	61
Fig. 3-23 Output crosstalk versus D of case 3.....	62
Fig. 3-24 Dynamic crosstalk of case 3.....	62
Fig. 3-25 Waveguide layouts of case 3.....	63
Fig. 3-26 Dynamic power flow of case 3.....	63
Fig. 3-27(a) Variation of crosstalk versus device length ratio in different lengths ($D = 2 \sim 4.5$).....	64
Fig. 3-27(b) Variation of crosstalk versus device length ratio in different lengths ($D = 5 \sim 7.5$).....	64
Fig. 3-28(a) Power in guide 1, case 3, scanned from 1.29 to 1.7um....	65
Fig. 3-28(b) Power in guide 2, case 3, scanned from 1.29 to 1.7um.....	65
Fig. 3-28(c) Loss comparisons of case 3, scanned from 1.29 to 1.7um.....	66

Fig. 4-1	Phase constants of different states in a switch.....	72
Fig. 4-2	The switch layouts.....	73
Fig. 4-3	Output powers of two switch states.....	74
Fig. 4-4(a)	Crosstalk in guide 1 of switched state.....	74
Fig. 4-4(b)	Crosstalk in guide 2 of unswitched state.....	75
Fig. 4-5	Output power of different states with different lengths....	75
Fig. 4-6(a)	Crosstalk of adiabatic filter in guide 1 of switched state.....	76
Fig. 4-6(b)	Crosstalk of adiabatic filter in guide 2 of switched state.....	76
Fig. 4-7(a)	Matched waveguides with different dimensions.....	77
Fig. 4-7(b)	Variation of phase constant versus wavelength.....	77
Fig. 4-8	Filter layouts.....	78
Fig. 4-9	Output power of the conventional and adiabatic filters.....	79
Fig. 4-10	Output power of the adiabatic filters with different lengths.....	79

Chapter 1

Introduction and Overview

1.1 Preface and overview

In early years before the invention of low loss fiber, the band mainly used for communications are of microwave or radio wave. Many microwave devices are proposed in that era and one of them relating to my thesis is the one called single tapered mode coupler invented in 1955[1]-[3]. The coupler was analyzed using the normal modes, which are just alternative expression of the traditional modal modes. For the simplest example of normal modes is the even and odd mode used for explaining the power distribution in a parallel waveguides. But the even and odd modes are just subset of the normal mode, the normal modes can further survive in a uniform mismatched coupler. For a non-uniform coupler the ideas of local normal modes must be used. For a non-uniform waveguide, we can approximate the guide by the series of uniform sections. As expressed in Fig. 1-1, the profile is independent of z within each section and is defined at the center $z=z_c$, where it coincides with the profile of the non-uniform waveguide. Now we approximate the normal modes in each section as it is infinitely long. It is clear that the model will be exactly correct only when the device length is infinitely long. Due to the finite length of a real device, we often just can use the local mode to model approximately a non-uniform waveguide. The accuracy depends on the relation between the slope of variation and the device length, which will be covered more in chapter 2. A coupler is called adiabatic when it varies very slowly avoiding the coupling of the two normal modes. Fig. 1-2 shows the general layout of this coupler. The phase constants of the two composite guides vary with reverse direction and cross over at some point of the coupler, depend on its purpose. For example, if a full coupler is needed, we often put the matched point at the center of the coupler and mismatched the two guides at the two ends largely. We are not going to discuss further and more information about full coupler will be covered in chapter 3. Since the principle of adiabatic coupler is the power sustained in only one normal mode, it is apparently different with the conventional coupler which is power redistributed through the interference of the two normal modes. Interference will suffer the conventional coupler sensitive to polarization, wavelength and then device length. This is the main reason adiabatic coupler insensitive to all these parameters.

Since it is impractical for microwave application due to the need of 5 to 10 times of coupling length of the parallel transmission lines. The wavelength of microwave is about several centimeters and will make the single tapered mode coupler several meters long! Because of the reasons above, this coupler is just for fun and useless at that time. Until the developing of fiber-optic communication, extension of the use of this coupler from microwave to optical waveguides was firstly proposed by [4] for its tolerance to fabrication. The device is workable in optical domain since the optical wavelength is thousands shorter than that of microwave. Because the phase constants of two guides must match at certain point in this coupler, they called it “cross beta” coupler then. An analytic solution of the “cross beta” coupler was derived under the constraints of linear variation of propagation constants and constant coefficient [5]-[6]. A Fourier integral interpolation of the first order coupled-local-mode theory of the mode-conversion loss in adiabatically tapered waveguide is presented in [7]. Tapering in both dimension and refractive index of different special profiles were solved numerically and analytically in [8]-[11]. The first switch using adiabatic principle is called digital optical switch in [12]. And many variations of the digital switch are proposed under different structures [13]-[15]. The filters, multiplexers and half power dividers using adiabatic device are proposed in [16]-[20]. Among these papers, there are some who announce they proposed a new profile that exhibits better or optimal profiles but we found that they just change the form of the profiles which had been provided in [3]. Although through many years from [3], we still discuss this thesis partly based on it.

1.2 Motivation of this thesis

Originally, my job is to design a waveguide structure which is used as the front end of an optical transceiver. As Fig. 1-3 shows, the laser emits signal of the band near 1.31 μm . and transport it to the fiber and the received signals of the bands of 1.55 μm must go through another way avoiding destroy the laser emitter. It seems we need a filter which can tell the two wavelengths. However, we know the bands of 1.55 μm are ranged from C band 1.53 μm to L band of 1.62 μm . We need a broadband filter which can well cover all the bands. We found that only the adiabatic device can satisfy our requirement and then we focused on studying each profiles of this coupler with some constraints. That's the place we entrance the gate of adiabatic devices.

1.3 Outline of this thesis

In the follow-up chapter we will introduce the normal modes of a coupler, which is the transformation of the conventional modal modes. It is very necessary because using the alternative modes we can explain and design the adiabatic coupler easier. In chapter 3 we will discuss three cases of different constraints containing ten profiles overall. In each case we examine the differences or relations between theoretical and BPM crosstalk. The bandwidth of each profiles are listed for comparison, too. Two examples of application are covered in chapter 4, which are optical switches and filters. The functions of tapering the propagation constant and coupling will be lightened through some simple comparison. And finally we give a conclusion to this device in chapter 5.

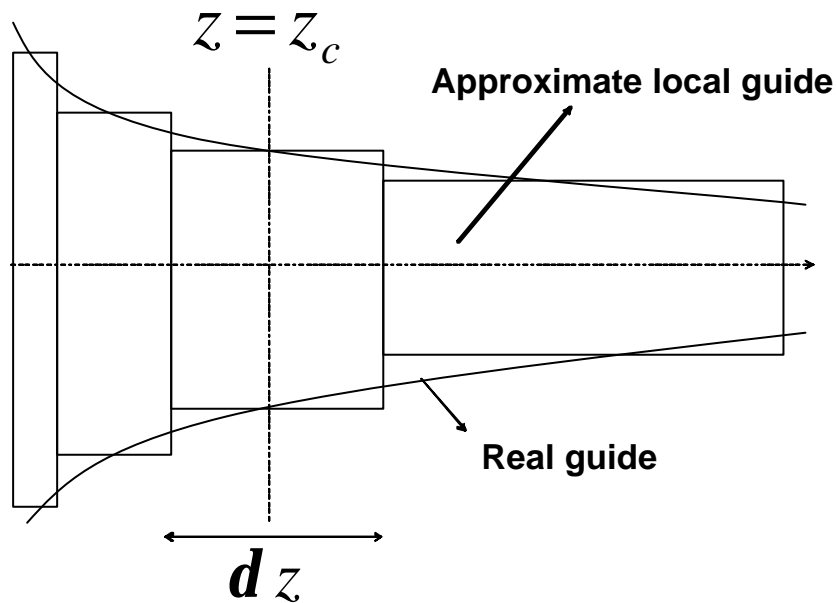


Fig. 1-1 Real guide approximated as the series local guides.

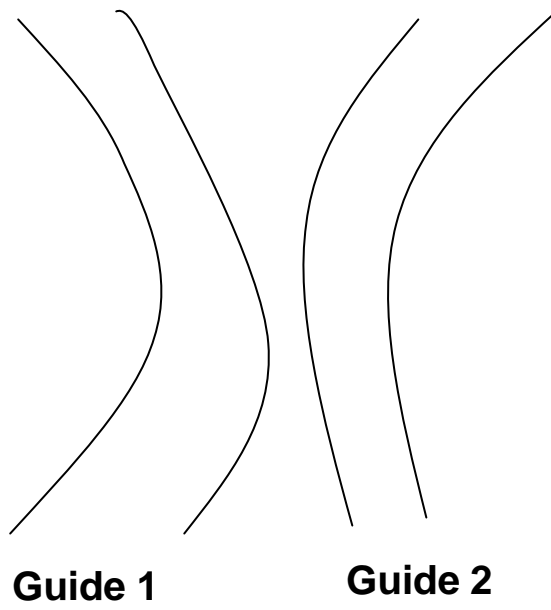


Fig. 1-2 General layout of an adiabatic coupler

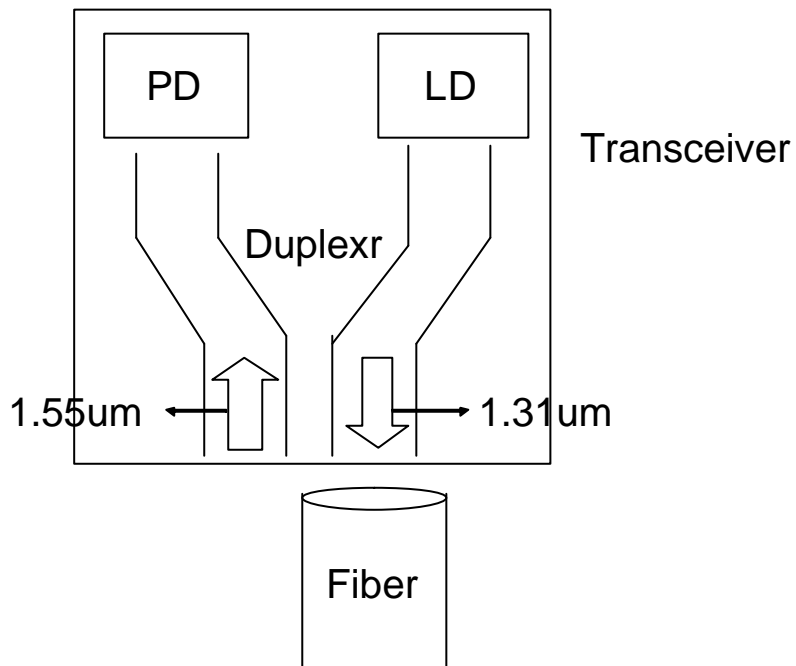


Fig. 1-3 Function of the front end of a transceiver

Chapter 2

The coupling principle and model

In this chapter we will discuss the conventional coupler using the principle of interference of normal modes and then introduce the adiabatic direction coupler to the reader. Which coupler has some advantage such as wavelength, polarization insensitive and more tolerances to fabrication over the conventional one. In order to get a clear picture of adiabatic coupler, we must give the reader an introduction of what is normal modes in a coupled waveguides firstly, which is the job of the follow-up section. Then the conventional coupler will be explained by the interference of the normal modes in section 2. And we will focus on the quasi-normal modes of a tapered couplers and one of its application, the adiabatic coupler, in section 3 and 4, respectively. In addition, the broadband aspect, another issue in this thesis, will be covered conceptually in section 5.

2.1 Normal modes of uniform coupled waveguides

As we all know there are four normal modes that two ideal uniform lossless optical waveguides can support, that is, two are in the forward and the others are in the backward direction. Here we focus on the co-directional coupler so the backward normal modes will be disregarded. The following equations govern the two forward modal modes for such a system. The wave amplitudes for the two coupled waveguides may be written in the form

$$\begin{aligned}\frac{dA_1}{dz} &= -j(\mathbf{b}_1 + C)A_1 + jCA_2 \\ \frac{dA_2}{dz} &= jCA_1 - j(\mathbf{b}_2 + C)A_2\end{aligned}\tag{2-1}$$

in which

$A_{1,2}(z)$ = wave amplitudes in guides 1 and 2, respectively

$\mathbf{b}_{1,2}$ = uncoupled propagation constants of guides 1 and 2, respectively

C = mutual and self-coupling coefficient between the guides

Two assumptions had been made that the guides are lossless, and the mutual and self-coupling coefficients are identical. Keep in mind that energy conservation will require C be real. The wave amplitudes are normalized so that the power in either

guide is equal to the square of the wave amplitudes.

One may ever seen eq(2-1) in many text books and its solution can be derived directly. Here we proceed to transform its solution to another form we care instead of the direct form, that is, we are more eager for the normal modes representations implicitly in eq(2-1). Taking out a common phase factor and introducing the normal coordinates $N_A(z)$ and $N_B(z)$, we get

$$\begin{aligned} A_1 &= e^{-j(b+c)z} \left[\cos\left(\frac{1}{2}\mathbf{q}\right)N_A(z) - \sin\left(\frac{1}{2}\mathbf{q}\right)N_B(z) \right] \\ A_2 &= e^{-j(b+c)z} \left[\sin\left(\frac{1}{2}\mathbf{q}\right)N_A(z) + \cos\left(\frac{1}{2}\mathbf{q}\right)N_B(z) \right] \end{aligned} \quad (2-2)$$

where we define

$$\begin{aligned} \mathbf{b} &= \frac{1}{2}(\mathbf{b}_1 + \mathbf{b}_2) \\ \mathbf{d} &= \frac{1}{2}(\mathbf{b}_1 - \mathbf{b}_2) \\ \cot(\mathbf{q}) &= M = \frac{\mathbf{d}}{C} \\ \Gamma &= \sqrt{\mathbf{d}^2 + C^2} = C\sqrt{1+M^2} \equiv \frac{C}{F} \\ \cos\left(\frac{\mathbf{q}}{2}\right) &= \sqrt{\frac{\Gamma+\mathbf{d}}{2\Gamma}} \\ \sin\left(\frac{\mathbf{q}}{2}\right) &= \sqrt{\frac{\Gamma-\mathbf{d}}{2\Gamma}} \end{aligned} \quad (2-3)$$

Among them, we define a new parameter $M = \frac{\mathbf{d}}{C}$, which is called mismatch parameter

that measure the asynchronicity between the two guides.

Substituting (2-2) in (2-1), we find that the normal coordinates satisfy the uncoupled equations:

$$\begin{aligned} \frac{dN_A}{dz} - j\Gamma N_A &= 0 \\ \frac{dN_B}{dz} + j\Gamma N_B &= 0 \end{aligned} \quad (2-4)$$

The normal mode solutions may be written down immediately as

$$\begin{aligned} N_A(z) &= N_A(0)e^{j\mathbf{b}_A z} \\ N_B(z) &= N_B(0)e^{j\mathbf{b}_B z} \end{aligned} \quad (2-5)$$

where $N_A(0)$ and $N_B(0)$ are the initial values at the start ends and $\mathbf{b}_{A,B}$ are phase

constants of the two normal modes, which equals to $\pm\Gamma=\pm C/F$ respectively according to eq(2-3). From eq(2-5) it is clear that unlike the modal modes in guides A_1 and A_2 , the normal modes N_A and N_B never couple through the guides. $N_A(z)$ is called the fast normal mode and $N_B(z)$ is called the slow normal mode. The amplitudes in the two guides are given by substituting equations (2-5) into equations (2-2). $|N_A(0)|^2$ represents the amount of power excited in the fast normal mode and $|N_B(0)|^2$ represents the amount of power excited in the slow normal mode.

The amplitudes are normalized so that $|N_A(0)|^2 + |N_B(0)|^2 = 1$. The wave amplitudes in the two guides for the fast normal mode are

$$\begin{aligned} A_1'(z) &= \cos\left(\frac{1}{2}\mathbf{q}\right) e^{-j(\mathbf{b}+\mathbf{c}-\mathbf{b}_A)z} \\ A_2'(z) &= \sin\left(\frac{1}{2}\mathbf{q}\right) e^{-j(\mathbf{b}+\mathbf{c}-\mathbf{b}_A)z} \end{aligned} \quad (2-6)$$

while the voltage amplitudes for the slow normal mode are

$$\begin{aligned} A_1''(z) &= -\sin\left(\frac{1}{2}\mathbf{q}\right) e^{-j(\mathbf{b}+\mathbf{c}-\mathbf{b}_B)z} \\ A_2''(z) &= \cos\left(\frac{1}{2}\mathbf{q}\right) e^{-j(\mathbf{b}+\mathbf{c}-\mathbf{b}_B)z} \end{aligned} \quad (2-7)$$

The fast normal mode has the same phase in each guide and is called the in-phase normal mode, while the slow mode is called the out-of-phase normal mode.

To get a clear picture of normal modes, we can write the overall field as

$$\begin{aligned} \mathbf{y} &= A_1 \mathbf{y}_1 + A_2 \mathbf{y}_2 \\ &= N_A \mathbf{y}_A + N_B \mathbf{y}_B \end{aligned} \quad (2-8)$$

where the $\mathbf{y}_{1,2}$ and $\mathbf{y}_{A,B}$ are the waveguide fields of each core in isolation and the normal mode fields, respectively. After some simple manipulation, we can rewritten it

as

$$\begin{aligned} \mathbf{y}_A &= \cos\left(\frac{\mathbf{q}}{2}\right)\mathbf{y}_1 + \sin\left(\frac{\mathbf{q}}{2}\right)\mathbf{y}_2 \\ \mathbf{y}_B &= -\sin\left(\frac{\mathbf{q}}{2}\right)\mathbf{y}_1 + \cos\left(\frac{\mathbf{q}}{2}\right)\mathbf{y}_2 \end{aligned} \quad (2-9)$$

So the normal mode fields are the linear compositions of modal fields of the uncoupled guides, and the coefficients are related to the mismatch parameter, M. In the case of identical guides M=0, and the two normal fields can be formed as

$$\begin{aligned} \mathbf{y}_A &= \frac{1}{\sqrt{2}}\mathbf{y}_1 + \frac{1}{\sqrt{2}}\mathbf{y}_2 \\ \mathbf{y}_B &= -\frac{1}{\sqrt{2}}\mathbf{y}_1 + \frac{1}{\sqrt{2}}\mathbf{y}_2 \end{aligned} \quad (2-10)$$

Which two match to the even and odd modes of the two identical guides.

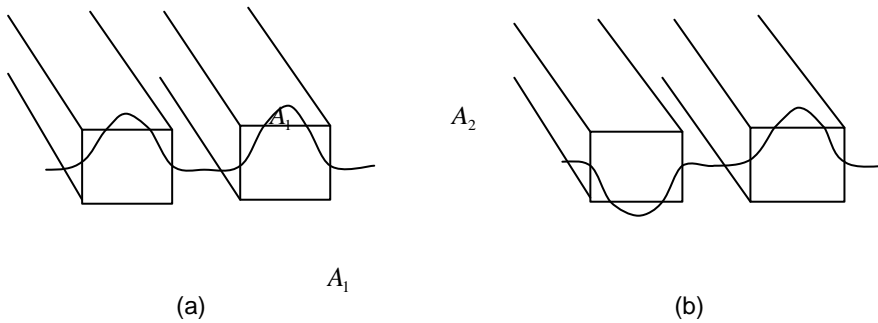


Fig. 2-1 (a) Even mode (b) Odd mode Of a coupler

2.2 Mode Interference Directional Couplers

The two coupled uniform waveguides treated above can be used as a directional coupler. From equations (2-2) and (2-5) it is seen that the power in guide 1 is given by

$$P_1(z) = |A_1(z)|^2 = |N_A(0)|^2 \cos^2\left(\frac{1}{2}\mathbf{q}\right) + |N_B(0)|^2 \sin^2\left(\frac{1}{2}\mathbf{q}\right) - \sin(\mathbf{q}) \operatorname{Re}(N_A(0)N_B^*(0)e^{2j\Gamma z}) \quad (2-11-a)$$

and the power in guide 2 is given by

$$P_2(z) = |A_2(z)|^2 = |N_A(0)|^2 \sin^2\left(\frac{1}{2}\mathbf{q}z\right) + |N_B(0)|^2 \cos^2\left(\frac{1}{2}\mathbf{q}z\right) + \sin(\mathbf{q}z) \operatorname{Re}(N_A(0)N_B^*(0)e^{2j\Gamma z})$$

(2-11-b)

where Γ is defined in (2-3)

From eq(2-11) we can tell immediately that the two guide powers are formed by the interference of the two normal modes in eq(2-2).

It is clear that if only one normal mode is excited in the coupler, that is, $N_A(0)$ or $N_B(0)$ equals zero and then there will no power transfer between the guides. To be a directional coupler both normal modes excited is necessary. Due to the interference of the two normal modes, we call this kind of coupler as mode interference directional couplers (MICs').

The beat length of the coupler is defined as the minimum distance between two points along the guides at which the power in a given guides has its maximum value. And the half distance of beat length is defined as coupling length $L_c = p/2C$ which means the minimum distance between the power maximum point and its nearest minimum point. In the following chapter we will use the minimum local beat length to be the basic length or distance unit. The coming plot shows the definition of beat and coupling length.

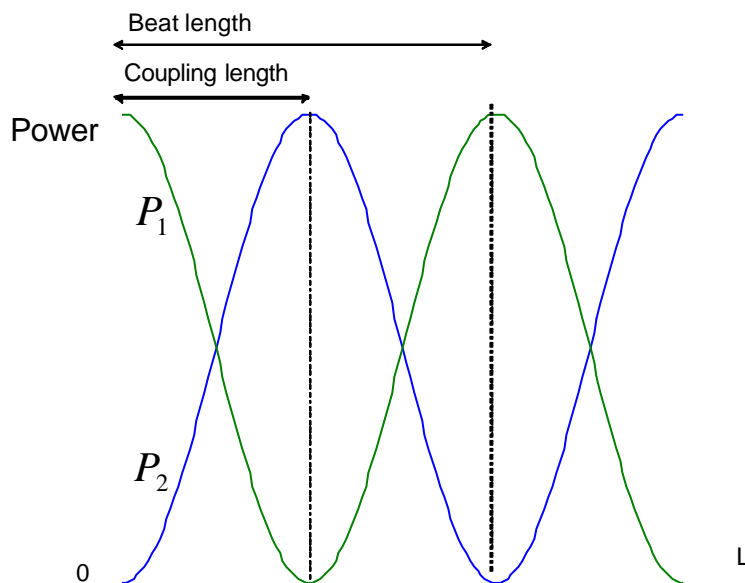


Fig. 2-2 Beat and Coupling length

Often the directional coupler can redistribute the powers in the two guides. For the sake of simplicity, we can define a new variable, transfer loss T , which stands for the ratio of power flowing to the other guide when only one guide mode is excited at the coupler head end. That is,

$$T = \frac{P_2(L)}{P_1(0)} = \text{Transfer Loss} \quad (2-12)$$

If, for example, $P_1(0)=1$ (all power initially in guide 1) and $T=1$ then all the power is transferred from guide 1 to guide 2. This will be called a full or zero-db coupler. If $P_1(0)=1$ and $T=1/2$, half the power is transferred from guide1 to guide 2. This will be called half or 3db couple. T can thus have any value from 0 to 1 and serves as a parameter to describe “conventional” mode interference couplers(MIC’ s).

If $\mathbf{b}_1 = \mathbf{b}_2$ (a matched coupler), $P_1(0)=1$, $N_A(0)=1/\sqrt{2} = -N_B(0)$, then from eq(2-11), it is seen that

$$P_1(z) = \cos^2(Cz)$$

and

$$P_2(z) = \sin^2(Cz)$$

so that $I_{b0} = \mathbf{p} / C$. The transfer loss is given by

$$T = \frac{P_2(L)}{P_1(0)} = \sin^2\left(\frac{\mathbf{p}L}{I_{b0}}\right)$$

To get a 3db coupler in this case, the coupler is made 1/4 of a beat length long while a full coupler is made 1/2 of a beat length long.

In general, when $\mathbf{b}_1 \neq \mathbf{b}_2$ if both modes are equally excited, so that $N_A(0) = -N_B(0) = 1/\sqrt{2}$, then from eq(2-11), it is seen that the power in the two guides becomes

$$P_1(z) = \frac{1}{2} + \frac{1}{\sqrt{M(z)^2 + 4}} \cos(2\Gamma z)$$

and

$$P_2(z) = \frac{1}{2} - \frac{1}{\sqrt{M(z)^2 + 4}} \cos(2\Gamma z) \quad (2-13)$$

Here we plot the transfer loss for several values of mismatch parameter, M. However, it can be seen from eq(2-13) that if $|M| \gg 1$, there is practically no power transfer,

$$\begin{aligned}
P_1(z) &= \frac{1}{2} + \frac{1}{\sqrt{M(z)^2 + 4}} \cos(2\Gamma z) \approx \frac{1}{2} \\
P_2(z) &= \frac{1}{2} - \frac{1}{\sqrt{M(z)^2 + 4}} \cos(2\Gamma z) \approx \frac{1}{2}
\end{aligned} \tag{2-14}$$

while if $|M| \ll 1$, there is practically complete periodic power transfer between the guides.

$$\begin{aligned}
P_1(z) &= \frac{1}{2} + \frac{1}{\sqrt{M(z)^2 + 4}} \cos(2\Gamma z) \approx \frac{1 + \cos(2Cz)}{2} = \cos^2(Cz) \\
P_2(z) &= \frac{1}{2} - \frac{1}{\sqrt{M(z)^2 + 4}} \cos(2\Gamma z) \approx \frac{1 - \cos(2Cz)}{2} = \sin^2(Cz)
\end{aligned} \tag{2-15}$$

which return to the case of identical waveguides.

The conventional couplers as we know are very sensitive to frequency, device length and polarization etc. Sensitive to frequency means the device will not work over a large frequency band, and sensitive to device length tell us we can't accurately expect the performance of the coupler cause of the fabrication process. And the last polarization is also important cause it always introduce extra phase delay such will disturb the signal's pulse shape. By adding more coupling elements and by means of an ingenious variation of the strength of the coupling. Papers have shown that the bandwidth may be increased, although there is a fundamental limit to the bandwidth obtained by such schemes.

2.3 Quasi (Local)-Normal modes In Tapered Coupled Waveguides

In this subsection we start to describe the quasi-normal modes in adiabatic couplers. We must say there exists no normal modes in non-uniform waveguides but as the title implied there exist quasi-normal modes instead. The word "quasi" is easy to understand that it means some quantity change very slow so we can assume it is still a constant. Here the slowly varying parameter is the phase constant or the coupling coefficient. If it changes sufficiently slow, we can assume it be a constant and the quasi-normal modes exist now. The following work we will focus on the coupler whose composite guides are function of z in phase constants, $\mathbf{b}_{1,2}(z)$, or the coupling coefficient, $C(z)$.

In order to see what restrictions must be placed on the variations of \mathbf{b}_1 , \mathbf{b}_2 , and

C, consider the following. For symmetry, assume the variation of \mathbf{b}_1 and \mathbf{b}_2 with z can be expressed by

$$\begin{aligned} \mathbf{b}_1 &= \mathbf{b} - \mathbf{d}(z) \\ \mathbf{b}_2 &= \mathbf{b} + \mathbf{d}(z) \\ C &= C(z) \end{aligned} \tag{2-16}$$

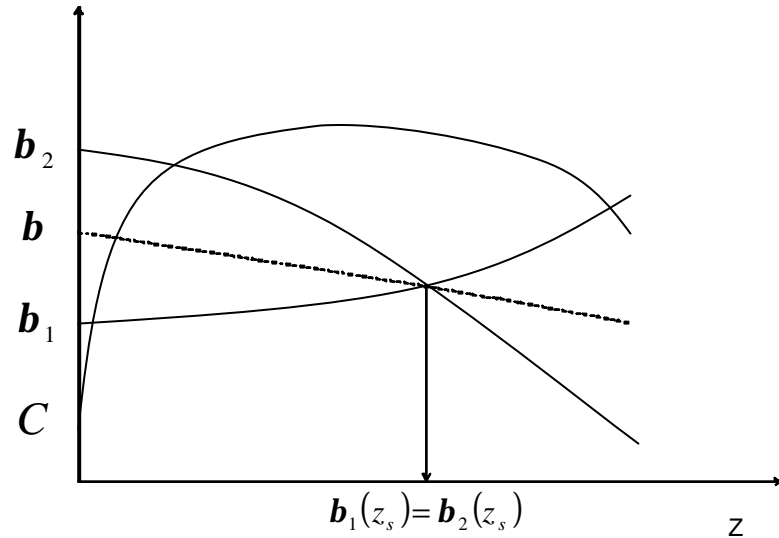


Fig. 2-3(a) Variation of the phase constant \mathbf{b} and coupling coefficient C

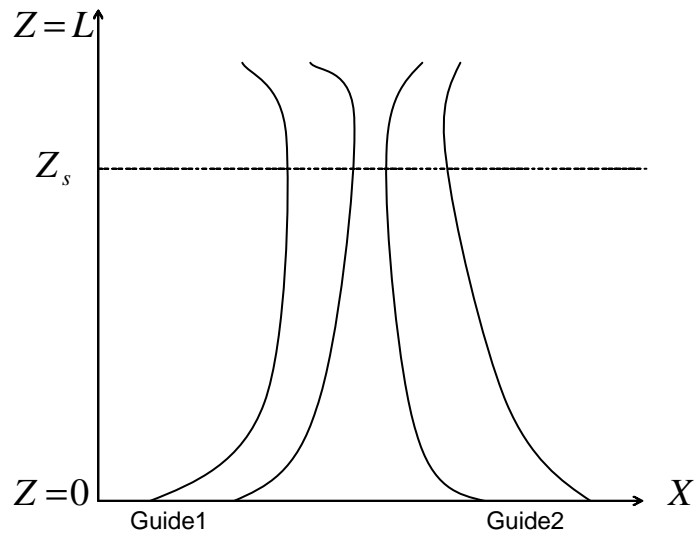


Fig. 2-3(b) The corresponding waveguide layout of (a)

where $\mathbf{b} = \text{constant}$ and $\mathbf{d}(0) \geq 0$. The equations for the wave amplitudes in the two guides are given by eq(2-1) with \mathbf{b}_1 , \mathbf{b}_2 , and C given by eq(2-16). As the same treated

in eq(2-1) with normal coordinates, here we introduce the local normal coordinates $N_A(z)$ and $N_B(z)$. The local normal coordinates are related to $A_1(z)$ and $A_2(z)$ by

$$\begin{aligned} A_1(z) &= \exp\left(-j\left[\mathbf{b}z + \int_0^z c(z')dz'\right]\right) \left\{ \cos\left(\frac{1}{2}\mathbf{q}(z)\right)N_A(z) - \sin\left(\frac{1}{2}\mathbf{q}(z)\right)N_B(z) \right\} \\ A_2(z) &= \exp\left(-j\left[\mathbf{b}z + \int_0^z c(z')dz'\right]\right) \left\{ \sin\left(\frac{1}{2}\mathbf{q}(z)\right)N_A(z) + \cos\left(\frac{1}{2}\mathbf{q}(z)\right)N_B(z) \right\} \end{aligned} \quad (2-17)$$

where all symbols are defined by eq(2-3) but where it is to be understood that Γ , \mathbf{d} , C and \mathbf{q} are now functions of z . Then, substituting eq(2-17) into eq (2-1) where C , \mathbf{b}_1 and \mathbf{b}_2 have the form of eq(2-16), we find after simple manipulation that N_A and N_B must satisfy

$$\begin{aligned} \frac{dN_A}{dz} - j\Gamma(z)N_A &= \frac{1}{2} \frac{d\mathbf{q}}{dz} N_B \equiv -C_{AB}N_B \\ \frac{dN_B}{dz} + j\Gamma(z)N_B &= -\frac{1}{2} \frac{d\mathbf{q}}{dz} N_A \equiv C_{AB}N_A \end{aligned} \quad (2-18)$$

where $C_{AB} = \frac{-1}{2} \frac{d\mathbf{q}}{dz} = \frac{1}{2(1+M^2)} \frac{dM}{dz}$

The difference of eq(2-4) and eq(2-18) is the coupling term in the right hand side of eq(2-18). If \mathbf{q} or M is constant along the guides, eq(2-18) will return to eq(2-4) which describes a uniform coupler. Since it is belong to the mode interference couplers and had been discussed in preceding section, we are not going to consider it here. It is clear, then, that there will be some coupling between quasi-normal modes in a tapered mode coupler. Such coupling between quasi-normal modes will be called ‘‘hypercoupling’’ to distinguish it from ordinary modal coupling between two waveguides (as represented by the parameter C). A ‘‘hypercoupling coefficient’’ $\mathbf{h}(z)$ may be defined by

$$\mathbf{h}(z) = \frac{1}{2\Gamma(z)} \frac{d\mathbf{q}}{dz} = \frac{-C_{AB}(z)}{\Gamma(z)} \equiv \frac{1}{2} \frac{d\mathbf{r}}{dz} \quad (2-19)$$

which gives a measure of the strength of the coupling between the quasi-normal modes.

In order for the quasi-normal modes have very little hypercoupling, we would like to make the hypercoupling coefficient very small. That is $\mathbf{h}(z) \ll 1$, which equals to

$$l_b \frac{dq}{dz} \ll 2p \quad (2-20)$$

where $l_b = \frac{p}{\Gamma(z)}$ is the local beat length in the coupler.

So the variation of q with respect to z must be slow enough compared to the local beat length. When eq(2-20) had been achieved, there will be a negligible change in the power of the local normal modes. We can then write down approximate solutions of eq(2-18) which proceed essentially in powers of the hypercoupling coefficient. Thus the In- Phase Quasi-Normal Mode is given approximately by

$$N_A(z) \cong e^{jr(z)} \left(N_A(0) + \frac{1}{2} N_B(0) \int_0^z \frac{dq}{dz'} e^{-2jr(z')} dz' - \frac{1}{4} N_A(0) \int_0^z \frac{dq}{dz'} e^{-2jr(z')} \int_0^{z'} \frac{dq}{dz''} e^{2jr(z'')} dz'' dz' \right) \quad (2-21)$$

and the Out-of-Phase Quasi-Normal Mode by

$$N_B(z) \cong e^{-jr(z)} \left(N_B(0) - \frac{1}{2} N_A(0) \int_0^z \frac{dq}{dz'} e^{2jr(z')} dz' - \frac{1}{4} N_B(0) \int_0^z \frac{dq}{dz'} e^{2jr(z')} \int_0^{z'} \frac{dq}{dz''} e^{-2jr(z'')} dz'' dz' \right) \quad (2-22)$$

where

$$r(z) = \int_0^z \Gamma(z') dz' \quad (2-23)$$

If $dq/dz=0$, it is seen that these become the ordinary normal modes of eq(2-5).

2.4 Adiabatic Directional Couplers

The power in the two tapered guides [by eq(2-17)] is

$$P_1(z) = |A_1(z)|^2 = \cos^2 \left(\frac{q(z)}{2} \right) |N_A(z)|^2 + \sin^2 \left(\frac{q(z)}{2} \right) |N_B(z)|^2 - \sin(q(z)) \text{Re}(N_A(z)N_B^*(z)) \quad (2-24-a)$$

$$P_2(z) = |A_2(z)|^2 = \sin^2 \left(\frac{q(z)}{2} \right) |N_A(z)|^2 + \cos^2 \left(\frac{q(z)}{2} \right) |N_B(z)|^2 + \sin(q(z)) \text{Re}(N_A(z)N_B^*(z)) \quad (2-24-b)$$

Choosing $q(0)=0$, which means the two guides are completely uncoupled at the input end, we can write down the above two equations at the input end as

$$P_1(0) = |N_A(0)|^2$$

$$P_2(0) = |N_B(0)|^2$$

If at the input end the power only exists in guide 1, ie $P_1(0)=1$ and $P_2(0)=0$, only one of the quasi-normal modes will be excited under such condition, $N_A(0)=1$ and $N_B(0)=0$. And we can derive the dynamic power flow in the two guides as

$$P_1(z) = \cos^2\left(\frac{1}{2}\mathbf{q}(z)\right)\{1+v(z)\} + \sin^2\left(\frac{1}{2}\mathbf{q}(z)\right)\mathbf{m}(z) + \sin(\mathbf{q}(z))\Delta(z) \quad (2-25-a)$$

$$P_2(z) = \sin^2\left(\frac{1}{2}\mathbf{q}(z)\right)\{1+v(z)\} + \cos^2\left(\frac{1}{2}\mathbf{q}(z)\right)\mathbf{m}(z) - \sin(\mathbf{q}(z))\Delta(z) \quad (2-25-b)$$

where

$$\begin{aligned} \mathbf{m}(z) &= \frac{1}{4} \left| \int_0^z \frac{d\mathbf{q}}{dz'} e^{2j\mathbf{r}(z')} dz' \right|^2 = \left| \int_0^z C_{AB} e^{j \int_0^{z'} (b_A - b_B) dz''} dz' \right|^2 \\ v(z) &= -\frac{1}{2} \operatorname{Re} \left(\int_0^z \frac{d\mathbf{q}}{dz'} e^{-2j\mathbf{r}(z')} \int_0^z \frac{d\mathbf{q}}{dz''} e^{2j\mathbf{r}(z'')} dz'' dz' \right) = -\mathbf{m}(z) \\ \Delta(z) &= \frac{1}{2} \operatorname{Re} \left(e^{2j\mathbf{r}(z)} \int_0^z \frac{d\mathbf{q}}{dz'} e^{-2j\mathbf{r}(z')} dz' \right) \end{aligned} \quad (2-26)$$

Equation (2-25) holds when $h \ll 1$.

Since power must be conserved, we must have $\mathbf{m}(z) + v(z) = 0$. This requirement may easily be verified in the specific examples treated. If, furthermore, $\mathbf{d}(z)$ and $C(z)$ are chosen so that $\mathbf{q}(L) = \mathbf{p}$ (a full coupler), it is seen from eq(2-25) that power can be transferred almost completely from guide 1 in the in-phase quasi-normal mode to guide 2 in the same quasi-normal mode by exciting power in one line only. In fact, by eq(2-21) – (2-26) we have for a full coupler

$$\begin{aligned}
P_1(L) &= |N_B(L)|^2 = \mathbf{m}(L) \\
P_2(L) &= |N_A(L)|^2 = 1 + \nu(L)
\end{aligned} \tag{2-27}$$

where \mathbf{m} and ν are given in equation (2-26). Thus, $\mathbf{m}(L)$ gives a measure of the error involved in making a complete power transfer coupler of length L in which only the w_1 -mode is excited if $\mathbf{d}(z)$ and $C(z)$ are selected so that: (1) $\mathbf{h}(z) \ll 1$, all z , and (2) $\mathbf{q}(0) = 0$ and $\mathbf{q}(L) = \mathbf{p}$. Since $\mathbf{m}(L) = |N_B(L)|^2$, $\mathbf{m}(L)$ also gives a measure of the power in the initially nonexcited mode that is present at the end of the coupler. It is therefore appropriate to call it the ‘‘mode crosstalk’’. Since the input power in guides is redistributed through the almost unchanged quasi-normal mode, we call this kind of coupler as ‘‘adiabatic directional couplers’’ (ADCs’).

In addition, we can express the ‘‘mode crosstalk’’ $\mathbf{m}(L)$ in Fourier transform which we are more familiar [7].

$$\begin{aligned}
\mathbf{m}(L) &= \frac{1}{4} \left| \int_0^L \frac{d\mathbf{q}}{dz} e^{2j\mathbf{r}(z)} dz \right|^2 = \frac{1}{4} \left| \int_0^1 \left(\frac{d\mathbf{q}}{Lds'} \right) e^{j2L \int_0^{s'} \Gamma(s'') ds''} (Lds') \right|^2 = \frac{1}{4} \left| \int_0^1 \frac{d\mathbf{q}}{ds'} e^{juL} ds' \right|^2 \\
&= \frac{1}{4} \left| \int_0^f \frac{d\mathbf{q}}{du} e^{iuL} du \right|^2
\end{aligned} \tag{2-28}$$

where $u(s') = 2 \int_0^{s'} \Gamma(s'') ds''$,

$$f = u(1)$$

we can see that the crosstalk related to length L is proportional to the square of Fourier transform of $d\mathbf{q}/du$, so it provide a method to see its performance under any profiles if du/ds is not a complex form.

2.5 Broadband Aspect of Adiabatic Directional Couplers

With the developing of wavelength division multiplexing in fiber-optic communication system, insensitive to wavelength will be a necessary property of any device in the fiber links. For the coupler, the conventional MICs’ always cut as certain length of some designed transfer ratio but the length can only support only the

designed wavelength working properly. That is, almost all devices are wavelength dependent. We don't believe any coupler can completely independent of wavelength but the adiabatic coupler will work almost as that in the frequency band of communication usage, that is, 1.3um and 1.55um. For enlarge the capacity of fiber links, the OH^{-1} free fiber which flatten the peak near 1.45um might be used for more broadband WDM system. So here we present the ADCs' which working cover all the region from 1.29um to 1.7um well, their performance will be shown through the follow-up chapter.

Chapter 3

Analysis and simulation of adiabatic couplers

In general, a compromise must be made between bandwidth and length of tapered mode couplers. Several classes of tapered mode couplers will be considered to illustrate this. Maybe other variations of $\mathbf{d}(z)$ and $C(z)$ will eventually prove better than those considered here but until they are discovered we must be content with what we have. The ones illustrated here are chosen primarily for mathematical simplicity, but it will be shown that they should be useful for bandwidths of the order of 3:1, although physical length of no more than about three minimum local beat lengths are required. Three Classes of couplers will be considered which will be called, respectively, constant local beat length couplers, uniform single tapered mode couplers and the linearization of both widths and separation couplers. The first two cases are mainly from [3], and the third is from [19]. We provided several new profiles in the formal two and we got an exact numerical solution in case 3.

3.1 Case 1. Constant Local Beat Length Couplers

3.1.1 The crosstalk issue:

This case is characterized by

$$\Gamma(z) = \sqrt{\mathbf{d}^2(z) + C(z)} = \mathbf{p}/\mathbf{l}_{b0} = \text{cons tan } t. \quad (3-1)$$

The constraint we put is help simplifying the exponential term in the crosstalk formula.

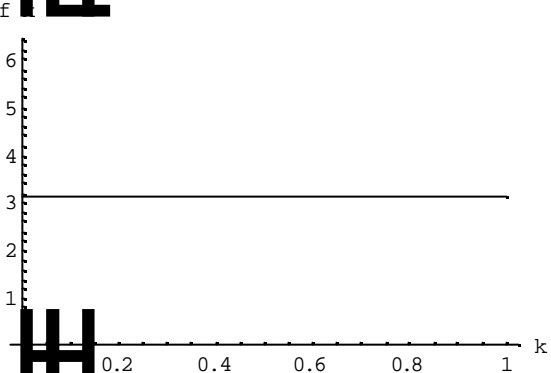
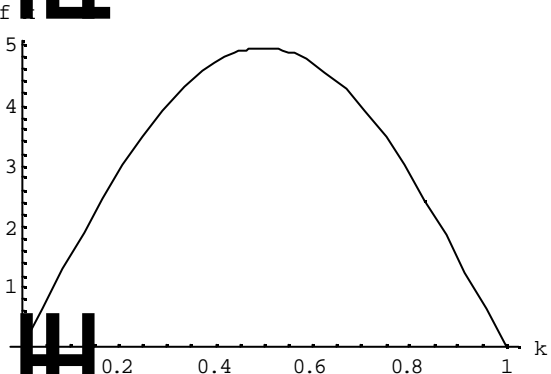
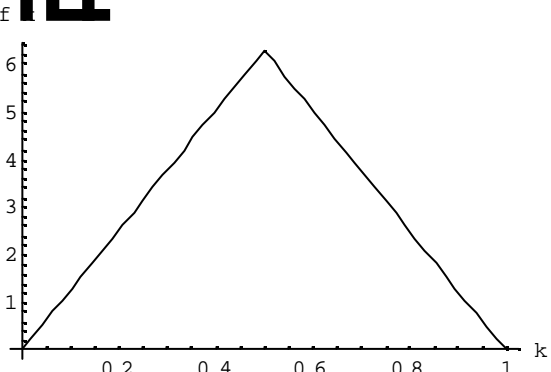
$$\mathbf{m} = \frac{1}{4} \left| \int_0^z \frac{d\mathbf{q}}{dz} e^{2j\Gamma(z)} dz \right|^2 = \frac{1}{4} \left| \int_0^k \frac{d\mathbf{q}}{dk} e^{j\frac{2pL}{l_{b0}}k} dk \right|^2$$
$$\mathbf{m}(k, D) = \frac{1}{4} \left| \int_0^k f(k') e^{j2pDk'} dk' \right|^2 \quad (3-2)$$

where $f(k) = \frac{d\mathbf{q}}{dk}$, $k = \frac{z}{L}$ and $D = \frac{L}{l_{b0}}$. This rewritten version of \mathbf{m} will help us

addressing all complex functions. From eq(2-27), we can see that it is Fourier Transform like formula if $k=1$ and $f(k)$ is zero outside the range $1 \geq k \geq 0$. We can say the crosstalk at the ends of guides $\mathbf{m}(1, D)$ is the ‘‘Frequency Domain’’ of $f(k)$. In

order to get the better performance, that is, the minimum crosstalk(m) and the shortest device length (D), we should select some profiles of $f(k)$ which have narrower mainlobe and smaller sidebands to let the coupler can achieve the desired crosstalk at shorter length.

But what kind of functions exhibit this property discussed above? The paper in [3] had proposed three profiles to comparison, had claimed the Raised_cosine function performs the best. For here, we just retain them and provide another three profiles to comparison their crosstalk between theoretical and BPM simulation and the broadband performance. The following table shows the six profiles.

Profiles $f(k)$	Plot $f(k)$
(a) $f(k) = p$	
(b) $f(k) = \frac{p^2}{2} \sin(pk)$	
(c) $f(k) = \begin{cases} 4pk & 1/2 \geq k \geq 0 \\ 4p(1-k) & 1 \geq k > 1/2 \end{cases}$	

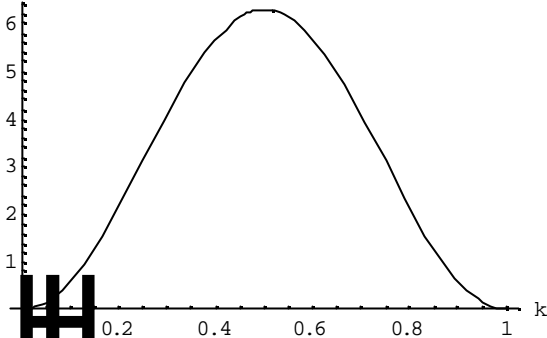
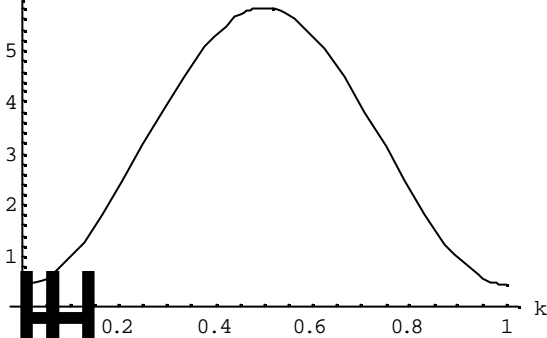
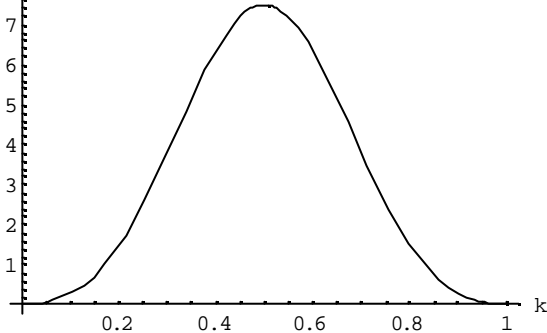
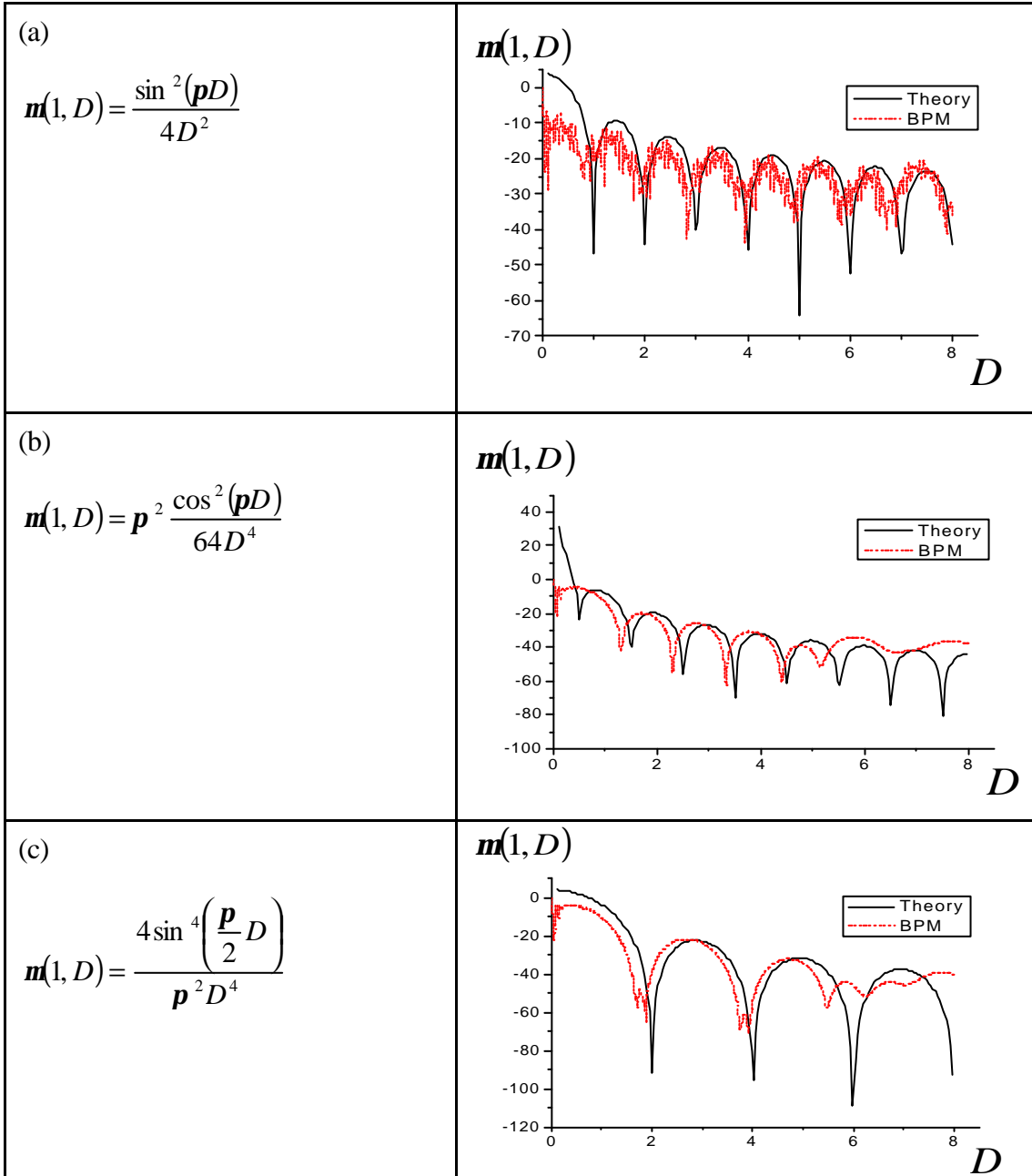
<p>(d) $f(k) = p(1 - \cos(2pk))$</p>	
<p>(e) $f(k) = p(1 - 0.852 \cos(2pk))$</p>	
<p>(f) $f(k) = p(1 - 1.19 \cos(2pk) + 0.19 \cos(4pk))$</p>	

Table 3-1 Functions and profiles of f(k)

The profiles (a),(b)and (d) is presented in [3], others are provided here. In fact, there have been exist some profiles which can minima the sidelobes developed in DSP, The digital signal processing, in which the profiles are used in the windowing of digital filter design. For example, Fig. 3-1 is a low pass filter. One can divide it into three parts as (A)Pass band, (B)Transition band, (C)Stop band. As you see in Fig. 3-1, there exists ripples in the edge of Pass band, this is caused by sidelobes of Fourier transform of windowing function. And we often hate the region of transition band, which is better as short as it can. That is affected directly by the width of main lobe of Fourier Transform of windowing function. So for an ideal filter we must use a profile which exhibit narrower main lobe and smaller side lobes, there are four profiles

famous in DSP design. That is, Hanning, Hamming, Blackman, and the last Kaiser functions. The profiles (d), (e), (f) are corresponding to Hanning, Hamming, Blackman functions. The Kaiser is too complex to addressed, so we drop it here for simplicity.

Next we show the plots of mode crosstalk at the guide ends $m(1, D)$ related to the device length D . Note that the theoretical prediction only correct when $D \gg 1$.



<p>(d)</p> $m(1, D) = \frac{\sin^2(pD)}{4D^6}$	
<p>(e)</p> $m(1, D) = \frac{p^2(a - bD^2)^2 \sin^2(pD)}{D^6}$ <p>$a = 0.159155$ $b = 0.0235549$</p>	
<p>(f)</p> $m(1, D) = \frac{p^2(p - qD^2)^2 \sin^2(pD)}{D^6(D^4 - 8D^2 + 16)}$ <p>$p = 0.636618$ $q = 0.0684366$</p>	

Table 3-2 Functions and profiles of output crosstalk

The BPM simulation results will be discussed in the next subsection.

From the theory of crosstalk prediction, we can say the profile(d), (e), (f) are all have small sidebands indeed. The side lobes in profile(d) are decreasing with D, and profile(e) has nearly equal sidelobes excepting the second. The profile(f) had the smallest sidelobes, but it has a wider main lobe that will make it need longer length to reach the first sidelobe. But once it reaches the sidelobe region, it really exhibits pretty small crosstalk. So we can say that if the crosstalk constraint were not so strict, smaller than -40dB, profiles(d)and (e) are prefer; if strict, the profile (f) might be a better choice.

And we also interested in the variation of crosstalk through the length given device to help observe the dynamic power flow in the two guides. We have knew that

the crosstalk is correct under the condition of $D \gg 1$ and crosstalk will be smaller when length is longer, we will compare these profiles at three device length, $D = 2$, to see if the prediction made by eq(2-27) will be distortion a lot; $D = 3.5$, to be a normal one to compared to $D = 6$ to see if longer length will get a better performance.

In Fig. 3-2, we can observe the crosstalk is zero at the beginning of the couplers. Excepting crosstalk in profile(a), which behave as sinusoidal variation along the coupler, others are all nearly increasing in the foresection and decreasing in the back section. It will falls at the ends of the level computing in Table 3-2. We also can judge that the maximum crosstalk along the couplers will decrease with the longer device length D . Another important point will be highlighted in next subsection of BPM simulation.

Knowing the variation of crosstalk along the couplers can help us confer the dynamic power flow in the coupler. From eq(2-25) we can predict the power flowing in guides, we add the BPM simulation here for comparison with the theoretical model . Also three device length are discussed, the same as above, $D = 2, 3.5, 6$.

BPM simulation

Before we can proceed to compare theoretical model and the BPM simulation, the first thing essentially is to transform the mathematical model to a real device layout. In the case we have assumed that the local beat length be a constant, that is,

$$\Gamma(k) = \frac{P}{I_{b0}} \equiv \Gamma.$$

which is fixed through the coupler. But remember the relation in eq(2-3)

$$\Gamma(k) = \sqrt{d^2(k) + C^2(k)}.$$

we can write

$$d(k) = \frac{P}{I_{b0}} \cos q(k)$$

$$C(k) = \frac{P}{I_{b0}} \sin q(k) \tag{3-3}$$

So the phase constants and the coupling coefficients must obey the two functions given above. The six profiles are different on the parameter $q(k)$, which is the

integration of function $f(k)$ and the boundary conditions are considered, $q(0)=0$ and $q(1)=p$.

(a)	$q(k) = pk$
(b)	$q(k) = p \sin^2\left(\frac{p}{2}k\right)$
(c)	$q(k) = \begin{cases} 2pk^2 & 1/2 \geq k \geq 0 \\ 2p(2k - k^2) & 1 \geq k > 1/2 \end{cases}$
(d)	$q(k) = p\left(k - \frac{1}{2p} \sin(2pk)\right)$
(e)	$q(k) = p\left(k - \frac{0.852}{2p} \sin(2pk)\right)$
(f)	$q(k) = p\left(k - \frac{1.19}{2p} \sin(2pk) + \frac{0.19}{4p} \sin(4pk)\right)$

Table 3-3 Functions of $q(k)$

And the corresponding plots of $q(k)$ are shown in Fig. 3-3

In this figure we observe the slope of profile(d) and (f) at both ends trend to zero, such a shape we will show you later that it gets better results in crosstalk and broadband applications.

And the corresponding functions $C(k)$ and $d(k)$ which are expressed normalized to $\frac{p}{I_{b0}}$ are shown in Fig. 3-4, where the I_{b0} is the minimum local beat length.

Here we select the minimum local beat length to be 2000um at 1.57um, $I_{b0} = 2000um$, and we are now ready to use all these parameters to design couplers. We have known that $d(k)$ is half the difference of the phase constants when waveguides are in isolation. We can change the refractive index or the widths of the waveguides along the propagation direction to satisfy $d(k)$, but the latter seems more

practical in real device so we will adopt it. We use the waveguide core index $n_{co}=1.544$, cladding index $n_{cl}=1.523$ to simulate the model. The next figure (Fig. 3-5) shows variations of effective index related to the waveguide widths.

Here we select the widths at the two ends of one waveguide starting at 5.52um and ending at 6.56um and the other waveguide starting at 6.56um and ending at 5.52um. These two values are selected in order to satisfy the boundary condition of

$$d(0) = -d(1) = \frac{P}{I_{b0}} = 1570.8. \text{ So we can get a pair of waveguides shown in Fig. 3-6.}$$

The coupler shown surely hadn't considered the variation of coupling coefficient $C(k)$. Due to the evanescent field is the exponential function of the distance away from the waveguide core, the $C(k)$ is approximately related to the gap function $G(k)$ as follow.

$$C(k) = Ae^{-(G(k)-G_0)}$$

where A and G_0 are constants.

So the gap of the two waveguides is proportional to $\log C(k)$, we can complete the overall device layout now.(see Fig. 3-7)

From the structure of real devices, we can further divide them into three groups:
Group1: (a) and (e), these two structures are bending seriously at the two ends. This group is proven higher loss and smaller bandwidth later.

Group2: (b) and (c), their ends are bending outward naturally

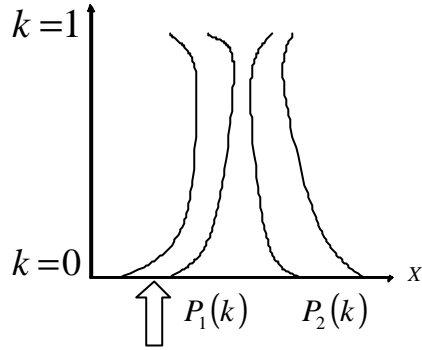
Group3: (d) and (f), Ends intend to extend parallelly with the propagation direction. This group is proven lower crosstalk and broader bandwidth later.

From eq(2-25), we can derive the dynamic power flow in the two guides.

$$P_1(k) = \cos^2\left(\frac{1}{2}q(k)\right)\{1 - m(k)\} + \sin^2\left(\frac{1}{2}q(k)\right)m(k) + \sin(q(k))\Delta(k)$$

$$P_2(k) = 1 - P_1(k)$$

we will compare it with those computed from BPM simulation at length of $D = 2, 3.5$ and 6 in Fig. 3-8. The power pumps into guide1 and we check the power in two guides through the coupler.



We found that the theoretical model and the BPM simulation results are matched more when length D increases. The reason is simple that the theoretical model only correct when $D \gg 1$. Another note is that the model tell us at some lengths the crosstalk will be reduced to zero, but we know it is impossible to reach such a good result due to the length needed is very critical. We must say there are some estimations when transforming the theoretical model to a BPM layout, the critical length of layout might randomly distribute with some variance around the exactly “zero“ place. The probability to choose such a exactly value is equal the one who choose some real number exactly in continuous domain, which is zero indeed. Another possible reason is the limit of the machine size value, each value computing is just an approximation.

We also found profile(a) has some quivers along the guides especially $D = 6$. The reason is the crosstalk in Fig. 3-2 exhibits sinusoidal variation, which quivers the dynamic power flow.

In Table 3-2 we had shown the BPM results of crosstalk versus D . We might find several things interesting. The fist, the apparent jitters on profile(a)and(e). Which is induced from the sharp bends at the ends of layouts in (a) and (e). Second, the phase terms are ignored automatically as D large enough, which can be seen from (b) to (f). The blurred phase in longer length possibly induced from the randomized factor existed in real device, longer device will suffer easier to the random factors. The last is the mismatched between the theoretical models and the BPM results in (d), (e), and (f). This is somehow like the case in DSP. If the functions used getting more complex, it will require the dimension of the device more critically. Such a critical requirement will distortion the real device layout.

We list all the data of crosstalk at the guide ends below in favor of comparisons.

Profiles	D value	Theoretical Crosstalk(dB)	BPM Simulation Crosstalk(dB)
(a)	2	-Inf	-22.4716
	3.5	-16.902	-19.5721
	6	-Inf	-30.7608
(b)	2	-19.5994	-23.7932
	3.5	-Inf	-35.2440
	6	-39.1843	-34.9464
(c)	2	-Inf	-37.7262
	3.5	-31.7057	-38.8535
	6	-Inf	-46.1206
(d)	2	-Inf	-28.7733
	3.5	-37.9250	-37.8671
	6	-Inf	-43.7462
(e)	2	-Inf	-42.7092
	3.5	-35.5658	-39.0795
	6	-Inf	-51.8233
(f)	2	-16.2777	-25.7150
	3.5	-54.1956	-40.0238
	6	-Inf	-50.3644

Table 3-4 Output crosstalk comparisons of case 1

3.1.2 The Broadband Issue

Another interesting point of adiabatic coupler is the really broadband characteristic. We now scan the wavelength from 1.29 to 1.7 μ m to observe its behavior. Let's begin with the shortest device length of 2D. Here we are not only to give you the information of crosstalk but also the loss, which is another important subject of a device.

D = 2

In Fig. 3-9(a), almost all profiles perform well at longer wavelength but decay at shorter wavelength. Even higher than 10dB crosstalk are occurred at 1.3 μ m band.

For the purpose of convenient comparison, we defined the bandwidth as the dimension of wavelengths in which the output power in guide 2 (see Fig. 3-9(b)) exceeds 98% of input power. That is, the bandwidth is defined as the band when power P_2 exceeds -0.0877dB.

From Fig 3-9(b) we can get their bandwidth in Table 3-5.

Profiles	Bandwidth(nm)
(a)	0
(b)	0
(c)	0
(d)	176
(e)	0
(f)	164

Table 3-5 Bandwidths of each profile in case 1, D = 2

Only profile(d) and (f) have bands satisfy the requirement of the definition of bandwidth. Length limits their performance.

Now we proceed to see their loss aspects. We defined the loss as

$$Loss = 10 * \text{Log} \left(\frac{P_{1out} + P_{2out}}{P_{in}} \right)$$

and the average loss

$$Average_Loss = \frac{\sum_{i=1}^n Loss(i)}{n}$$

where n represents the number of wavelength scanned and i represents the index of wavelength scanned.

From Fig. 3-9(c) we can get Table 3-6.

Profiles	Max Loss(dB)	Location	Average Loss
(a)	-5.5247	1.648um	-3.3649
(b)	-0.6427	1.358um	-0.2950
(c)	-0.4975	1.37um	-0.2572
(d)	-0.0230	1.29um	-0.0049
(e)	-2.1225	1.29um	-0.6179
(f)	-0.0036	1.33um	-0.0012

Table 3-6 Loss comparisons of case 1, D =2

The ‘Location’ means the wavelength at which the maximum loss occurred.

Fig. 3-9(c) shows the loss of each device over the scan wavelength. It is expected the profiles (a) and (e) are higher loss devices since they bend sharply at the two ends. (Fig. 3-7) In addition to broader bandwidth, profile(d)and(e)are almost lossless devices.

To sum up the graphs shown above, profile (d) might perform best in both the bandwidth and loss considerations. And for profiles (a), it is the worst one in both bandwidth and loss. In profile (e) it is expected to perform well in theoretical prediction but is high loss device, too. The reason is that in the theoretical model it doesn’ t consider the bending effect that profile (e) has, the real model should consider both of them. We also show performance of $D= 3.5$ and $D = 6$ to see if any effect will be induced when the length are changed. .

D = 3.5

Now we add the sequence column in bandwidth table for convenient comparison.

From Fig. 3-10(b) we get the bandwidth in Table 3-7

Profiles	Bandwidth(nm)	Sequence
(a)	0	6
(b)	80	4
(c)	52	5
(d)	288	1
(e)	140	3
(f)	260	2

Table 3-7 Bandwidths of each profiles in case 1, D = 3.5

The length had changed to 7000um from 4000um, and it is clear that all the bandwidth become larger in Table3-7. Larger bandwidth of Profile(a) can also be seen through Fig. 3-10(b)). The first and the second are the same as the case in $D =2$. And the others are still less compared to the first two profiles.

For the loss aspect we get Table 3-8 from Fig. 3-10(c)

Profiles	Max Loss(dB)	Location	Average Loss
(a)	-7.2812	1.352um	-2.1762
(b)	-0.1693	1.302um	-0.0968
(c)	-0.1214	1.31um	-0.0750
(d)	-4.7377e-004	1.29um	-2.3126e-004
(e)	-1.3796	1.404um	-0.4161
(f)	-1.9706e-004	1.644um	-9.8625e-005

Table 3-8 Loss comparisons of case 1, D = 3.5

It is apparent that all the average loss are much reduced.

D = 6

We get their bandwidth in Table 3-9 from Fig. 3-11(b).

Profiles	Bandwidth(nm)	Sequence
(a)	0	6
(b)	410	1
(c)	266	4
(d)	388	2
(e)	150	5
(f)	356	3

Table 3-9 Bandwidths of each profile in case 1, D =6

Now the broadest one is changed to profile (b), which covers all scanning wavelength from 1.29 to 1.7um sustaining P_2 exceeds 98%. Profiles (d) is listed second and profile (f) is closely followed it. Profile (e), which is disappointed to us, just enhances 10 nm after being lengthened to 1.2cm, is surpassed by (c) easily. Profile (a) is still the last.

We get Table 3-10 from Fig. 3-11(c).

Profiles	Max Loss(dB)	Location	Average Loss
(a)	-5.1233	1.296um	-1.7777
(b)	-0.0286	1.292um	-0.0124
(c)	-0.0737	1.402um	-0.0204
(d)	-8.2157e-004	1.532um	-2.6200e-004

(e)	-0.8078	1.338um	-0.2750
(f)	-0.0021	1.532um	-5.0275e-004

Table 3-10 Loss comparisons of case 1, D = 6

After giving these figures, we can say that in this case there is no exception that longer length of the some profile can get broader bandwidth.

3.2 Case 2. Uniform Tapered Mode Couplers

3.2.1 The Crosstalk Issue

This case also follows the constraint of [3], which hold the hypercoupling coefficient be a constant through the coupler, that is

$$\mathbf{h}(k) = \frac{1}{2} \frac{d\mathbf{q}}{d\mathbf{r}} = p \quad (3-4)$$

where

$$p = -\frac{1}{L \int_0^1 C(\mathbf{V}) d\mathbf{V}} \quad (3-5)$$

is a constant. Which is the integration of C(z) over the device. In order for the weakly hypercoupling requirement is satisfied, $p \ll 1$.

For couplers to satisfy (2-22), it can be shown that $\mathbf{d}(k)$ and $C(k)$ must be related by

$$M(k) = \frac{\mathbf{d}(k)}{C(k)} = \frac{1 - 2\mathbf{s}(k)}{2\sqrt{\mathbf{s}(k) - \mathbf{s}^2(k)}} \quad (3-6)$$

where

$$\mathbf{s}(k) = \frac{\int_0^k C(\mathbf{V}) d\mathbf{V}}{\int_0^1 C(\mathbf{V}) d\mathbf{V}} \quad (3-7)$$

We again face the problem of mode crosstalk, that is

$$\mathbf{m}(k, D) = \frac{1}{4} \left| \int_0^k \frac{d\mathbf{q}}{dk'} e^{j2r} dk' \right|^2 = p^2 \sin^2(\mathbf{r}(k)) \quad (3-8)$$

From eq(2-3),and eq(2-18)

$$\Gamma = \sqrt{\mathbf{d}^2 + C^2} = C\sqrt{M^2 + 1} = \frac{C}{2} \sqrt{\frac{1}{\mathbf{s} - \mathbf{s}^2}}$$

$$\mathbf{r}(k) = L \int_0^k \Gamma(k') dk' = \frac{-1}{2p} \int_0^{\mathbf{s}(k)} \sqrt{\frac{1}{\mathbf{s}(k') - \mathbf{s}^2(k')}} d\mathbf{s}(k')$$

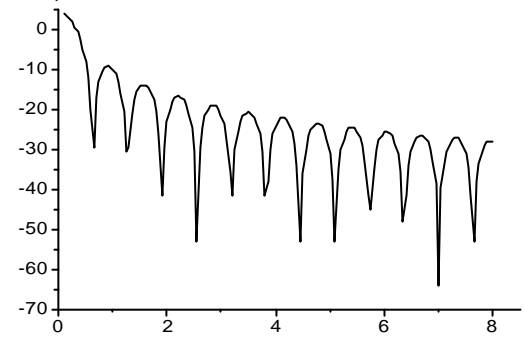
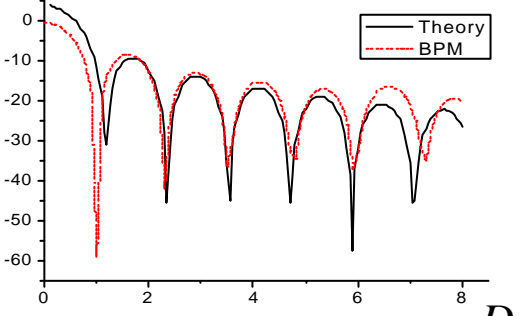
$$= \frac{-1}{2p} \sin^{-1}(1 - 2s(k')) \Big|_0^s(k)$$

where we have used the relation of $\frac{ds}{dk} = \frac{C(k)}{\int_0^1 C(k') dk'}$.

We can rewrite eq(32) as

$$m(k, D) = p^2 \sin^2 \left(\frac{\frac{p}{2} - \sin^{-1}(1 - 2s(k))}{2p} \right) \quad (3-9)$$

Here we provide four profiles.

Profiles	$m(1, D) = p^2 \sin^2 \left(\frac{-p}{2p} \right)$
(a) $C = \frac{p}{I_{b0}}$	$m(1, D)$ 
(b) $C(k) = \frac{p}{1.852 I_{b0}} (1 - 0.852 \cos(2pk))$	$m(1, D)$ 

<p>(c)</p> $C = \frac{p}{I_{b0}} e^{-t \left(k - \frac{1}{2} \right)^2}$ <p>$t = 10.1072$</p>	
<p>(d)</p> $C = \begin{cases} c_2 + mk & k \leq t \\ c_1 & t < k < 1-t \\ -m(k+t-1) + c_1 & 1-t \leq k \end{cases}$ <p>where</p> $c_1 = \frac{p}{I_0}$ $c_2 = 0.08 \frac{p}{I_0}$ $t = 0.430633$ $m = \frac{c_1 - c_2}{t}$	

Table 3-11 Functions of coupling and profiles of crosstalk

The BPM simulation results will be covered in the next subsection.

The crosstalk between profiles(b) and (c) are hard to differentiate because their p values are almost the same, see Fig. 3-12.

The crosstalk at the output of the coupler can be written as

$$m(1, D) = p^2 \sin^2 \left(\frac{-p}{2p} \right) = \frac{\sin^2 \left(\frac{p}{2} L \int_0^1 C(k) dk \right)}{\left(L \int_0^1 C(k) dk \right)^2} \quad (3-10)$$

Which told us its envelope is proportional to the inverse of the square of integration of $C(k)$ along the guides.

Since the hamming and the Gaussian profiles are nearly overlay, almost the

same area below the $C(k)$ can be imagined. So we can expect their performance of crosstalk and performance will be very alike.

As treated in case 1, we now consider the crosstalk through the guides when device lengths are given, D is known. Three values are provided here for comparison, $D = 2, 3.5, 6$. (In Fig. 3-13)

From Fig. 3-13 we observe that they have more than one maximum as in case 1 (excepting profile(a) in case 1), and the local maximum increases as D increases. Which a phenomenon will quiver all dynamic power flow, as case 1(a).

We also found that the peak value of crosstalk decreases as D increases.

Next we consider the real device layout.

BPM Simulation

Before we can start our layout to simulate, we need two parameters, $C(k)$ and $d(k)$.

The $C(k)$ we have known since its our choice, it seems simple the other one can be derived from eq(3-6). However, we find the values of $M(k)$ are positive and negative infinity at the guide ends. We can't use it without further reform.

In order to make the boundary values of $M(k)$ to be finite, we reform it below.

The original function,

$$M(k) = \frac{1 - 2s(k)}{2\sqrt{s(k) - s^2(k)}} = \frac{2\left(\frac{1}{2} - s(k)\right)}{\sqrt{1 - 2^2\left(\frac{1}{2} - s(k)\right)^2}} \quad (3-11)$$

Now we use a unknown to replace "2".

$$M(k) \cong \frac{a\left(\frac{1}{2} - s(k)\right)}{\sqrt{1 - a^2\left(\frac{1}{2} - s(k)\right)^2}} \quad (3-12)$$

For here we assume the boundaries of the two ends $M(0) = 10$ and $M(1) = -10$, respectively, and $a = \frac{20}{\sqrt{101}}$ can be derived directly. Profile of $M(s)$ is shown in Fig.

3-14

Now we can derive the $d(k)$ directly from eq(3-6) and its variation is plotted in Fig. 3-15.

Here we select the same parameters as case 1,

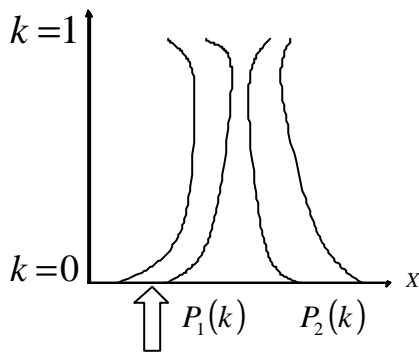
Minimum local beat length	$l_{b0} = 2000\mu m$
Waveguide Core Index	$n_{co} = 1.544$
Waveguide Cladding Index	$n_{cl} = 1.523$
Testing Wavelength	$\lambda = 1.57\mu m$

Table 3-12 Simulation parameters of case 2

We can get the device layout in Fig. 3-16. We can see the widths of the first profile changed from 2 μm to 10 μm , which a variation must leave the guide away from single mode and additional terrible loss. We will discuss it only theoretically but not BPM simulation.

We also compare the dynamic power variations in guides between theoretical model and BPM simulation in Fig. 3-17. As in case 1 treated, three device lengths will be considered, $D = 2, 3.5, 6$.

The power pumps into guide1 and we check the dynamic power in two guides through the coupler.



From Fig 3-17 we do observe the quivers in all profiles, and we might judge that the model and BPM simulation will not match well when the local maximums increase in Fig. 3-13..

We can find that the BPM simulation results in Table 3-11 are well matched with the theoretical model. In fact only case 2 can match so perfect through this chapter, and that represents in this case those functions used to built the device layout is not as critical as the case 1.

We also give the output crosstalk of the three values of D in this case.

Profiles	D value	Theoretical Crosstalk(dB)	BPM Simulation Crosstalk(dB)
(a)	2	-18.7616	NaN
	3.5	-19.6762	NaN
	6	-21.9860	NaN
(b)	2	-13.3564	-12.8775
	3.5	-29.5406	-34.0912
	6	-22.3619	-34.1155
(c)	2	-13.7311	-13.2864
	3.5	-27.2500	-43.2208
	6	-21.4461	-29.3768
(d)	2	-28.0485	-24.4709
	3.5	-15.9621	-16.1489
	6	-24.3844	-16.3809

Table 3-13 Output crosstalk comparisons of case 2

3.2.2 The Broadband Issue

In the subsection we scanned the three profiles using the same range from 1.29 to 1.7 μm as preceding case. And the definition of bandwidth and loss are the same as the preceding case.

D = 2

From Fig. 3-18(b) we get the bandwidth in Table 3-14. The line in Fig. 3-18(b) masked -0.877dB is just for the bandwidth measure.

Profiles	Bandwidth(nm)	Sequence
(b)	182	3
(c)	186	2
(d)	280	1

Table 3-14 Bandwidths of each profile in case 2, D = 2

Although the lengths of these devices are just 4000 μm , their bandwidths are larger than the ones in case 1. The first is profile (d), and the other two are almost the same.

From Fig. 3-18(c) we get the follow-up Table.

Profiles	Max Loss	Location	Average Loss(dB)
(b)	-0.0092	1.608um	-0.0028
(c)	-0.0099	1.602um	-0.0035
(d)	-0.0206	1.29um	-0.0035

Table 3-15 Loss comparisons of case 2, D = 2

All the three profiles exhibit pretty small loss. We can found that the loss even larger than zero near 1.7um, it means the power is enlarged through the device. That's surely impossible and the reason is probably limited by approximation of the beam propagation method.

D = 3.5

From Fig. 3-19(b) we get the bandwidth in Table 3-16.

Profiles	Bandwidth(nm)	Sequence
(b)	332	1
(c)	328	2
(d)	252	3

Table 3-16 Bandwidths of each profile in case 2, D = 3.5

The former champion has down to the last position in D =3.5 since there is a deep near 1.65um.

From Fig. 3-19(c) we get the device loss in Table 3-17

Profiles	Max Loss	Location	Average Loss
(b)	-0.0031	1.532um	0.0041
(c)	-0.0035	1.532um	0.0036
(d)	-0.0099	1.334um	5.3279e-004

Table 3-17 Loss comparisons of case 2, D = 3.5

The value of loss is not true but the trend might be right so we retain the results here. The loss are all reduced when length increases to D = 3.5, as is the same as case 1.

D = 6

From Fig. 3-20(b) we derived the Table 3-18.

Profiles	Bandwidth(nm)	Sequence
(b)	332	2
(c)	328	3
(d)	364	1

Table 3-18 Bandwidths of each profile in case 2, D = 6

Although profile (d) has large crosstalk near the band of 1.55um, but it perform better in the band of 1.6-1.7um and wins back. The others are exactly the same as in D =3.5. The broadband issue must consider all the bands but not only some critical wavelength, that is the job of the preceding crosstalk issue. Smaller crosstalk at some wavelength (1.57m) can not promise it can work over broader band. So there exists weakly relation between the results of Table 3-10 and all tables in this subsection.

From Fig. 3-20(c) the device loss are shown in Table 3-19(c).

Profiles	Max Loss	Location	Average Loss
(b)	-0.0011	1.54um	0.0040
(c)	-0.0013	1.53um	0.0036
(d)	-0.0037	1.628um	0.0011

Table 3-19 Loss comparisons of case 2, D = 6

Over the loss comparisons of this section, we can conclude profile(b) exhibits the lowest loss.

3.3 Case 3. Linearization of Device layout

3.3.1 The crosstalk issue

After following the preceding two cases, let's consider the constraint of linearization of the variation of widths and the separation of the two guides. Such a guide layout had been proposed in [19], which had provided an optimal design way. However, the process in that had ignored the phase terms and some mismatch between their models and the real device is expected. Here our job is to search the real optimal parameters without dropping the phase terms and compare the crosstalk among the two design ways

As fig. 3-21 shows, this kind of couplers can be divided into three regions. W is the widths of the guides, and G is the separation between the two guides, these two parameters both linearly vary with propagation distance. In order to get a clear picture

of the mode crosstalk in this case, we need consider the phase terms using eq(2-26)

$$\mathbf{m} = \frac{1}{4} \left| \int_0^k \frac{d\mathbf{q}}{dk} e^{j2\mathbf{r}(k')} dk' \right|^2 = \left| \int_0^k C_{AB}(k') e^{j2\mathbf{r}(k')} dk' \right|^2$$

where $C_{AB}(k) = \frac{1}{2(1+M^2)} \frac{dM}{dk}$, M is given as eq(2-3), $M = \frac{d}{C}$.

Now we define M_{10} and M_{20} , which are the asynchronicity parameters at the input of Region 1 and Region 2, respectively. Here we select $M_{10}=10$ and $M_{20}=0.8$ in order to let the C_{\max} (which is the value in Region 2, C_{20}) and C_{\min} (which is the value at the input of Region 1, C_{10}) to be the same as in case 2. We also denote the length of the Region “x” as $D_x = \frac{L_x}{I_{b0}}$, where the I_{b0} is the minimum local beat length. Here

we use the optimal design in [19] that

$$\mathbf{a}_{opt} = \frac{L_1}{L_2} = \frac{D_1}{D_2} = \left\{ \frac{1}{2 M_{20} (M_{20}^2 + 1)} \ln \left(\frac{M_{10}}{M_{20}} \right) \right\}^{\frac{2}{3}} = 0.97 \cong 1$$

So $D_1 = D_2 = D_3 = D/3$, which a ratio can minima the crosstalk under constant coupler length. Using all above parameters, we can plot the $C_{AB}(k)$ and $\mathbf{r}(k)$ and then integrate them using eq(2-26).(see Fig. 3-22)

Below (Fig 3-23) we show the relations between crosstalk, $\mathbf{m}_{phase}(1, D)$ and device length, D. And here we also draw the result of [19] for comparison, which is denoted as $\mathbf{m}_{envelope}(1, D)$. Since in [19] they didn't consider the phase term, they predict a higher crosstalk indeed and that is not a tight bound. And the BPM results in Fig. 3-23 will be discussed in latter subsection.

The following given (Fig. 3-24) is the dynamic crosstalk through the coupler. Two things are notable here. The one is the maximum of crosstalk decreases as D increases and the other is the number of peaks increases as D increases.

BPM Simulation

Almost through the same process as the preceding two cases, we get the device layout.

We here still use the wavelength of 1.57um to simulate the crosstalk.'

Minimum local beat length	$l_{b0} = 2000\mu m$
Waveguide Core Index	$n_{co} = 1.544$
Waveguide Cladding Index	$n_{cl} = 1.523$
Testing Wavelength	$\lambda = 1.57\mu m$

Table 3-20 Crosstalk simulation parameters of case 3

And the waveguide layout is drawn in Fig. 3-25. All parameters are the same as in case 2.

In Fig. 3-23, the variation of the crosstalk with the length is plotted. We found that the theory-phase included and BPM lines mismatch at longer device length. The line of BPM is apparently phase lead the theory one.

The following table compares the crosstalk of theoretical computing and BPM simulation. We can find that the phase included crosstalk not only more close to the BPM results but also predicts there is a peak near the length of $D=3.5$, which is impossible for the envelope prediction in the “without phase” crosstalk.

D value	Theoretical Xtalk(dB) (without phase)	Theoretical Xtalk(dB) (phase included)	BPM Xtalk(dB)
D = 2	-9.61	-29.12	-49.74
D = 3.5	-14.47	-19.354	-23.42
D = 6	-19.15	-31.56	-45.62

Table 3-21 Output crosstalk comparisons of case 3

Further Discussion

Does the “optimal” ratio a given in [19] really perform best result? We can change it to see if it is the one that exhibits the smallest mode crosstalk. Here we use BPM simulation to search the optimal a under different lengths.

The coming plot (Fig. 3-27(a)) shows that the theoretical prediction is well matched with the BPM simulation results if the device length is shorter than $D = 4.5$. But they start to mismatch when the length becomes longer.(Fig. 3-27(b)). In Fig. 3-27(b) we can see the difference is evident especially larger a . The reason of mismatch in longer device must be the random phase effect induced in device layout. Fortunately we often need a shorter device in real world so the theoretical model can still work correctly. No matter how the length of the device is, we found there is no fixed optimum length ratio existed. In [19], it is written as a form independent of device

length ($a = 1$ in this case) and now we prove this is not be true.

3.3.2 The Broadband issue

Here we focus on the comparison of bandwidths in different length. As the preceding cases treated, the bandwidth is defined as the power in guide2 exceeding 98% of input power at guide 1.

From Fig. 3-28(b) we get the following table.

Length	Bandwidth(nm)	Sequence
D = 2	302	3
D = 3.5	322	2
D=6	378	1

Table 3-22 Bandwidths of each profile in case 3

Longer device exhibits broader bandwidth. This has been proved again.

From Fig. 3-28(c) the loss are listed below.

Length	Max loss	Location	Average Loss
D = 2	-0.0204	1.700um	-0.0050
D = 3.5	-0.0068	1.700um	0.0010
D = 6	-0.0092	1.648um	-0.0015

Table 3-23 Loss comparisons of case 3



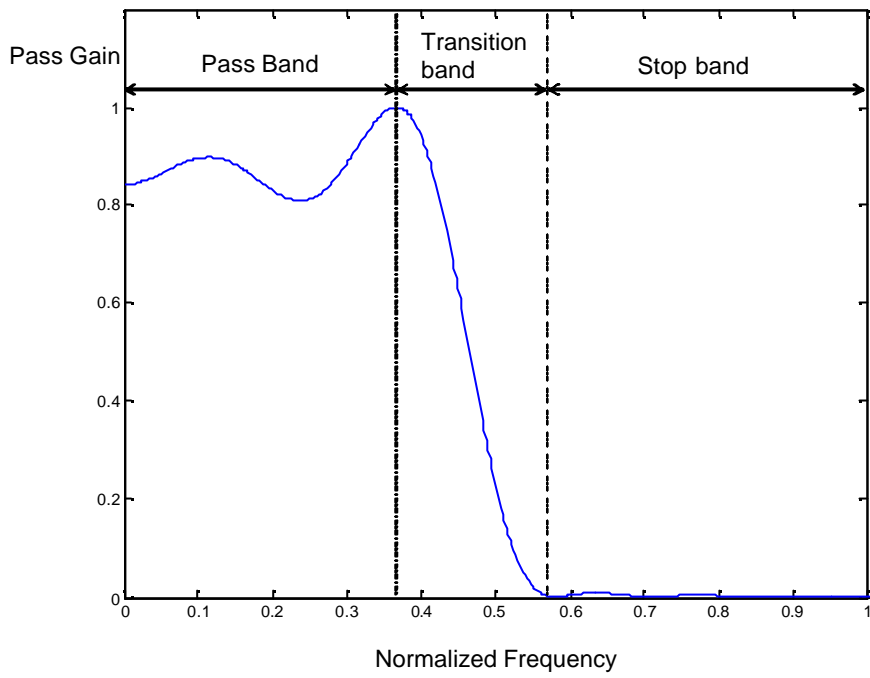


Fig. 3-1 A typical loss pass filter

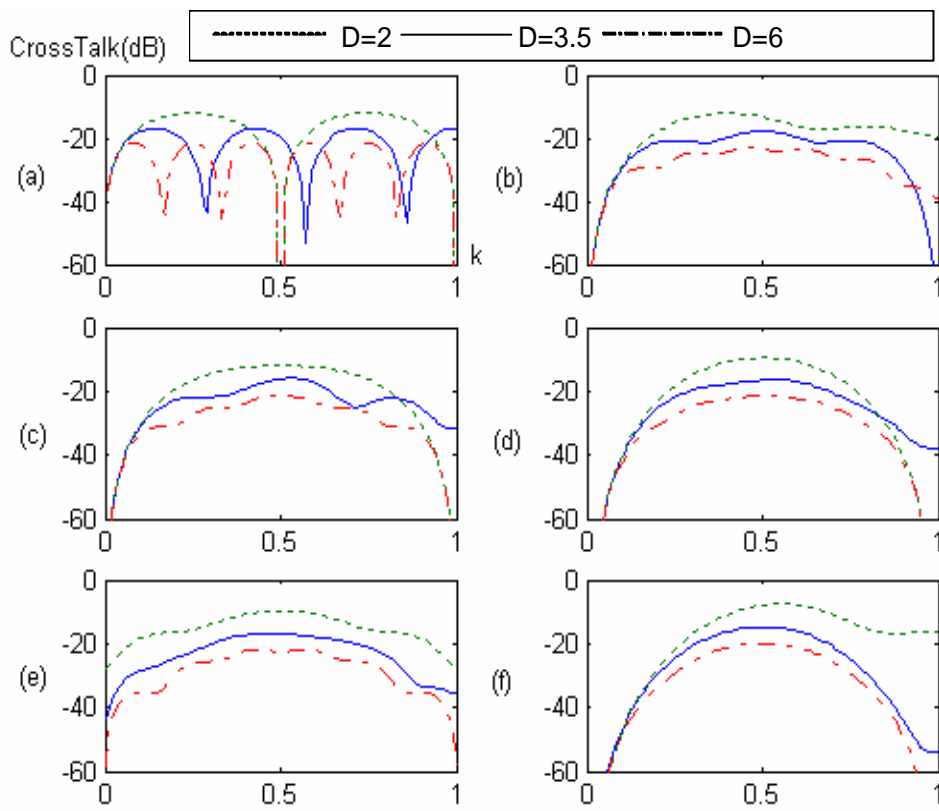


Fig 3-2 Dynamic crosstalk of case 1

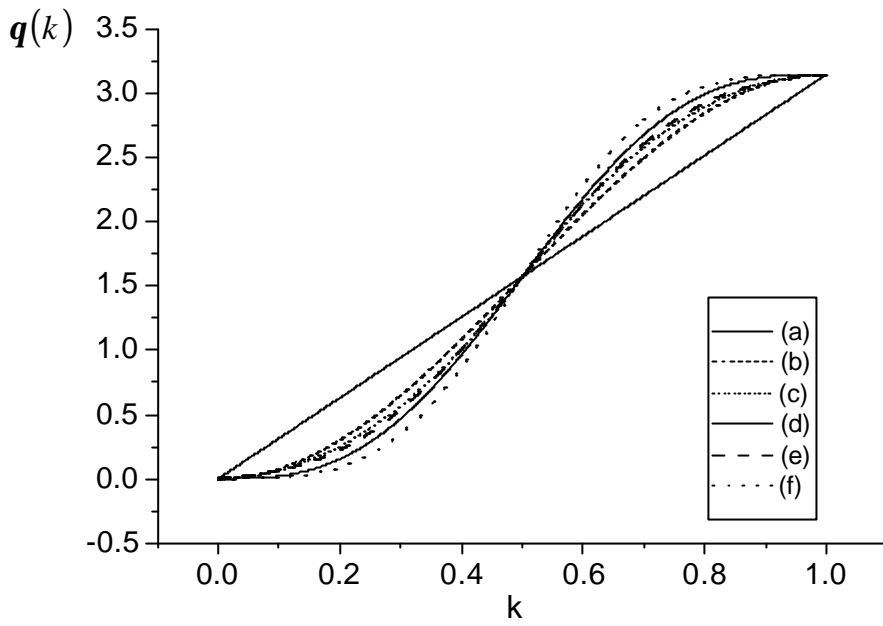


Fig. 3-3 Variations of $q(k)$ of case 1

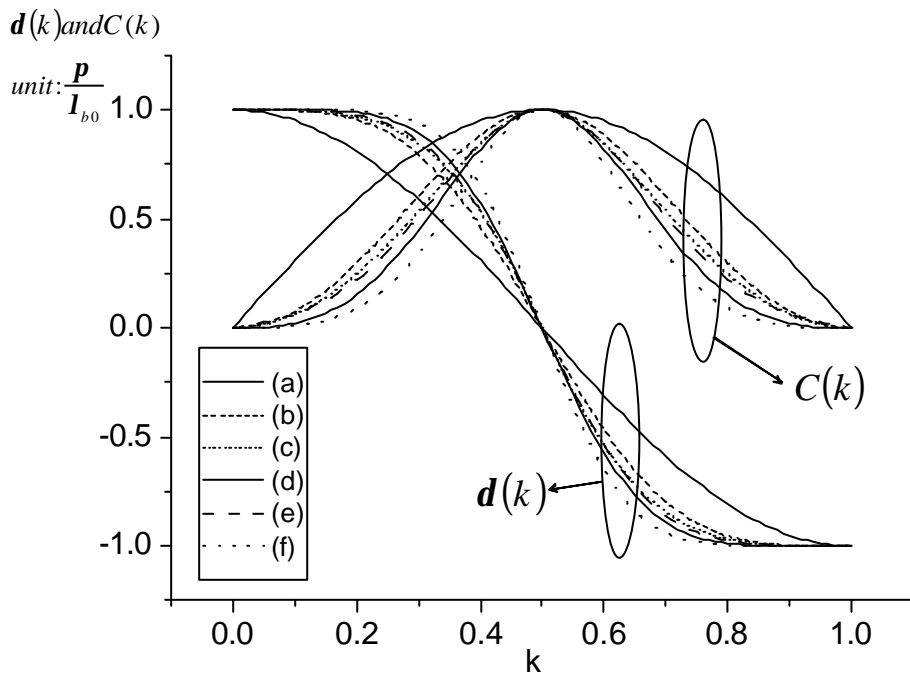


Fig. 3-4 Variations of $d(k)$ and $C(k)$ of case 1

Effective Index

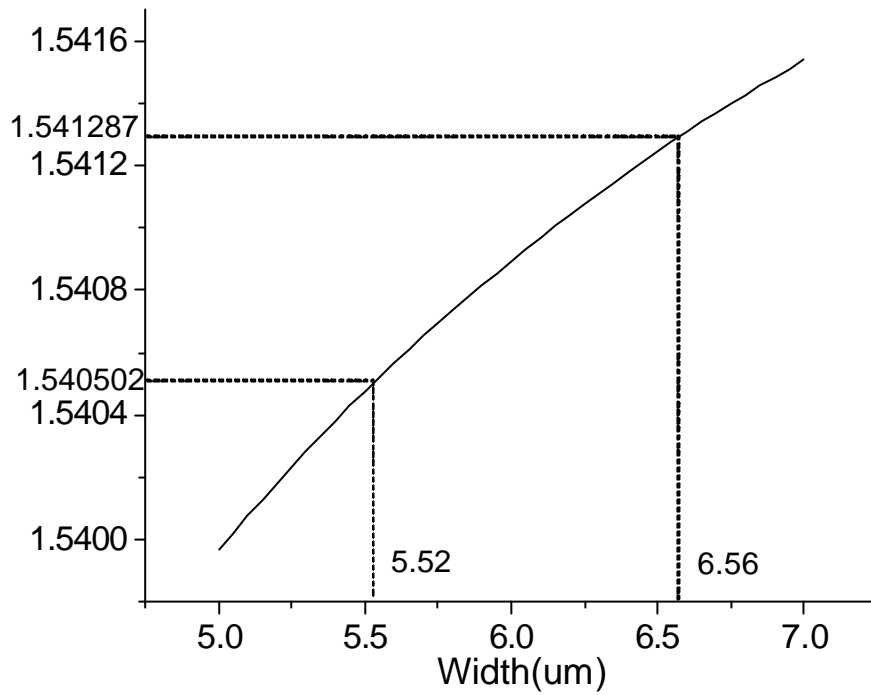


Fig. 3-5 Variation of effective index versus waveguide width

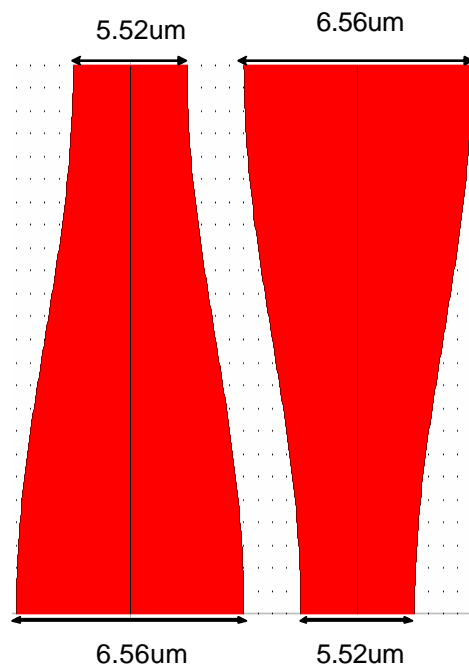
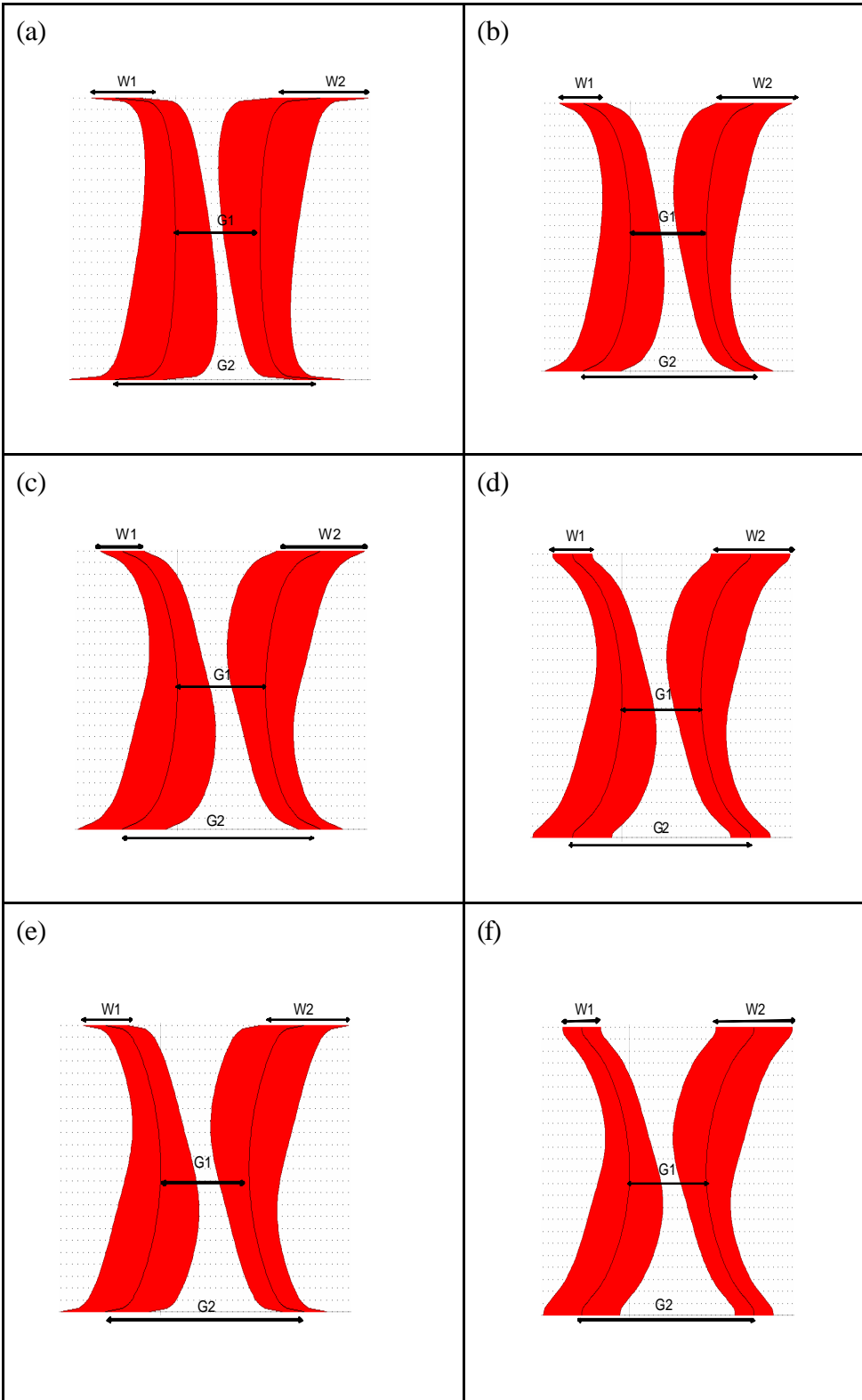


Fig. 3-6 Antisymmetric waveguide pairs



Units :um

$W1=5.52$

$W2=6.56$

$G1=7.6$

$G2=16$

Fig. 3-7 Waveguide layouts of case 1

D = 2

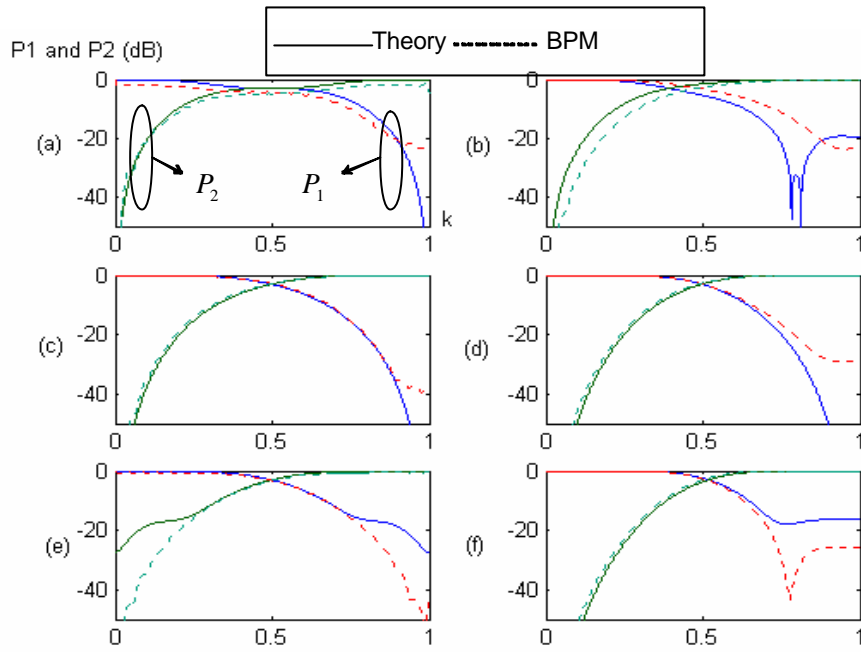


Fig. 3-8(a) Dynamic power flow of case 1, D = 2

D = 3.5

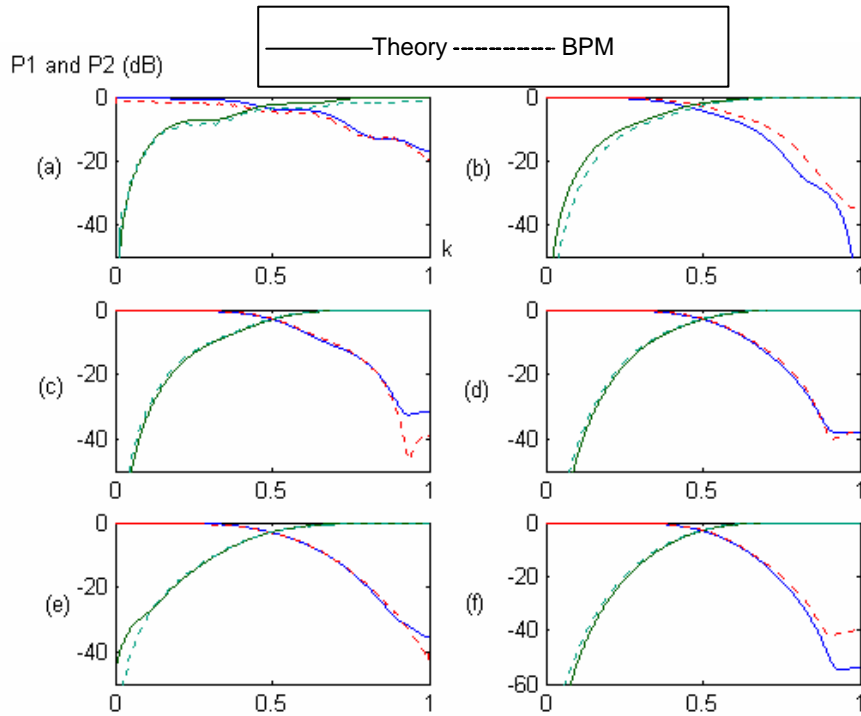


Fig. 3-8(b) Dynamic power flow of case 1, D = 3.5

D = 6

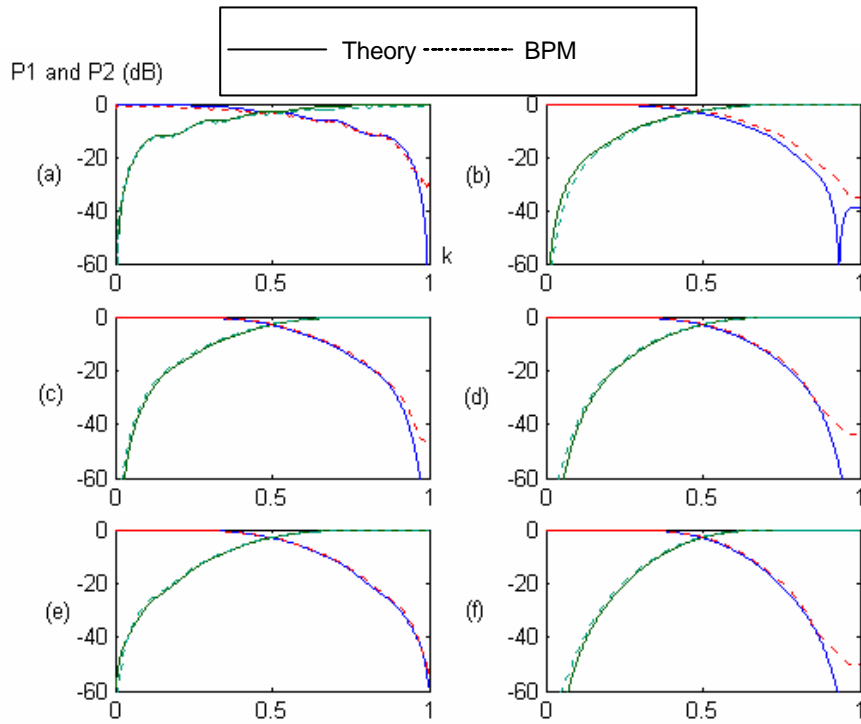


Fig. 3-8(c) Dynamic power flow of case 1, D = 6

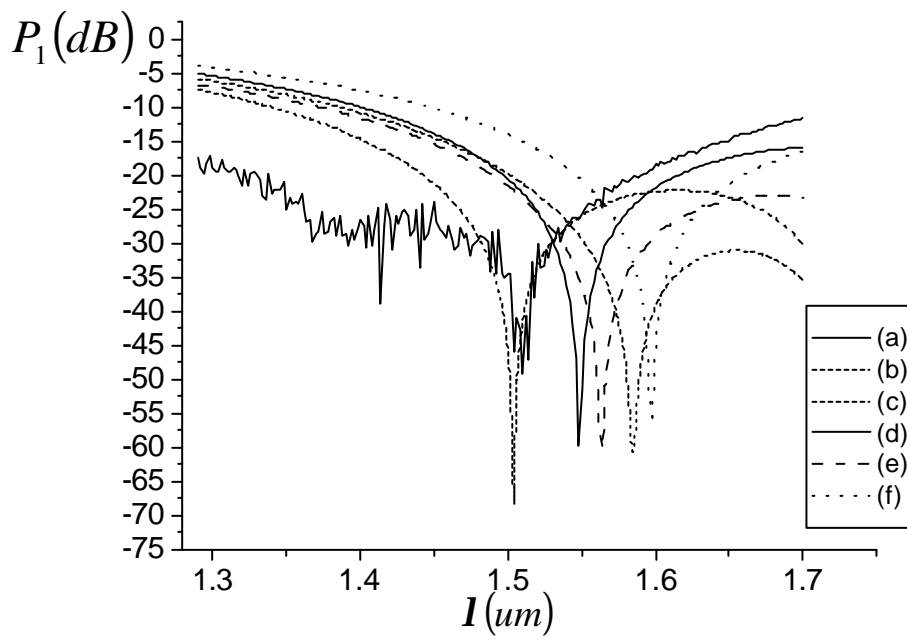


Fig. 3-9(a) Power in guide 1, case 1, D = 2, scanned from 1.29 to 1.7um

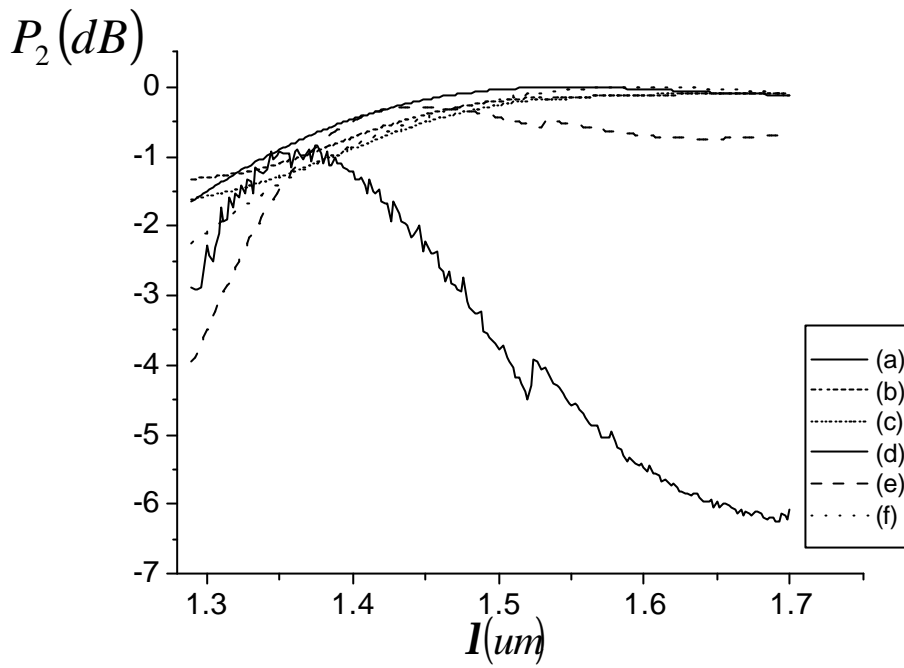


Fig. 3-9(b) Power in guide 2, case 1, D =2, scanned from 1.29 to 1.7um

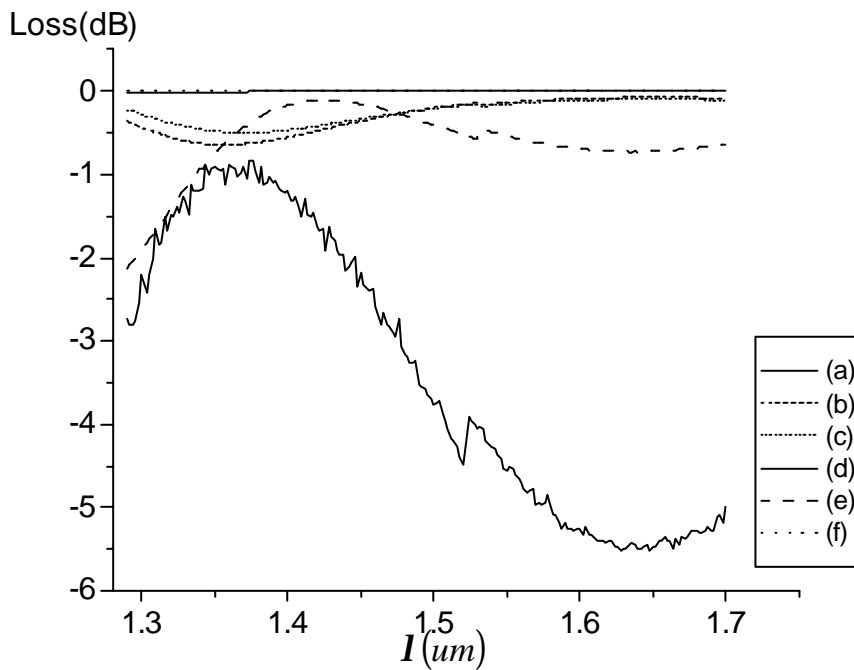


Fig. 3-9(c) Loss in case 1, D = 2, scanned from 1.29 to 1.7um

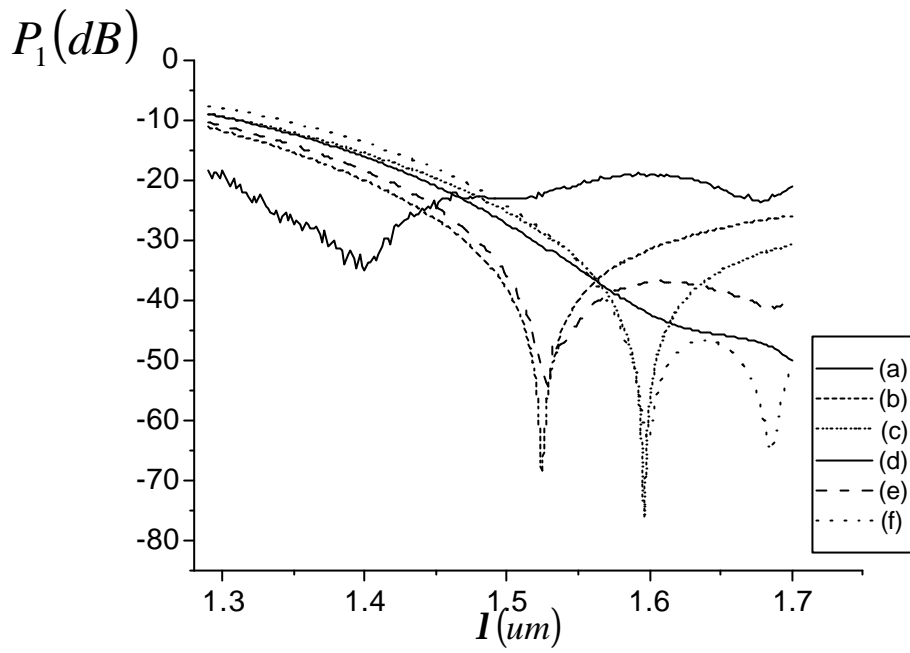


Fig. 3-10(a) Power in guide 1, case 1, $D = 3.5$, scanned from 1.29 to 1.7 μm

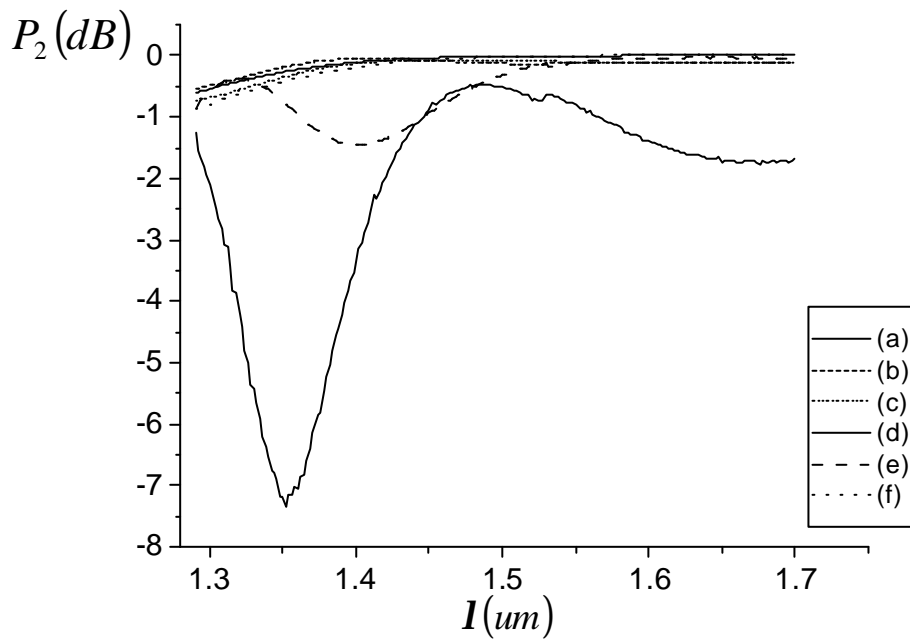


Fig. 3-10(b) Power in guide 2, case 1, $D = 3.5$, scanned from 1.29 to 1.7 μm

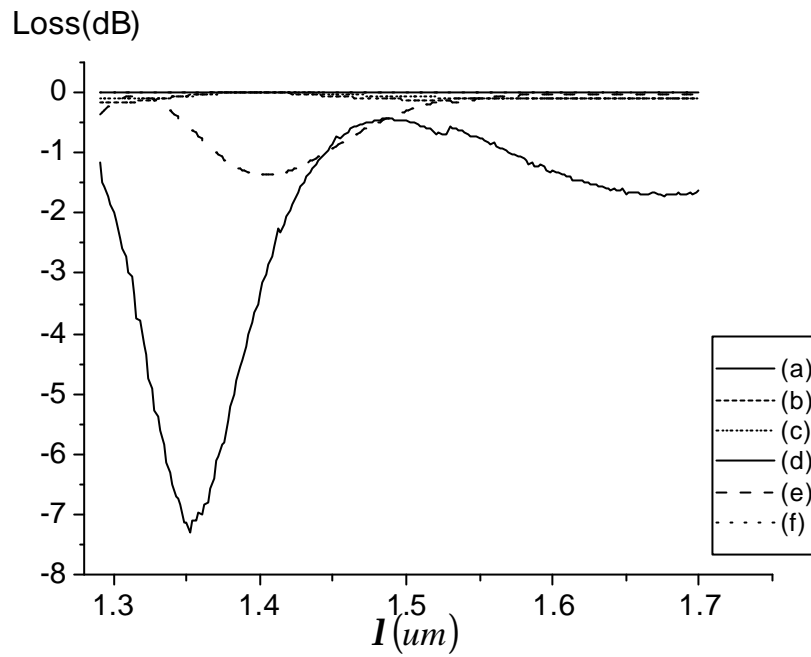


Fig. 3-10(c) Loss in case 1, D = 3.5, scanned from 1.29 to 1.7um

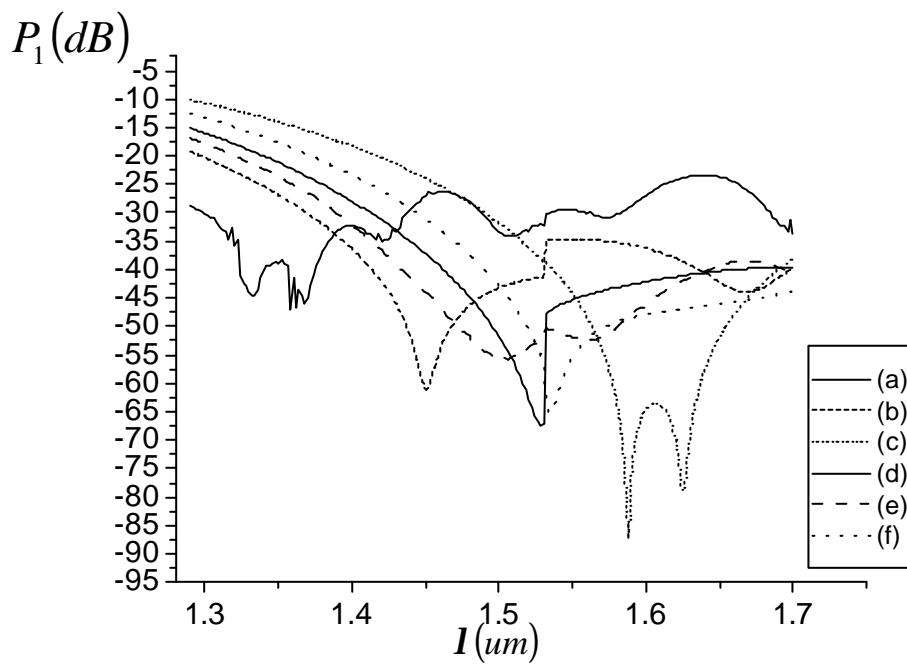


Fig. 3-11(a) Power in guide 1, case 1, D = 6, scanned from 1.29 to 1.7um

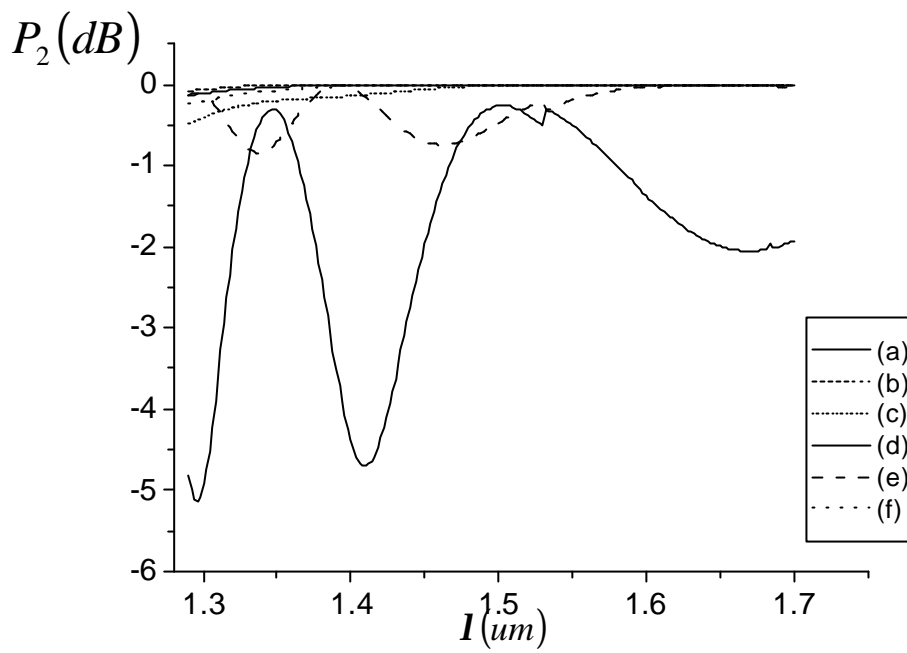


Fig. 3-11(b) Power in guide 2, case 1, D =6, scanned from 1.29 to 1.7um

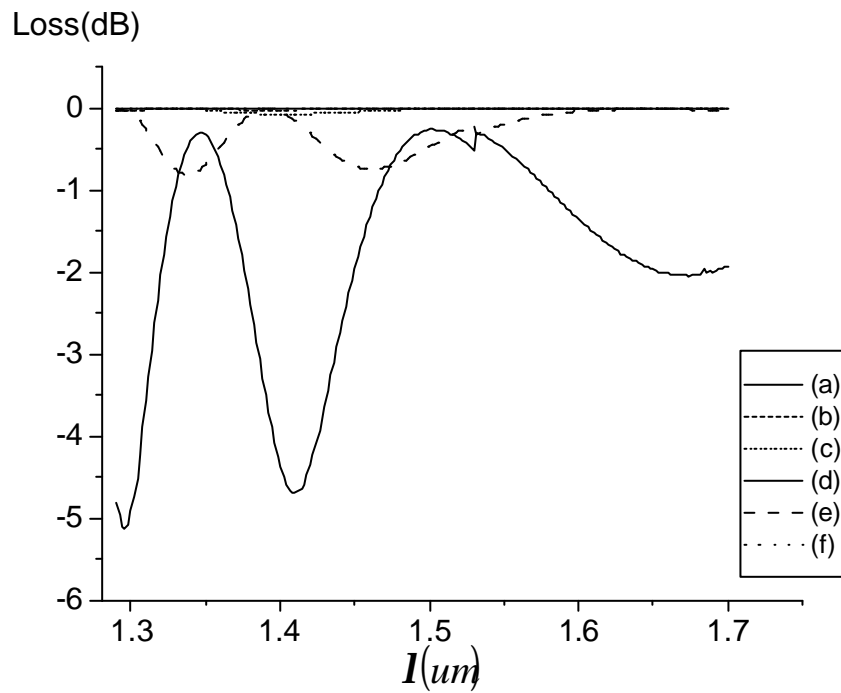


Fig. 3-11(c) Loss in case 1, D = 6, scanned from 1.29 to 1.7um

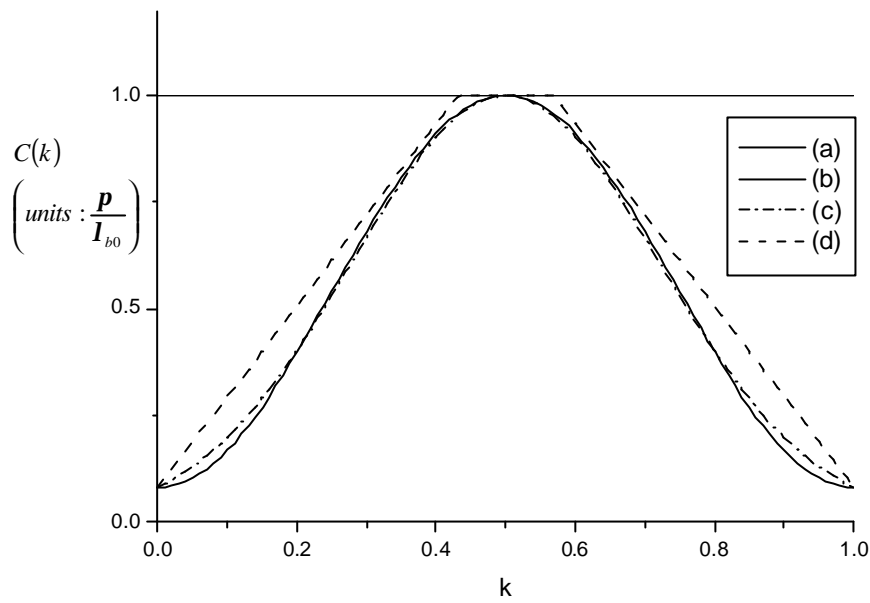
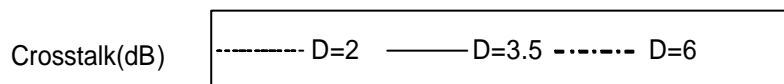


Fig 3-12 Variations of coupling coefficients of case 2



(a)

(b)

k

(c)

(d)

Fig. 3-13 Dynamic crosstalk of case 2

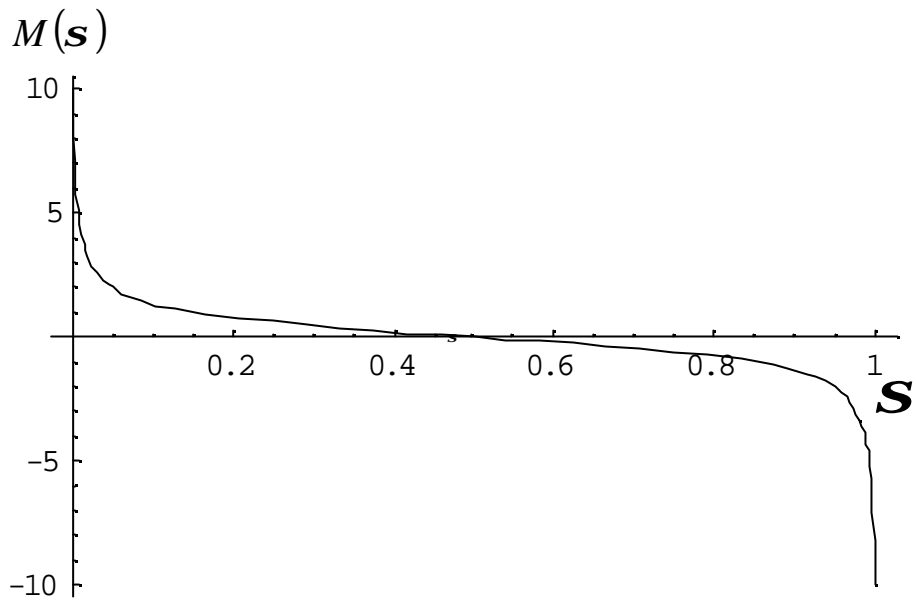


Fig. 3-14 Variations of the asynchronicity parameter of case 2

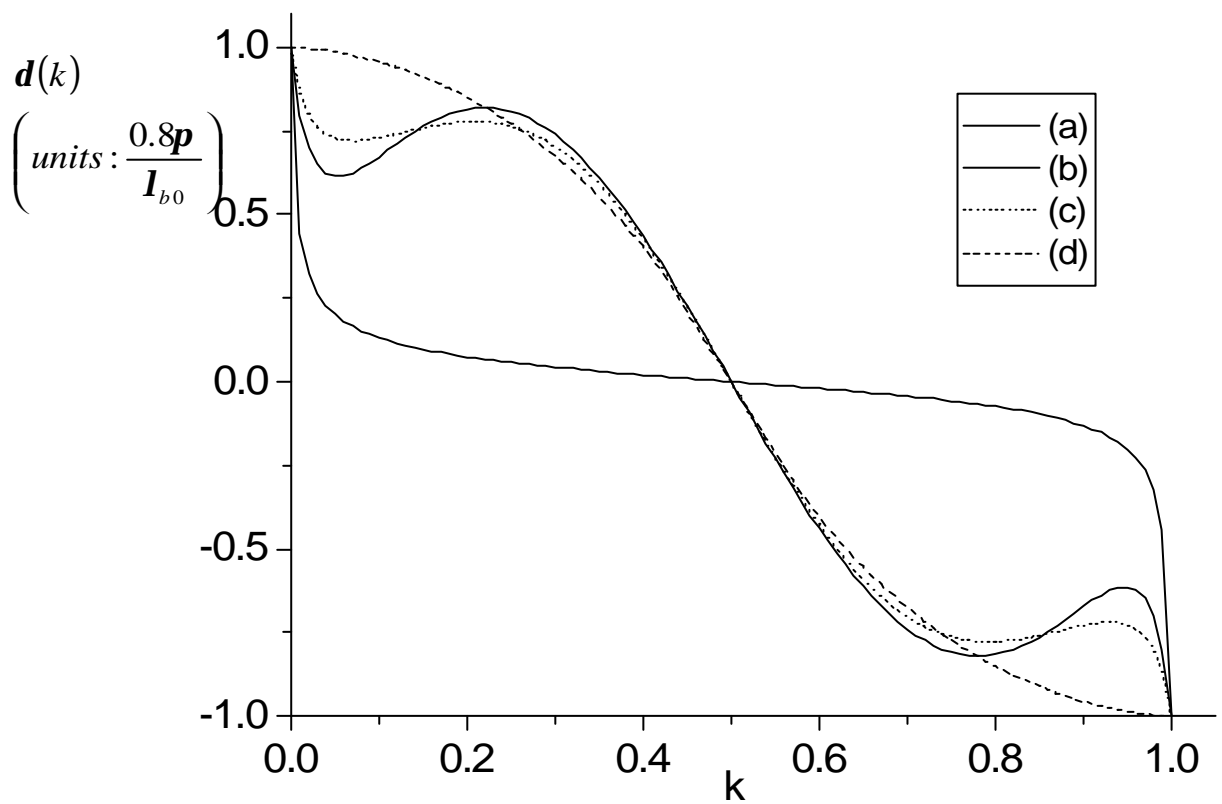
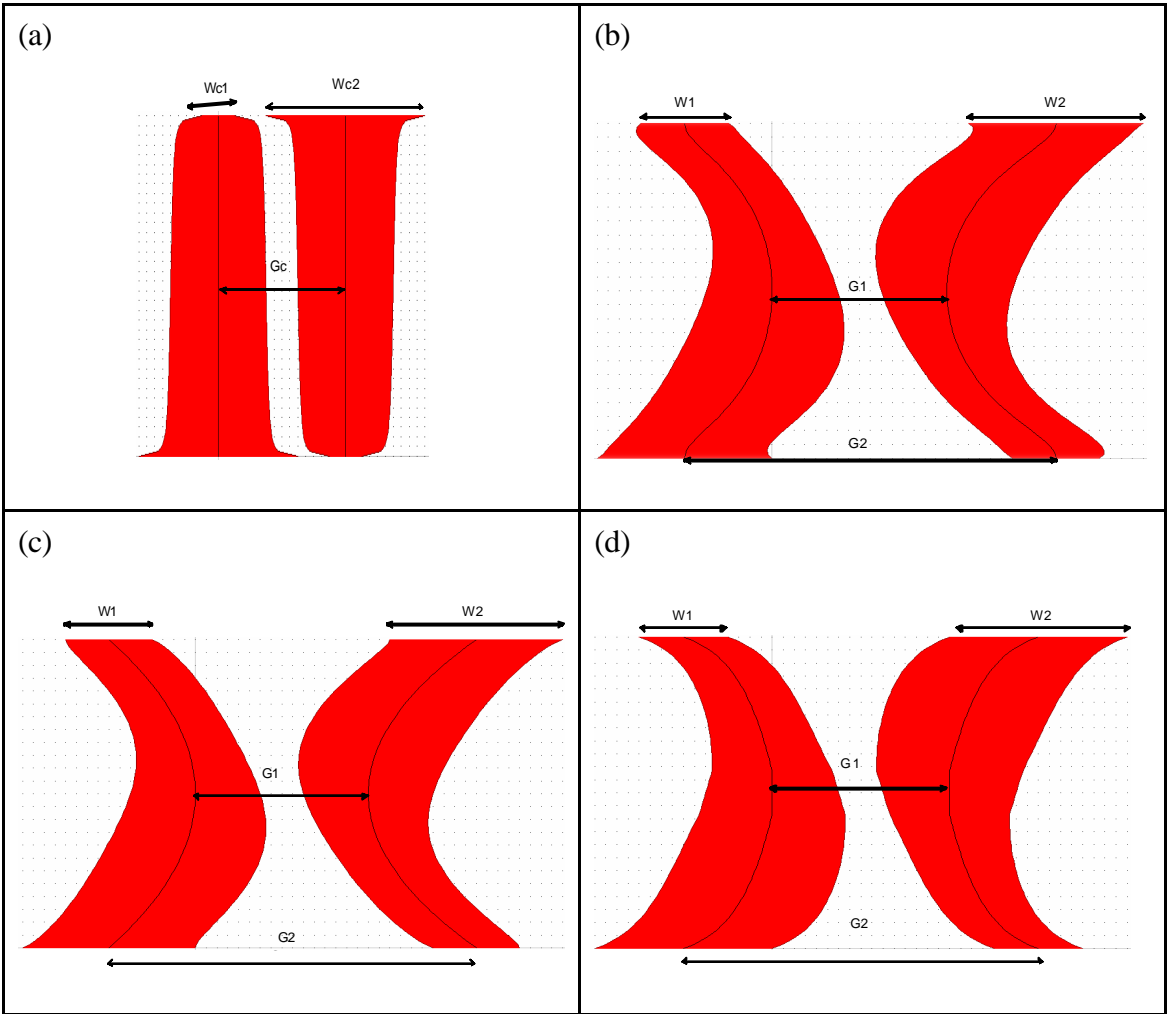


Fig. 3-15 Variations of half the difference of phase constants, $d(k)$



Units : μm

$W_{c1} = 2$

$W_{c2} = 10$

$G_c = 7.6$

$W_1 = 5.62$

$W_2 = 6.45$

$G_1 = 7.6$

$G_2 = 10.6$

Fig. 3-16 Waveguide layouts of case 2

D = 2

P1 and P2 (dB)

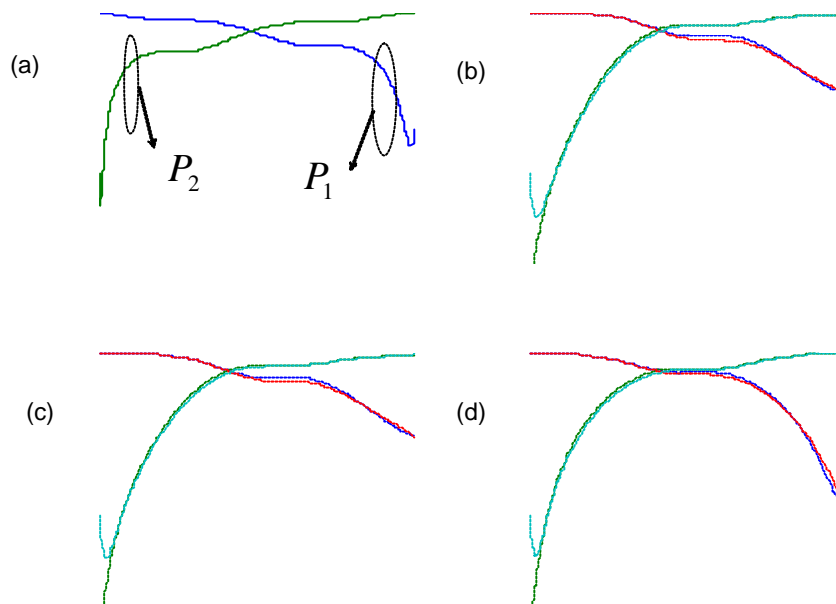
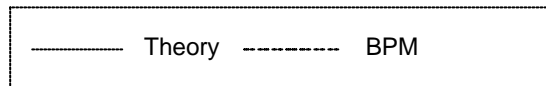


Fig. 3-17(a) Dynamic power flow of case 2, $D = 2$

D = 3.5

P1 and P2 (dB)

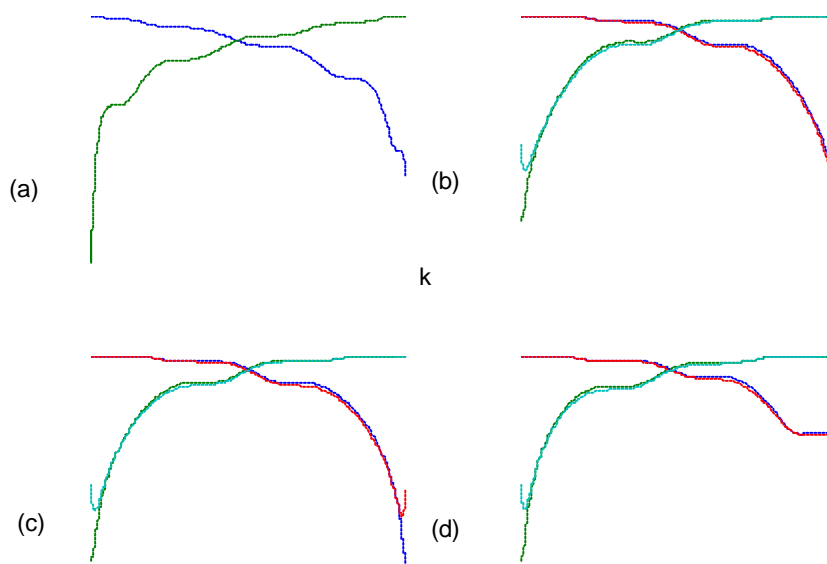
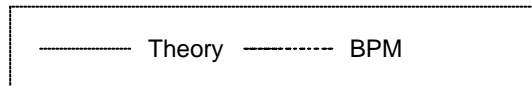


Fig. 3-17(b) Dynamic power flow of case 2, $D = 3.5$

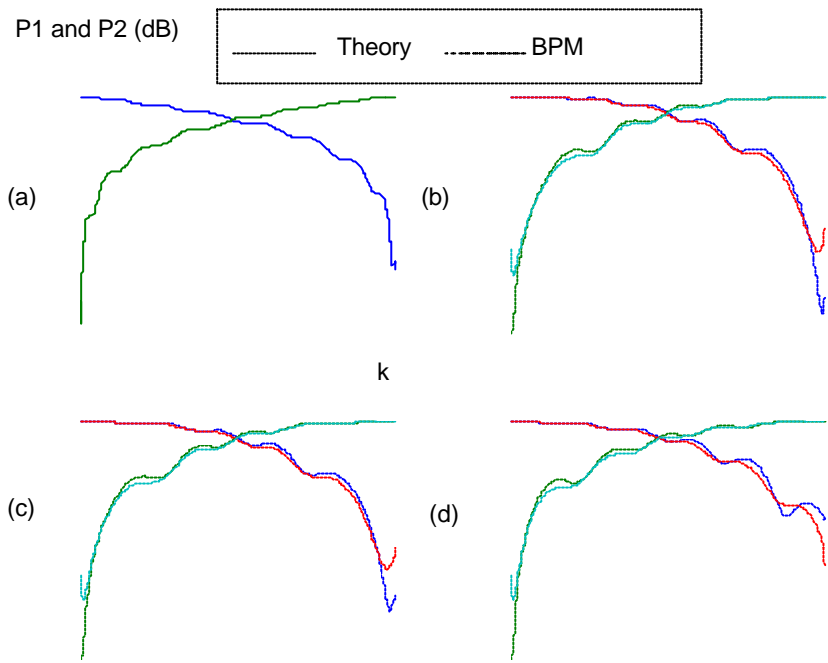


Fig. 3-17(c) Dynamic power flow of case 2, $D = 6$

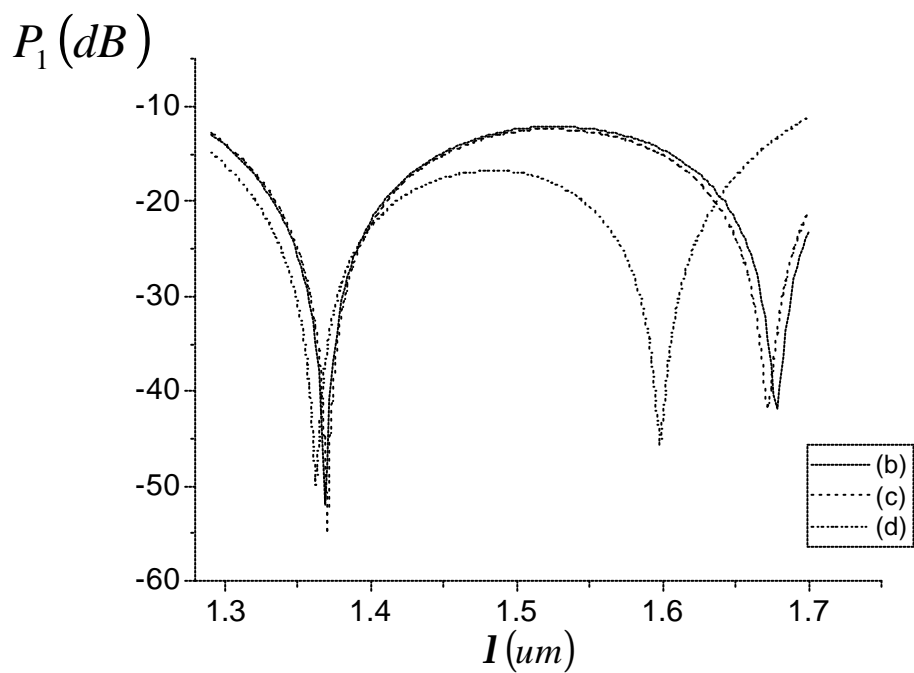


Fig. 3-18(a) Power in guide 1, case 2, $D = 2$, scanned from 1.29 to 1.7 μm

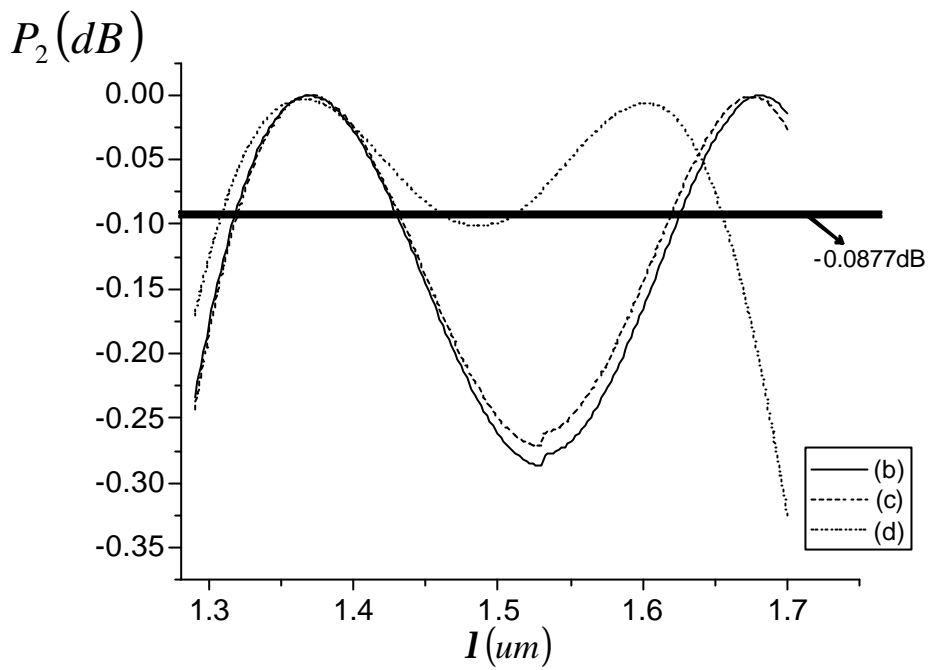


Fig. 3-18(b) Power in guide 2, case 2, $D=2$, scanned from 1.29 to 1.7 μm

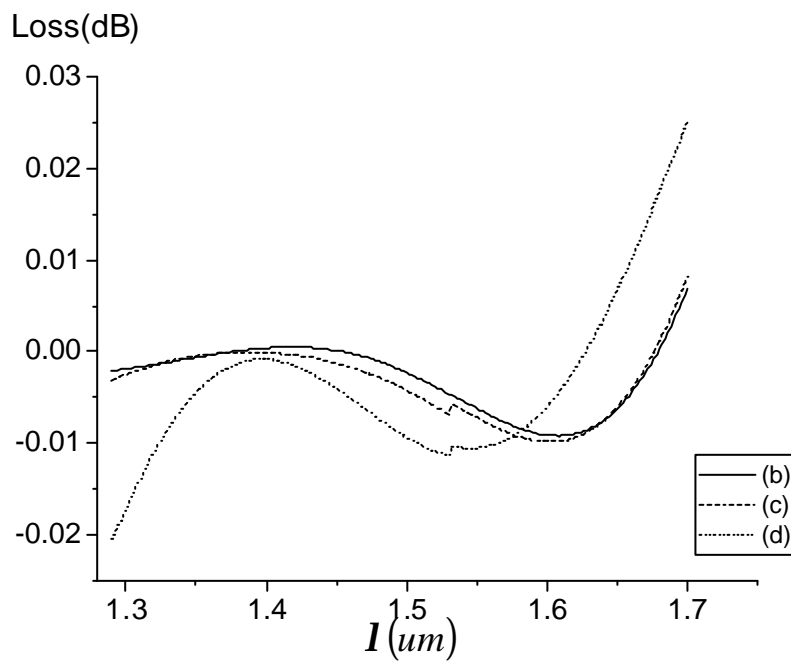


Fig. 3-18(c) Loss in case 2, $D=2$, scanned from 1.29 to 1.7 μm

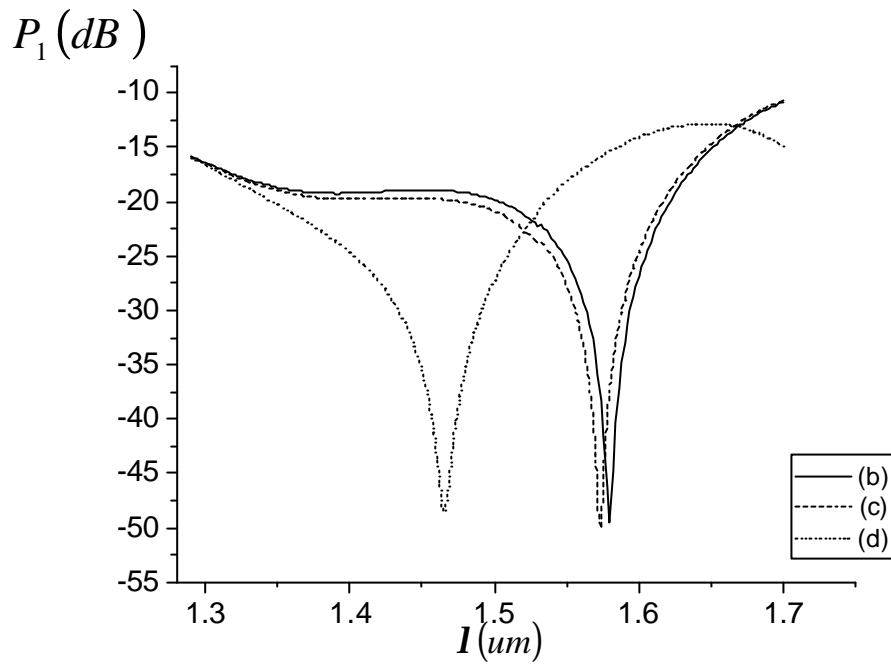


Fig. 3-19(a) Power in guide 1, case 2, $D = 3.5$, scanned from 1.29 to 1.7um

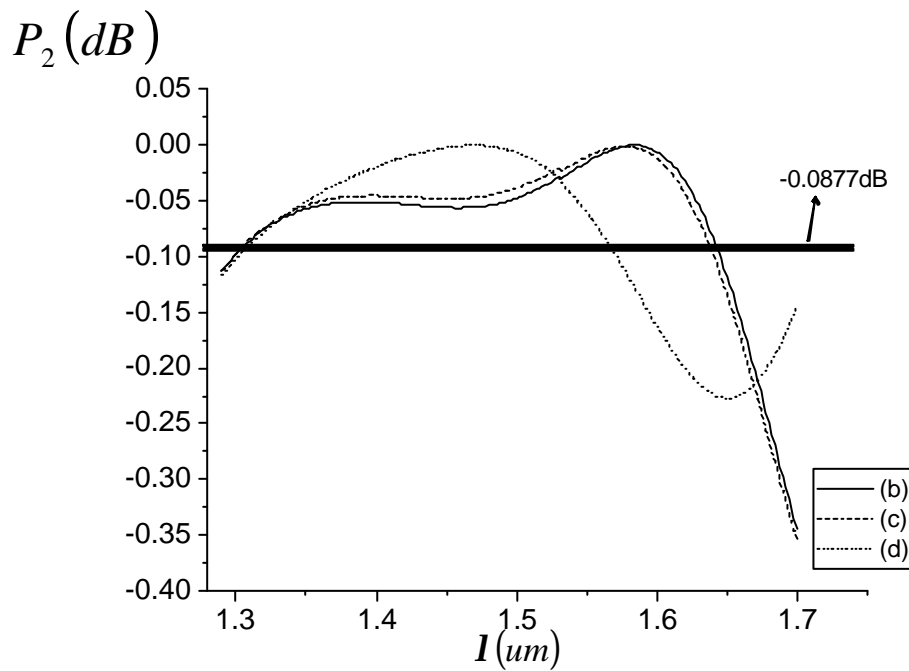


Fig. 3-19(b) Power in guide 2, case 2, $D = 3.5$, scanned from 1.29 to 1.7um

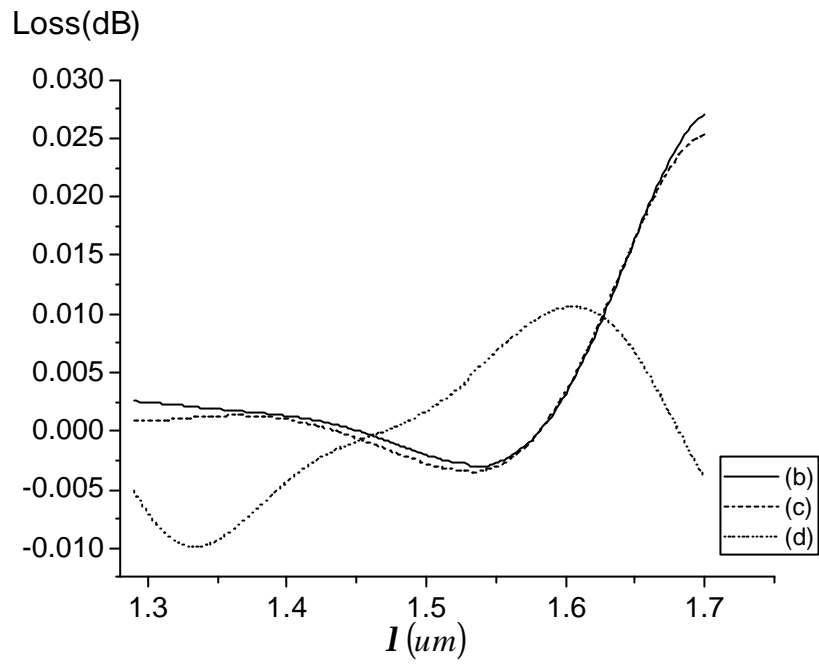


Fig.3-19(c) Loss comparisons of case 2, D =3.5

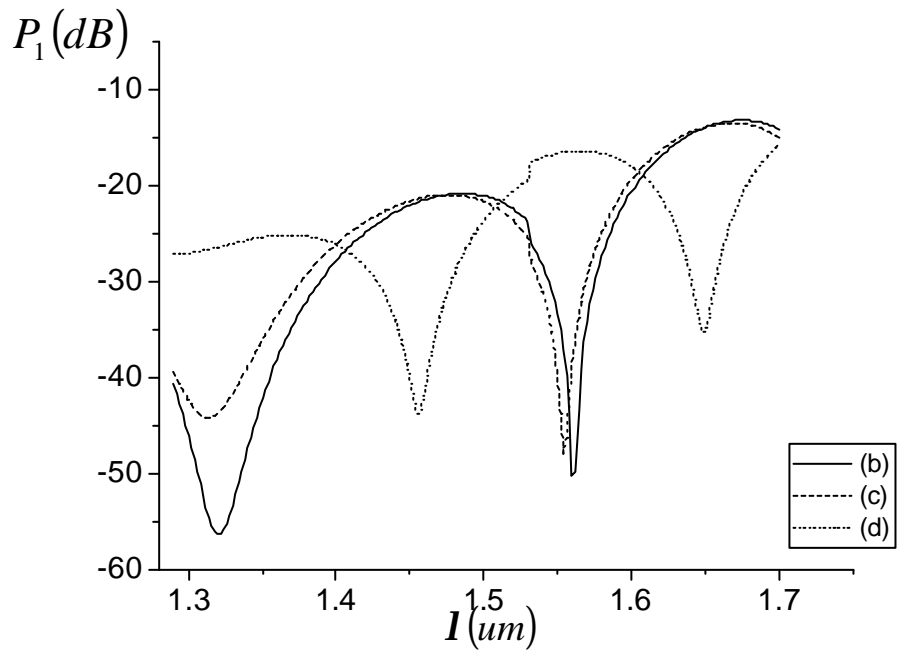


Fig. 3-20(a) Power in guide 1, case 2, D =6, scanned from 1.29 to 1.7um

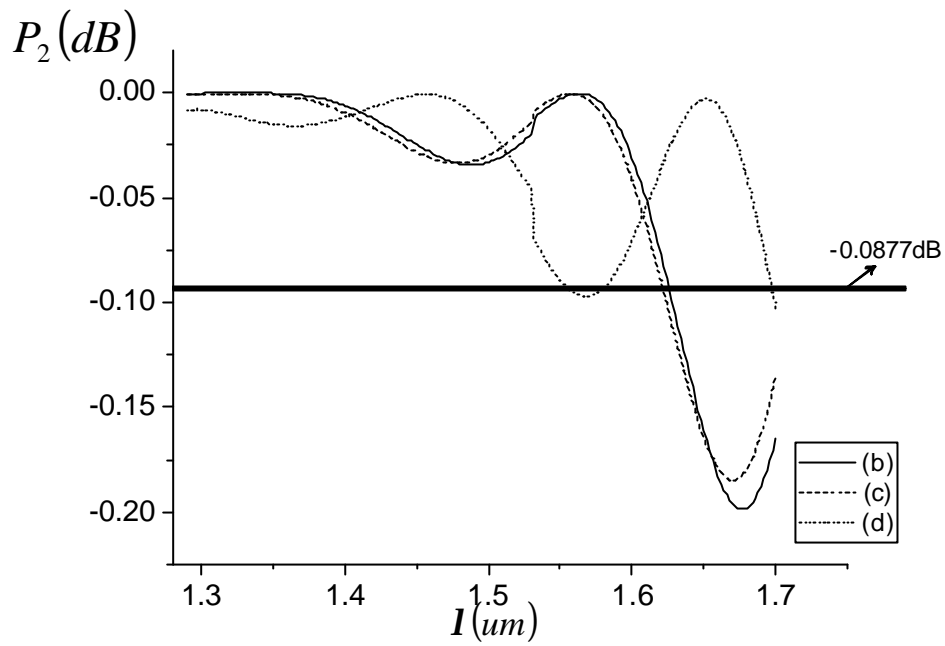


Fig. 3-20(b) Power in guide 2, case 2, D =6, scanned from 1.29 to 1.7um

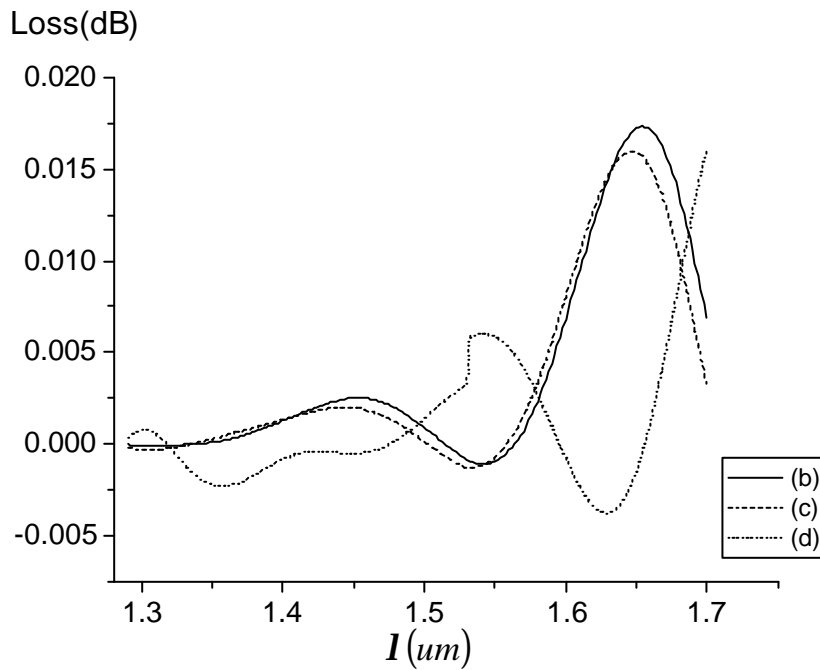


Fig. 3-20(c) Loss comparisons of case 2, D = 6

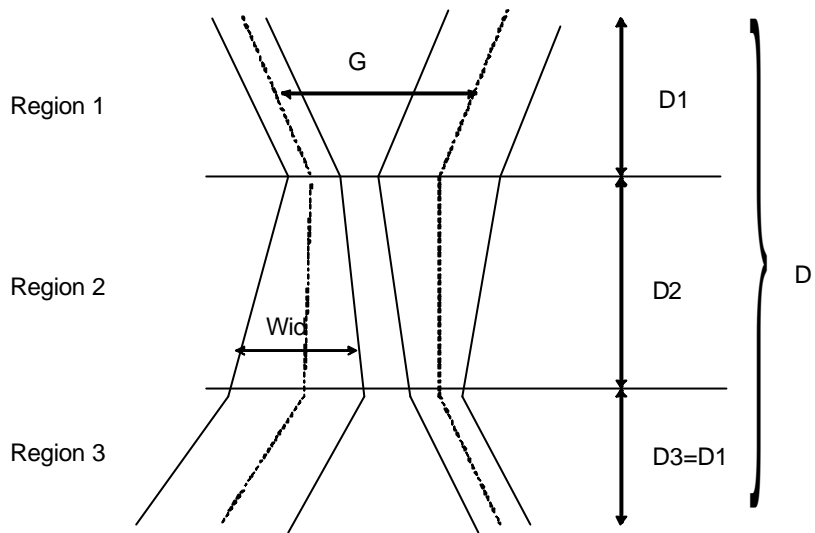


Fig. 3-21 Linearization of adiabatic coupler

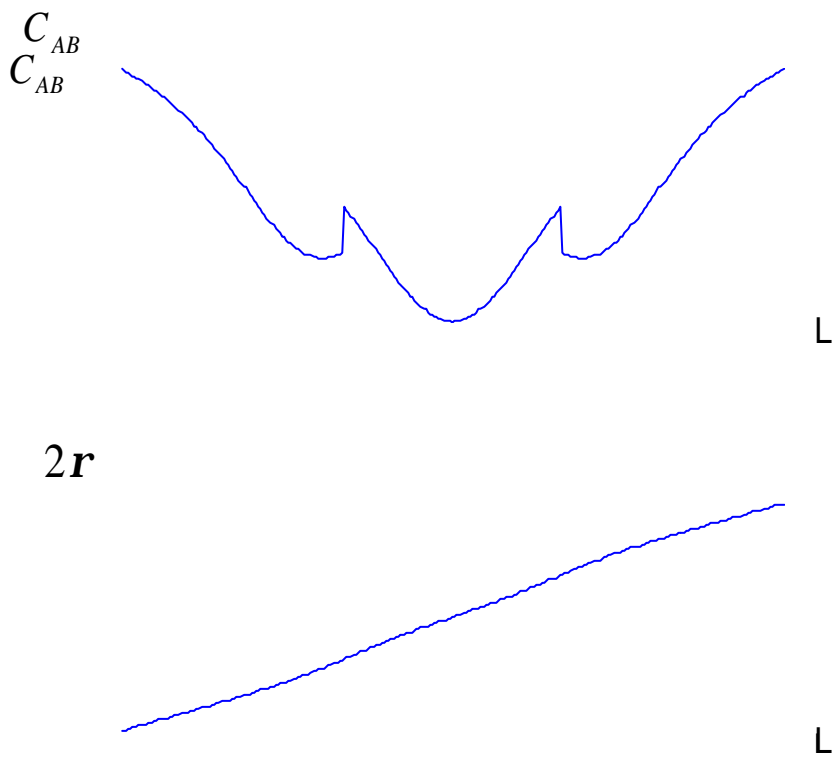


Fig. 3-22 Variations of $C_{AB}(z)$ and $r(z)$ of case 3

$m(1, D)$

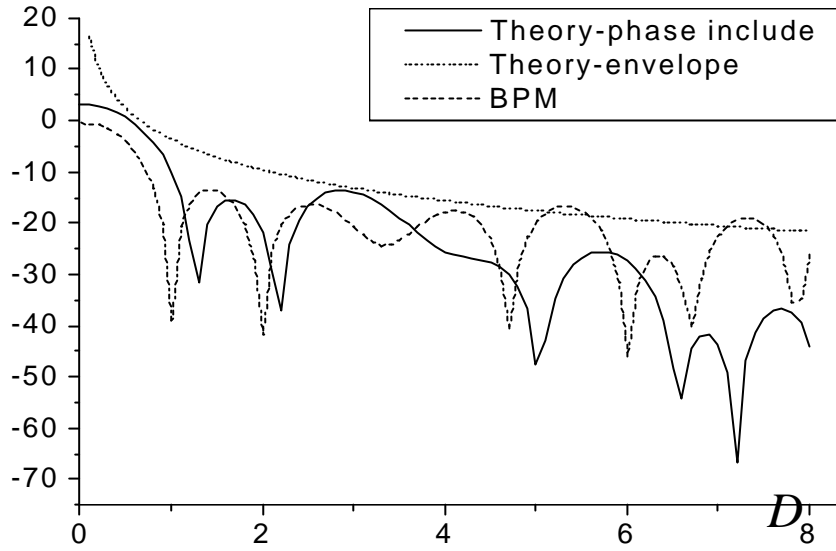


Fig.3-23 Output crosstalk versus D of case 3

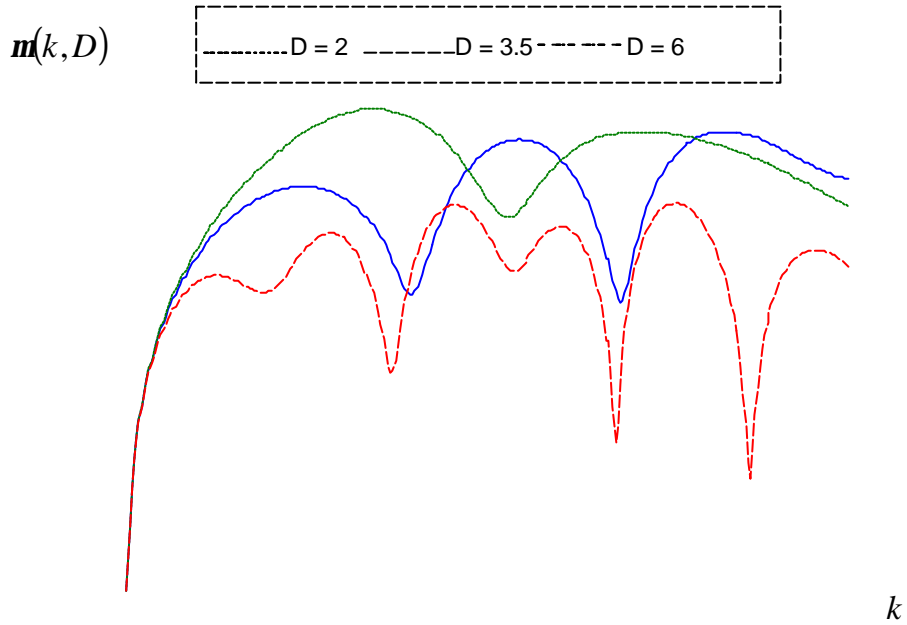


Fig. 3-24 Dynamic crosstalk of case 3

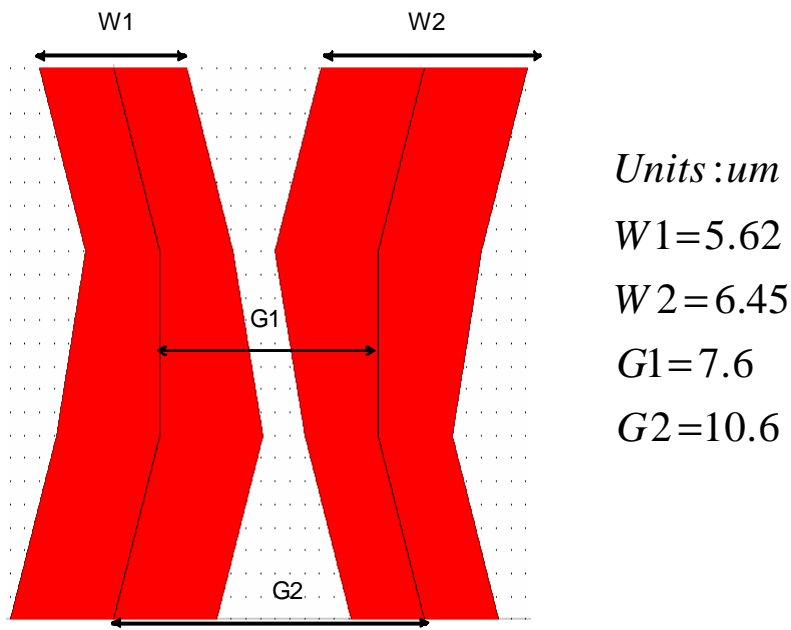


Fig. 3-25 Waveguide layouts of case 3

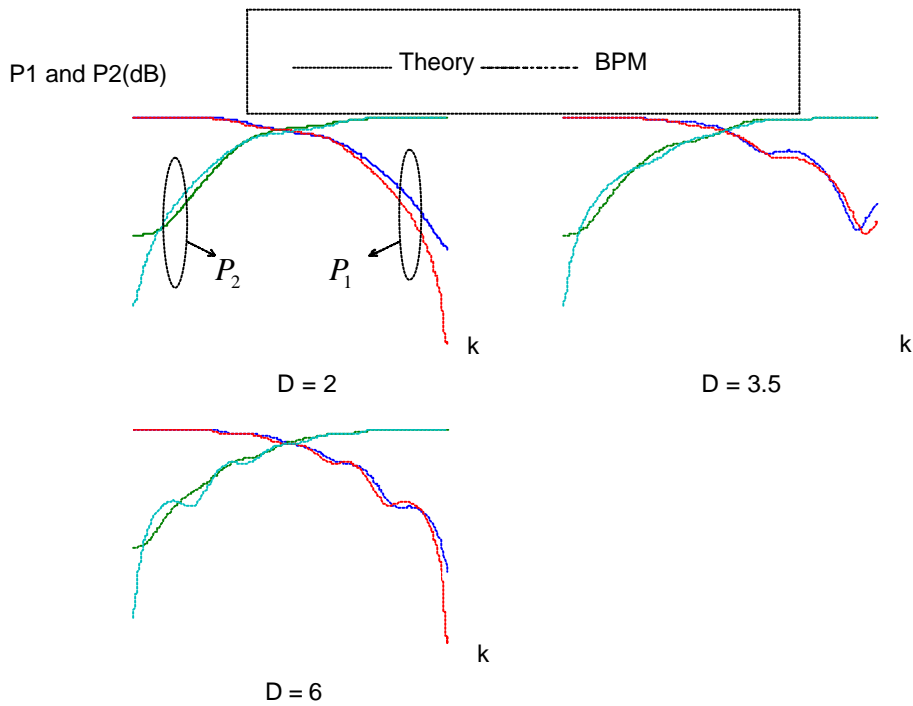


Fig. 3-26 Dynamic power flow of case 3

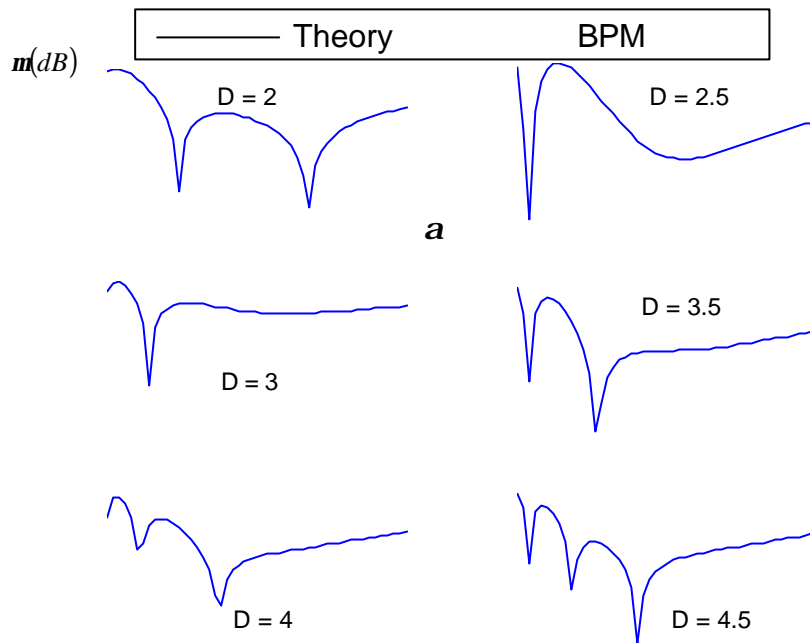


Fig. 3-27(a) Variation of crosstalk versus device length ratio in different lengths ($D = 2 \sim 4.5$).

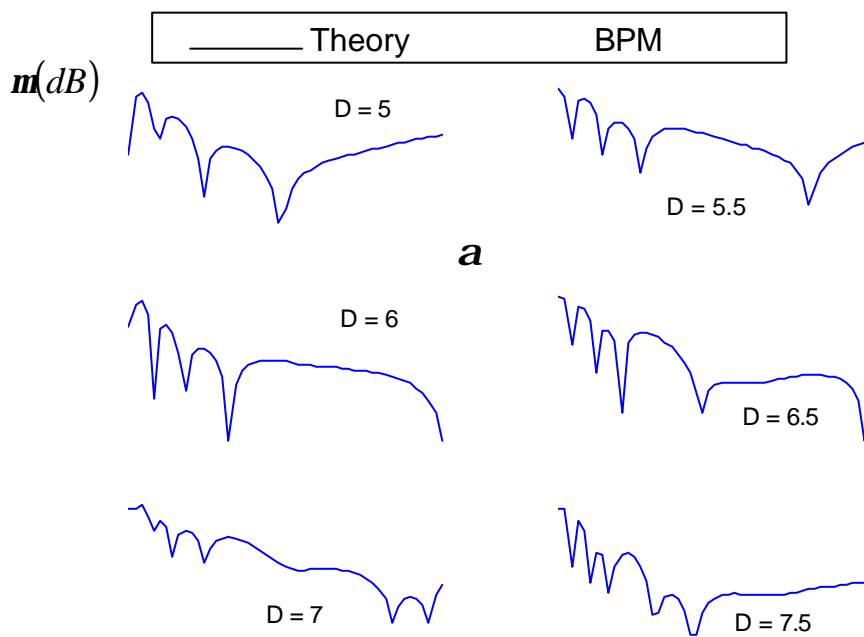


Fig. 3-27(b) Variation of crosstalk versus device length ratio in different lengths ($D = 5 \sim 7.5$).

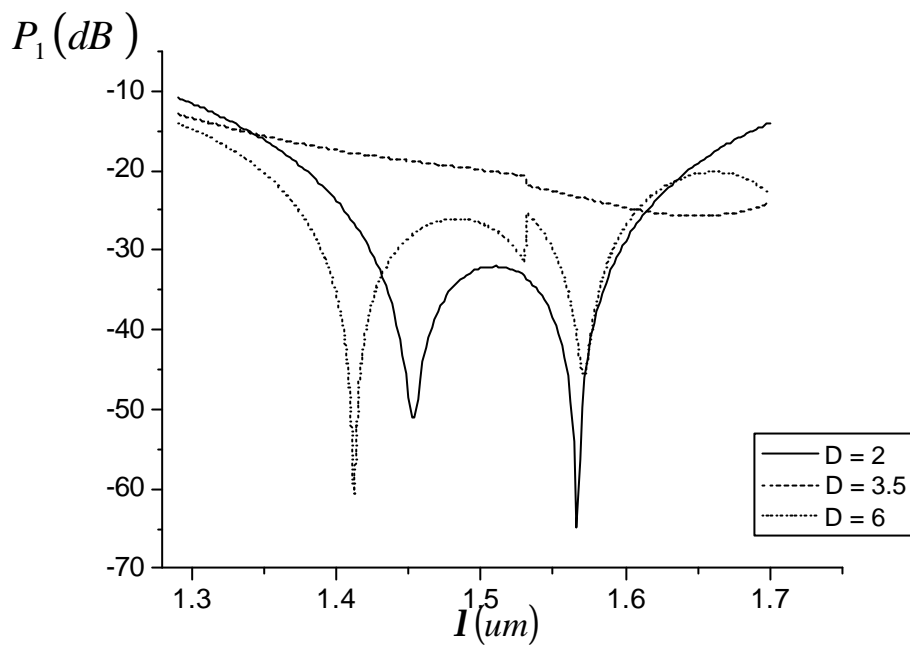


Fig. 3-28(a) Power in guide 1, case 3, scanned from 1.29 to 1.7um

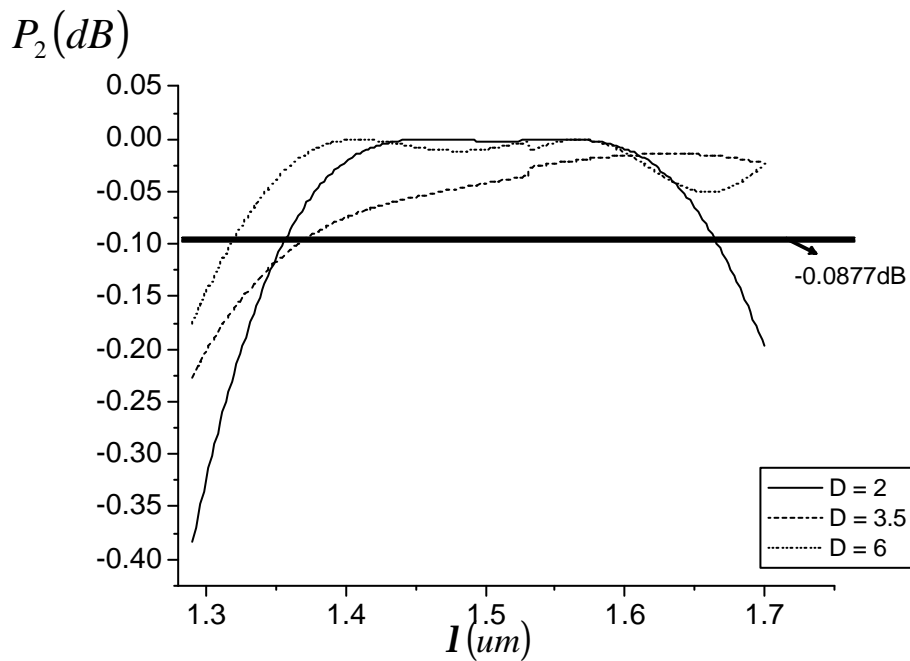


Fig. 3-28(b) Power in guide 2, case 3, scanned from 1.29 to 1.7um

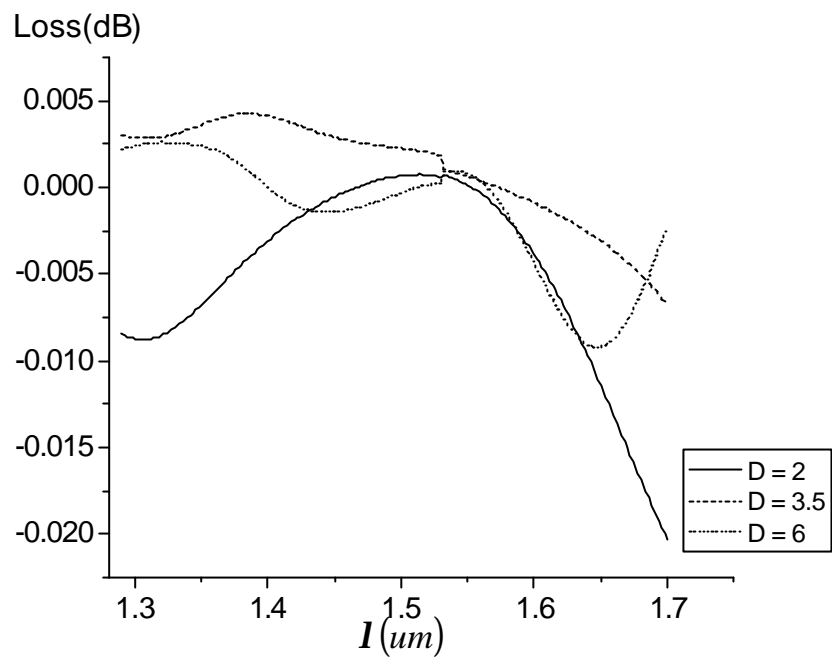


Fig. 3-28(c) Loss comparisons of case 3, scanned from 1.29 to 1.7um

Chapter 4

Application Aspect

One may wonder how we need a full coupler since all power flowing into another port that really makes no meaning. In this chapter two devices, switch and filter, using adiabatic principles will be covered, which are workable over larger bandwidth. And the influences of two basic characters of adiabatic device, tapered coupling and widths, are shown through comparison with the conventional device.

4.1 Broadband Optical Switch

Optical switch is one of the key components for optical communication and optical signal processing. With the developing technologies of WDM, we often need a broadband switch which can work well over the wavelength being used in communication, the band of 1.31 μm and 1.55 μm . Using the OH^{-1} free fiber the operating wavelength can even range from 1.30 μm to the L band of 1.62 μm . One of the candidate switch can support such a broad range of wavelength is the adiabatic switch, which can be formed only added a heater on one of the guides to tune the mismatch phase constants.

We have known the principle of adiabatic coupling is the crossing match of phase constants at the coupler center. If a heater is added to change the refractive index of one of the coupler guide, we can move the match point of phase constant out of the strong coupling region and finally mismatch the two guides.

Fig. 4-1 shows the two states of the switch. The phase constants b_1 and b_2 are assumed linear variation along propagation under switched state. If the turned on heater raises the temperature of guide 2 and changes its refractive index, the phase constant of guide 2 will turn to the unswitched state, b_2' , which will move the match point of phase constants away from the strong coupling region near the center of coupler and then stops the power flow across the two guides. The same structure can also be replaced by electro-optic material such as $LiNbO_3$ or carrier injected type method such as GaInAsP/InP [15] but for here we use the polymer material, BCB4024, which exhibits the thermal-optical coefficient of $-1.5 \times 10^{-4} / ^\circ C$.

Fig. 4-2(A) shows the adiabatic switch layout. Excepting the heater component added on guide 2, all parameters and materials are the same as in case 3, chapter 3. Other profiles discussed in chapter 3 can also be used for switch but picks this one

mainly due to its ease of fabrication

Another two structures are compared to the adiabatic switch, case A is consisted of two identical parallel guides formed a conventional coupler and case B is the same as the former excepting the tapered coupling. These two samples will help us see what are the advantages of the tapered width and the tapered coupling in adiabatic case. Their diagrams are in Fig. 4-2(A) and (B).

All three devices are 7000um long and a is defined in preceding chapter. The value of a selected in case (B) is for the coupling optimum. The refractive index of core n_{core} and $n_{cladding}$ are used of polymer materials, BCB4024 and BaK2, which are 1.544 and 1.523 at 1.55um, respectively. And the thermal-optic coefficient of BCB4024 is $-1.5 \times 10^{-4} / ^\circ C$.

Fig. 4-3 indeed shows the differences of parallel and tapered guides, and of constant and tapered widths. The coupler of parallel guides exhibits large sinusoid-like sidelobes through all scanning range. These sidelobes can always unstable the device controlled in a system, due to possible severely output power change even when very small shift of temperature control. In the tapered separation but non-tapered width guides coupler the side lobes are apparently mitigated and it converges to unswitched state very soon compared to the adiabatic coupler. Up to now, we have known the tapered guides exhibits the advantages of eliminating sidelobes. However, the tapered width in adiabatic coupler spoils the performance of transition since it has a larger mainlobe and thus will take more time to raise temperature of unswitch state. If this be true, why we need such a tapered widths coupler? The answer is in Fig. 4-4.

It is clear now that the tapered width can help the switch working in much more broad bandwidth in both switched ($\Delta T=0$) and unswitched ($\Delta T=12$) states. Figure4-4(a) and (b) show the crosstalk of unswitched and switched states, respectively. For now we can give a summary that the tapered coupling and widths of an adiabatic coupler can help eliminate the sidelobes in the switch transition state and give a broadband identity in such a device.

From the preceding chapter we have compared several profiles under different lengths, and now we also compare the switching characters of adiabatic switches with different lengths. In Fig. 4-5 we show the output power versus the temperature

changed over guide 2 at wavelength 1.55 μ m.

In the switched state, ie $\Delta T=0$, the dynamic coupling is the same as discussed in preceding chapter. When the temperature in guide 2 raises or lowers gradually, the power in guide 1, P_1 , starts to raise to 1. And in this diagram you can see longer the device length, faster P_1 approaches one, which might mean that it is unnecessary for longer device raise so high temperature as for shorter one and correspondingly reduces the switch time. Fig. 4-6 shows the issue of broadband.

In the switched state it is the same as discussed in chapter 3, but in the unswitched state we can see longer device length will exhibit less crosstalk which is different in the switched state that $D = 3.5$ induce more crosstalk than shorter length of $D = 2$. The two plots are just for a reference and we will not discuss them further.

4.2 Broadband Optical Filter (WDM Filter)

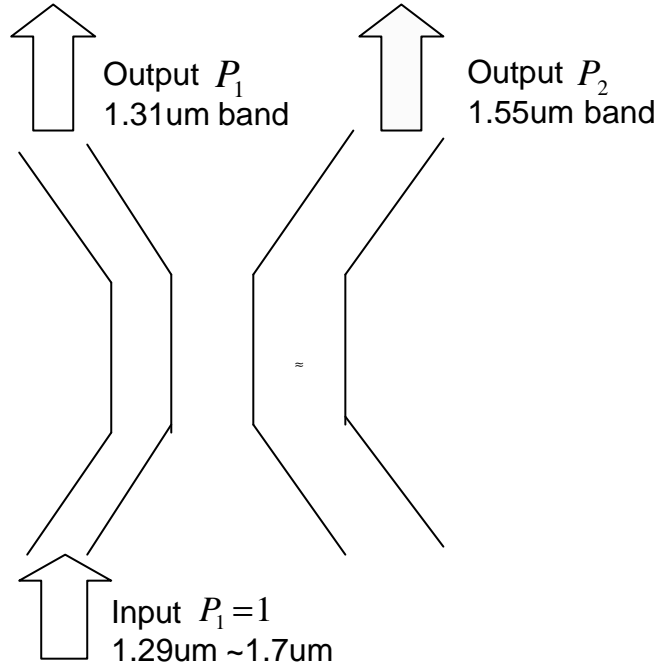
In a subscriber WDM system, filters separate the bands of 1.31 and 1.55 μ m are needed, and these filters are often called WDM filters. The passband of filters should be broad enough to cover all the using channels in C and L bands, that is, ranges from 1.53 to 1.62 μ m. Due to such a broad bandwidth needed in operation, the adiabatic filters are one of the candidates. The principles of directional coupler filter can be found in many text books so here we will just explain it conceptually. We all know only the phase match of two guides the power can flow completely to another port. If we tune the refractive index and structure of one of the guides to match at some designed wavelength, we will find that it will leave the matching condition when the operational wavelength shifts.

Excepting the designed wavelength, we see the two phase constant lines in Fig. 4-7 separate further when leaving away from the designed wavelength. Such a mechanism can clearly be used as a filter. For now we still provide three basic structures for comparison, which are all designed matched at wavelength of 1.55 μ m in Fig. 4-8.

The thinner guide is simulated using another polymer material, CN120-S80, of which the refractive index is 1.5547. The other guide and the cladding are both the same as the switch

All three structures in Fig. 4-8 are of two different guides designed matched at 1.55 μ m. And as the preceding switch case we provide the three to see what are the

functions of tapered coupling and tapered widths. Case A contains two guides of uniform coupling and widths. Case B (which had been proposed in [17], and the advantage of tapering of a filter is studied in [21]) adopt the tapered coupling but constant widths. Case C, which based on adiabatic coupler, surely has tapered structures of both coupling and widths. We should note the device lengths are slightly different due to tuning to its optimum filter function.



As the above indicated, we pumped all power of wavelength distributed from 1.29 to 1.7um into guide 1 and observed the outputs.

It's clear from Fig. 4-9 that the case A oscillates seriously outside the narrow stop band of guide 1 and lengthen the transition band making it ineffective in operation. Using the tapered coupling in case B, it apparently eliminates the sidelobes of case A. This behavior is like the case B in preceding section, which is in the temperature domain. The reason that the tapered coupling can eliminate the sidelobes is almost the same as the case of grating. When weakly coupling between two modes, the power can be written as the formula below [22]

$$A_2(L) \approx -j \int_0^L C(z) \exp(-2j\mathbf{d}z) dz$$

It is assumed that $A_2(0)=0$. So outside the strong coupling region, the behavior of power in guide 2 is proportional to the Fourier transform of the coupling coefficient. The case A in switch or filter holds coupling constant mapping to a sinc alike function

which has significant sidelobes, and the tapered coupling used for migrating the problems can be imaged now. The same method is often used in a grating, too.

Besides tapering the waveguide separation, tapering the widths can also provide additional advantage of broad bandwidth. If we need a crosstalk less than 10dB near the 1.55um band, then only the adiabatic can sustain over the range of 1.5 to 1.64um. The only price is the deterioration of crosstalk at exact 1.55um compared to case B.

Fig. 4-10 shows the adiabatic filter in different lengths. We can see when the device becomes longer, the filter exhibits more bandwidth and abbreviate the transition band between the bands of 1.3 and 1.55m.

We defined the bandwidth as the band of crosstalk lower than -20dB near the communication band of 1.55um.

Device Length(cm)	Range(um)	Bandwidth(nm)	Crosstalk at 1.31um(P2 in dB)
0.7	1.544~1.566	22	-24.35
1.2	1.514~1.596	82	-30.96
2.0	1.504~1.610	106	-35.58

Table 4-1 Bandwidths and crosstalk comparisons of adiabatic filters

For the three different lengths we found that longer device can exhibit broader bandwidth and lower crosstalk.

Summary

We had demonstrated two adiabatic devices of switch and filter, and compared with the conventional ones to point out the advantages of tapering in separation and widths. The tapered coupling can help mitigate the significant sidelobes and the tapered widths can enhance its working bandwidth. And we proposed filters that exhibit bandwidth of 106nm near 1.55um and low crosstalk less than -20dB whether in 1.31or 1.55 bands.

In both adiabatic devices, longer one can always reduce transition band obviously, but more space and cost are paid. There exists a trade off between the transition band (in wavelength or temperature domain) and the length of an adiabatic

device.

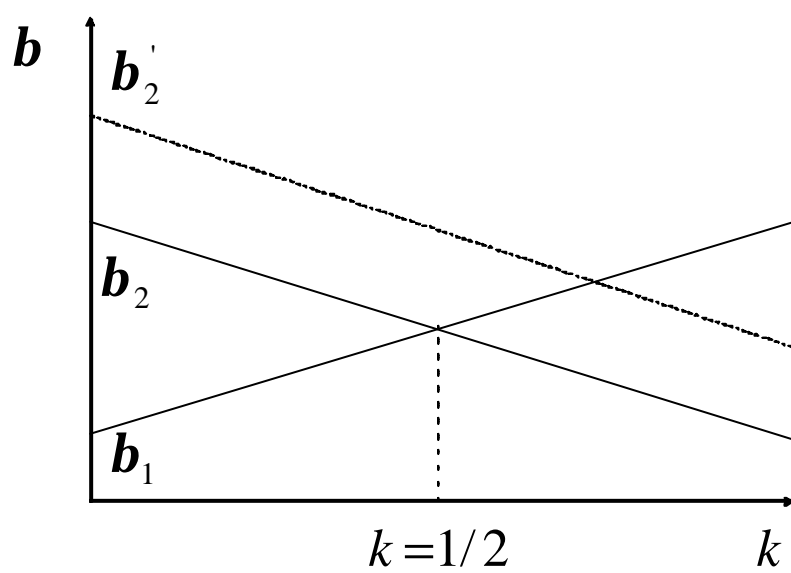


Fig. 4-1 Phase constants of different states

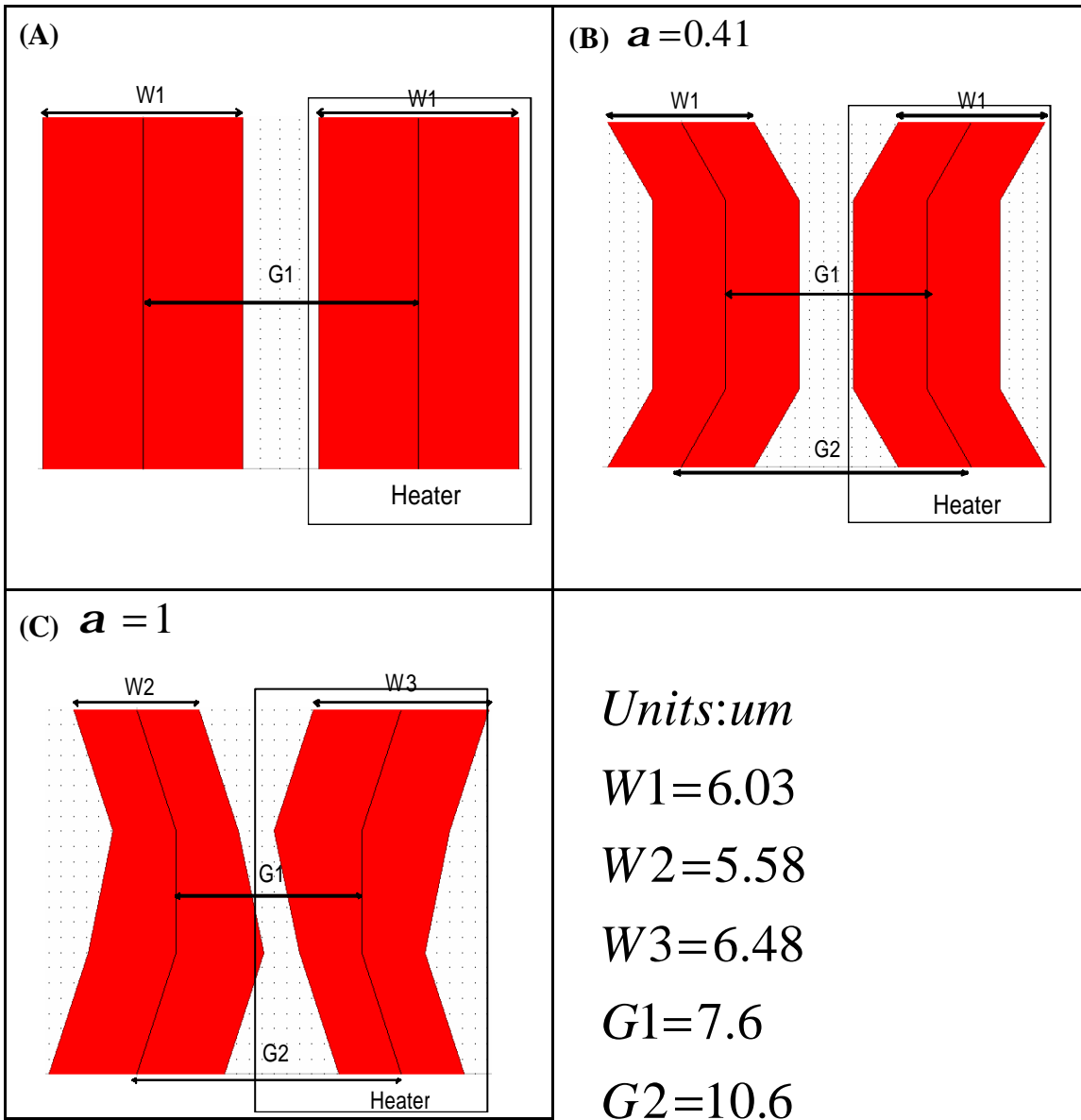


Fig. 4-2 The switch layouts

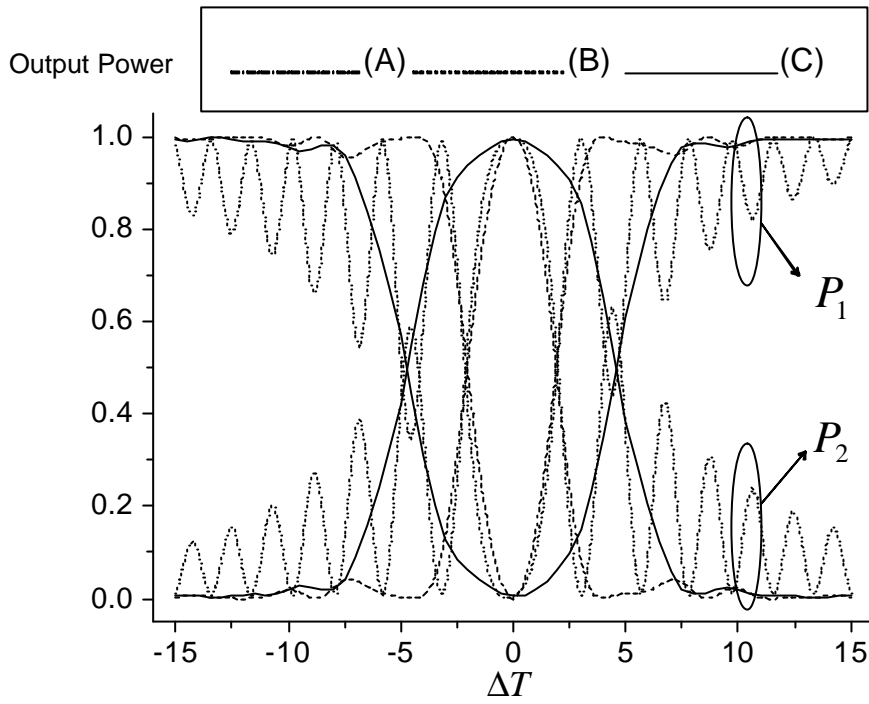


Fig. 4-3 Output powers of two switch states

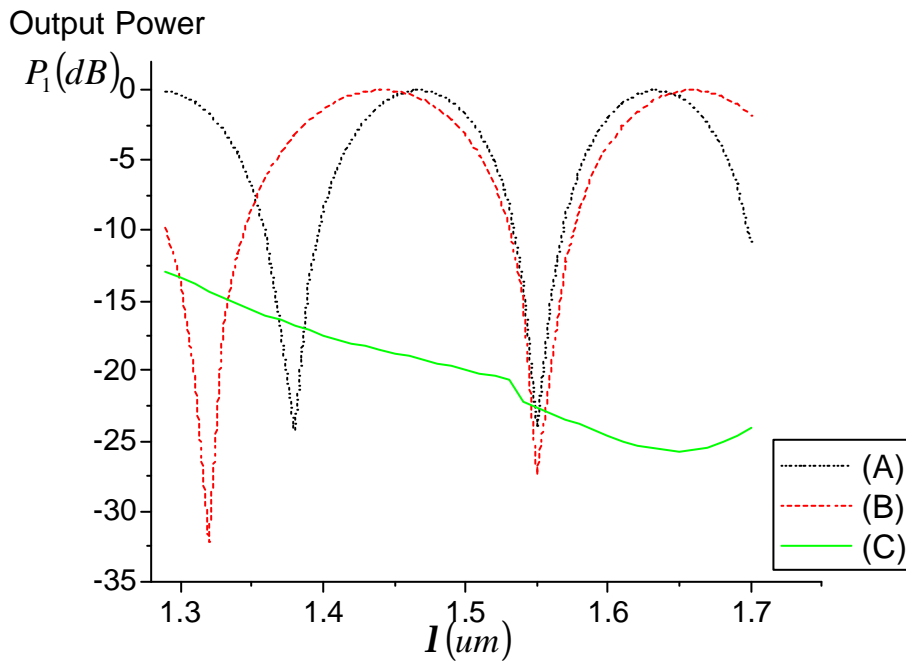


Fig. 4-4(a) Crosstalk in guide 1 of switched state

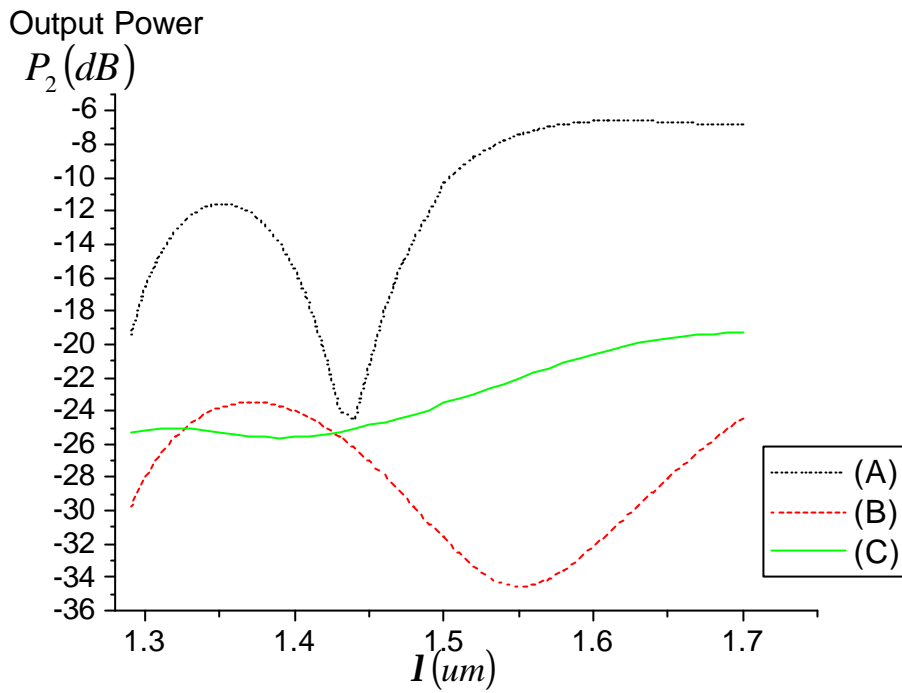


Fig. 4-4(b) Crosstalk in guide 2 of unswitched state

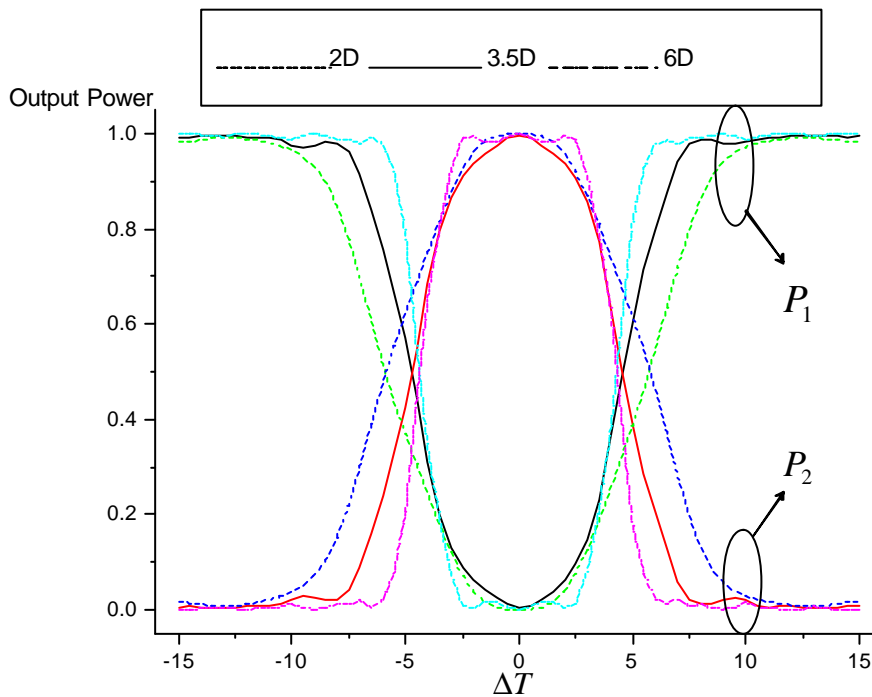


Fig. 4-5 Output power of different states with different lengths

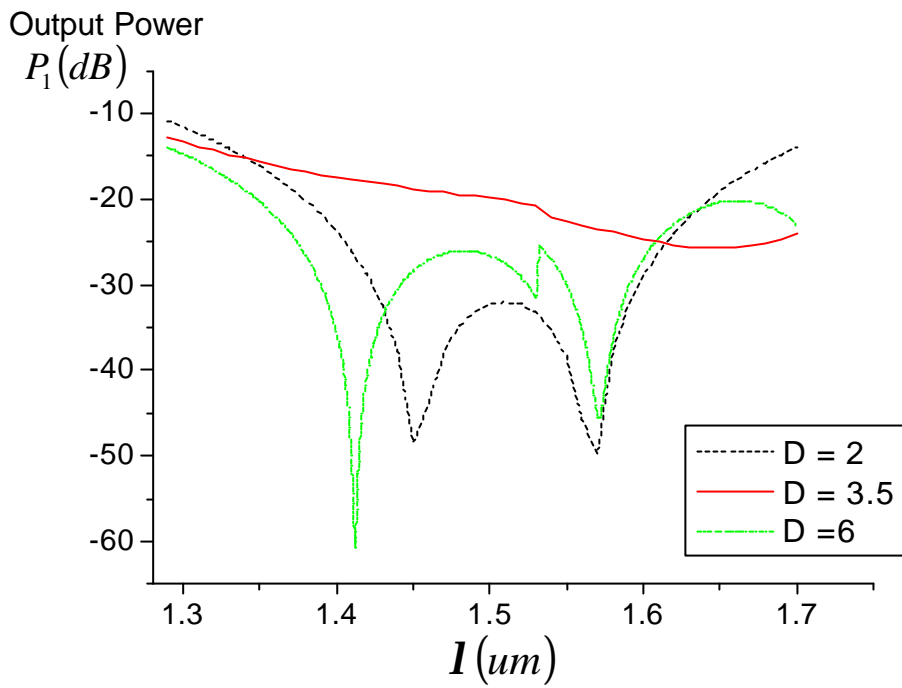


Fig. 4-6(a) Crosstalk of adiabatic filter in guide 1 of switched state

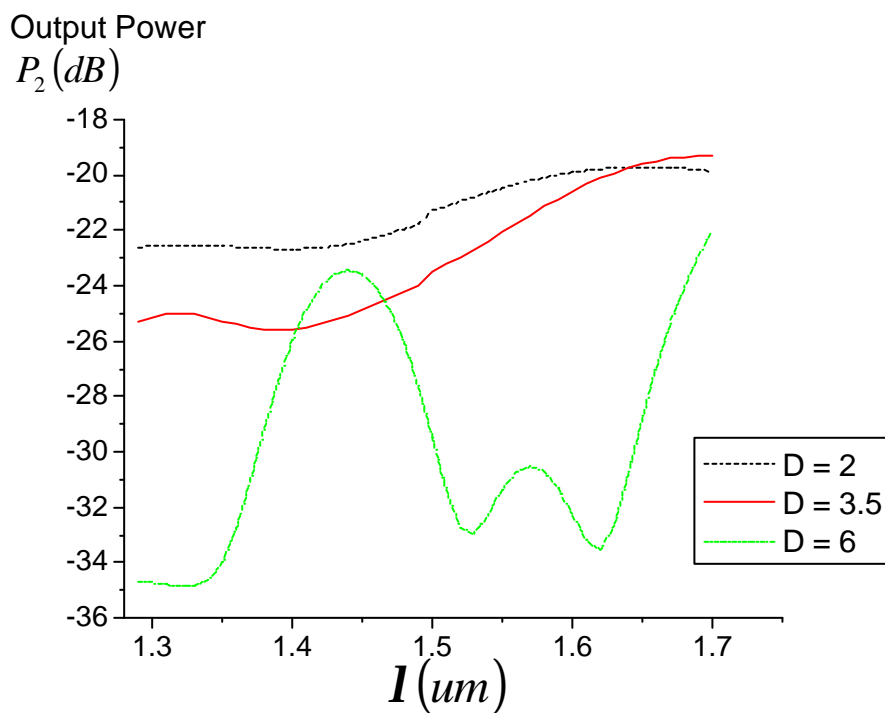


Fig. 4-6(b) Crosstalk of adiabatic filter in guide 2 of unswitched state

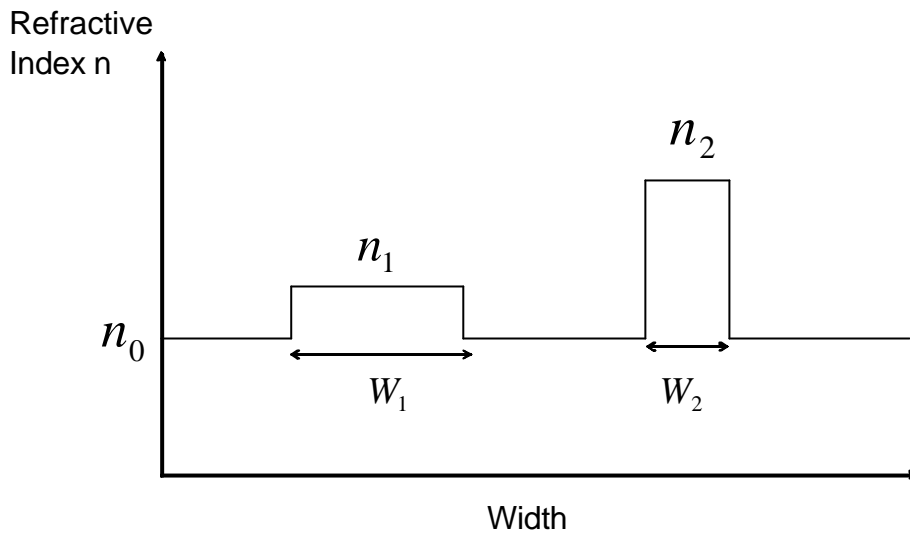


Fig. 4-7(a) Matched waveguides with different dimensions

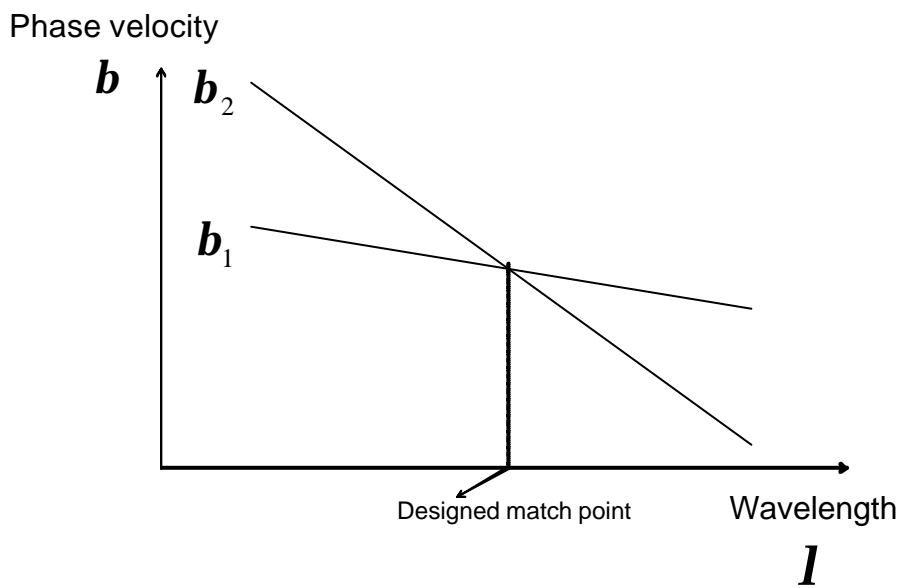


Fig. 4-7(b) Variation of phase constant versus wavelength

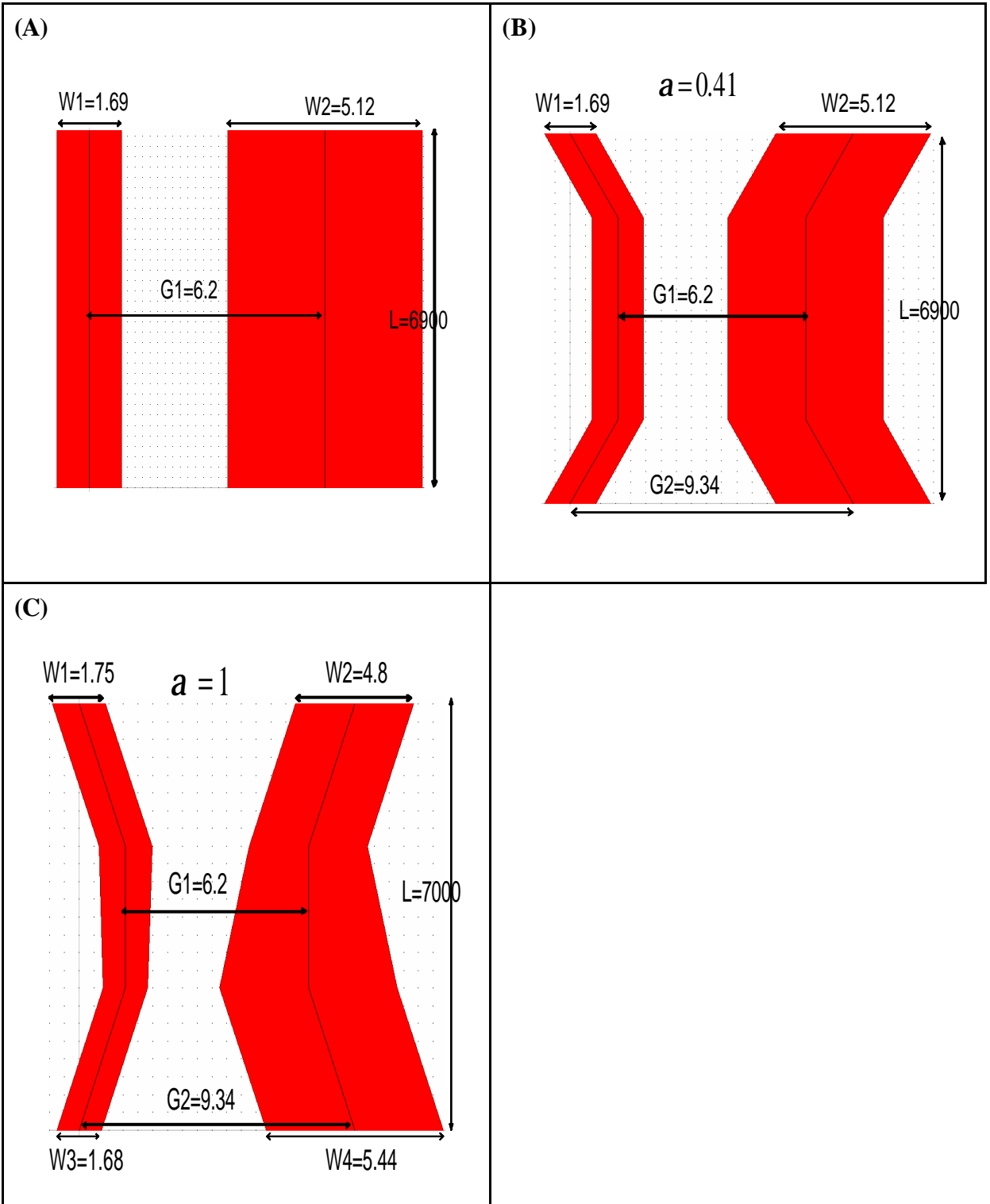


Fig. 4-8 Filter layouts. Unit:micro

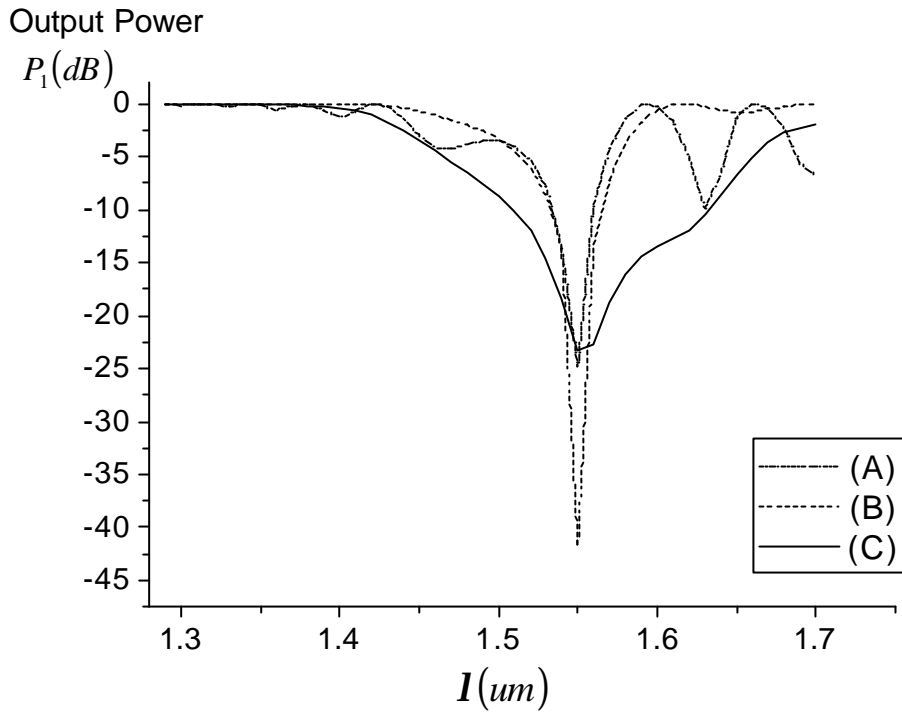


Fig. 4-9 Output power of the conventional and adiabatic filters

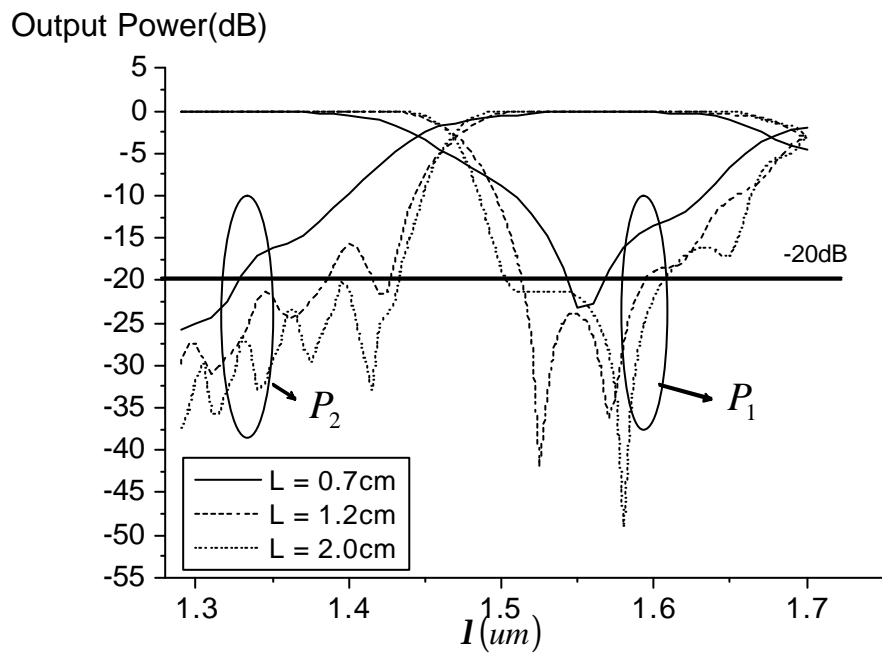


Fig. 4-10 Output power of the adiabatic filters with different lengths

Chapter 5

Conclusion

In this thesis we had done that:

1. We provided three additional profiles originally from DSP application to the adiabatic couplers and their analytic form of crosstalk are derived.
2. We predicted the performance of the dimension linearized coupler more accurately with phase considered and proved that the optimum length ratio in this case should depend on the length of the device.
3. We had shown two examples of applications in switches and filters and derived the filter of length of 2cm which had bandwidth of 106um.

Better performance can always be observed as long as we lengthen the device. We had not found the optimal profile of the adiabatic coupler since the complexity of mathematical form of crosstalk. Even if the optimum profile exists, that will be a complex function and require much critical parameters in fabrication. Another way of shorten the length instead of searching the optimum profile is to enlarge the evanescent wave and reduce the beat length and overall length can be shorten. This will be more practical compared to model computing. .

Reference

- [1] J. S. Cook, "Tapered velocity couplers," Bell Syst. Tech. J., pp. 807-822, 1955
- [2] A. G. Fox, "Wave coupling by warped normal modes," Bell Syst. Tech. J., pp. 823-852, 1955.
- [3] W. H. Louisell, "Analysis of the single tapered mode coupler," Bell Syst. Tech. J., pp. 853-870.
- [4] M. G. F. Wilson and G. A. The, "Improved tolerance in optical directional couplers," Electron. Lett., vol. 9, pp. 453-455, 1973
- [5] R. B. Smith, "Coupling Efficiency of the tapered coupler," Electron. Lett., vol. 11, pp. 204-206, 1975
- [6] R. B. Smith, "Analytical solutions for linearly tapered directional couplers," J. Opt. Soc. Amer., vol. 66, pp. 882-892, 1976
- [7] G. H. Song, W. J. Tomlinson, "Fourier analysis and synthesis of adiabatic tapers in integrated optics," J. Opt. Soc. Amer. A., vol. 9, pp. 1289-1300, 1992
- [8] A.W. Snyder, Y. Chen, D. Rowland, and D. J. Mitchell, "Mismatched directional couplers," Opt. Lett., vol. 15, pp. 357-359, 1990
- [9] D. R. Rowland, Y. Chen, and A.W. Snyder, "Tapered mismatched couplers," J. Lightwave Technol., vol. 9, pp. 567-570, 1991
- [10] R. R. A. Sym, "The digital directional coupler: Improved design," IEEE Photon. Technol. Lett., vol. 4, pp. 1135-1138, 1992
- [11] H. S. Kim, and R. V. Ramaswamy, "Tapered, both in dimension and in index, velocity coupler: Theory and experiment," IEEE, J. Quantum Electron., vol. 29, pp. 1158-1167, 1993
- [12] Y. Silberberg, P. Perlmutter and J.E. Baran, "Digital optical switch," Appl. Phys. Lett., vol. 51, pp. 1230-1232, 1987
- [13] U. Siebel, R. Hauffe, and K. Petermann, "Crosstalk-enhanced polymer digital optical switch based on a W-shape," IEEE, Photon. Technol. Lett., vol. 12, pp. 40-41, 1992
- [14] R. Moosburger, C. Kostrzewa, G. Fischbeck, and K. Petermann, "Shaping the digital optical switch using evolution strategies and BPM," IEEE, Photon. Technol. Lett., vol. 9, pp. 1484-1486, 1997
- [15] S. Xie, H. Heidrich, D. Hoffmann, H. P. Nolting, and F. Reier, "Carrier-injected GaInAsP/InP Directional coupler optical switch with both tapered velocity and

- tapered coupling,” IEEE, Photon. Technol. Lett., vol 4, pp. 166-169, 1992
- [16] Y. Shani, C. H. Henry, R. C. Kistler, R. F. Kazatinov, and K. J. Orlovsky, “Integrated optic adiabatic devices in silicon,” IEEE, J. Quantum. Electron., vol. 27, pp.556-566, 1991
- [17] W. P. Wuang, B. E. Little, “Power exchange in tapered optical couplers,” IEEE, J. Quantum. Electron., vol. 27, pp.1932-1938, 1991
- [18] R. Adar, C. H. Henry, R. F. Kazarinov, R. C. Kistler, and G. R. Weber, “Adiabatic 3-dB Couplers, filters, and multiplexers made with silica waveguides on silicon,” IEEE, J. Lightwave. Technol., vol 10, pp. 46-50, 1992.
- [19] T. A. Ramadan, R. S. Scarmozzino, and R. M. Osgood, “Adiabatic couplers.:design rules and optimization,” IEEE, J. Lightwave. Technol., vol 16, pp. 277-283, 1998.
- [20] S. T. Chu, W. Pan, T. Kato, T. Kaneko, and Y. Kokubun, “Broadband box-like filters using tapered waveguides,” Electron. Lett., vol 35, pp. 1462-1464, 1999
- [21] R. C. Alferness, P. S. Cross, “Filter characteristics of codirectionally coupled waveguides with weighted coupling,” IEEE, J. Quantum. Electron., vol.14, pp.843-847, 1978
- [22] R. Syms, J. Cozens, “Optical guided waves and devices,” Chapter 10, 1992